University of Szeged

Faculty of Pharmacy

Department of Pharmaceutical Technology

Head: Prof. Dr. Habil. Piroska Szabó-Révész DSc

Crystallinity changes of organic materials in pharmaceutical technology

Ph.D. Thesis

By

Csaba Martha

Pharmacist

Supervisor:

Prof. Dr. Habil. Piroska Szabó-Révész DSc

Szeged

2014

Content

Content 2
Publications related to the thesis 3
Other publications and presentations 5
1. List of abbreviations 6
2. Introduction 1
3. Aims 2
3. Literature background 3
3.1. The importance of the amorphous form in pharmaceuticals 3
3.2. Prediction of amorphization 6
3.3. The factor of excipients in an amorphous system 6
4. Method applied for investigation of the amorphous form 9
4.1. X-ray crystallography 10
4.2. Thermal analysis 11
4.3. Vibrational spectroscopy 11
4.4. Other methods 12
5. Materials and Methods 14
5.1. Model materials of the crystallinity decrease 14
5.2. Methods of sample preparation 18
5.3. Methods of investigation 20
6. Results 22
6.1. Investigation of sugar-alcohols 22
6.2. Investigation of crystallinity changes of meloxicam 30
6.3. Investigation of crystallinity change of clopidogrel bisulphate 36
7. Summary and practical relevance 44
References 46
ACKNOWLEDGEMENTS 51

Publications related to the thesis

1. **Mártha Csaba**, Jójártné Laczkovich Orsolya, Szabóné Révész Piroska: Amorf forma a gyógyszertechnológiai kutatásokban. *Acta Pharmaceutica Hungarica* (2011) 81. 37-42.

2. **Csaba Mártha**, Levente Kürti, Gabriella Farkas, Orsolya Jójárt-Laczkovich, Balázs Szalontai, Erik Glässer, Mária A. Deli, Piroska Szabó-Révész: Effects of polymers on the crystallinity of nanonized meloxicam during a co-grinding process. *European Polymer Journal* (2013) 49. 2426–2432 **(IF: 3.242; citations: 6)**

3. **Csaba Mártha**, Orsolya Jójárt-Laczkovich, Joachim Ulrich, Piroska Szabó-Révész: Investigation of the crystallinity of sugar alcohols co-ground with polymeric excipients. *Journal of Thermal Analysis and Calorimetry* (2013) 115. 2479–2486. **(IF: 2.206)**

4. **Csaba Mártha**, Orsolya Jójárt-Laczkovich, Piroska Szabó-Révész: Effect of co-grinding on crystallinity of clopidogrel bisulphate. *Chemical Engineering & Technology* (2014) 37/8. 1393–1398 **(IF: 2.175)**

Presentations related to the thesis

1. **Mártha Csaba**, Jójártné Laczkovich Orsolya, Ambrus Rita, Szabóné Révész Piroska: Hatóanyagok amorfizálhatóságának vizsgálata. *Congressus Pharmaceuticus Hungaricus XIV. P-64. 2009. 11. 13-15.* Budapest, Magyarország (poszter)

2. Jójárné Laczkovich Orsolya, **Mártha Csaba**, Szabó-Révész Piroska: Kristályos vagy amorf? Az amorfizálhatóság vizsgálata. *XVI. Országos Gyógyszertechnológiai Konferencia és VIII. Gyógyszer az Ezredfordulón Konferencia, 2010. 10. 20-22.* Siófok, Magyarország (előadás)

3. **Csaba Mártha**, Orsolya Jójárt-Laczkovich, Piroska Szabó-Révész: Amorphous form in pharmaceutical technological research. *Pharmaceutical Sciences for the future of medicines and Young Scientists Meeting P-50. 2011. 07. 13-17.* (poszter)

4. **Csaba Mártha**, Orsolya Jójárt-Laczkovich and Piroska Szabó-Révész: Amorphization of co-ground clopidogrel hydrogensulphate. *8th World Meeting on Pharmaceutics, Biopharmaceutics and Pharmaceutical Technology 2012. 03. 19-22.* Turkey, Istanbul. (poszter)

5. **Mártha Csaba**, Jójárt-Laczkovich Orsolya és Szabó-Révész Piroska: Polimerek befolyása egy hatóanyag kristályosságára ko-őrlés során. *XVII. Országos Gyógyszertechnológiai Konferencia és IX. Gyógyszer az ezredfordulón konferencia 2012. 09. 27-29.* Siófok, Magyarország (előadás)

6. **Csaba Mártha**, Kitti Korcsok, Orsolya Jójárt-Laczkovich and Piroska Szabó-Révész: Investigation of crystallinity of meloxicam co-ground with PVA. From Medicine to Bionics – 1st European PhD Conference *2013. 06. 13-15* Budapest, Hungary (poszter)

7. Jójártné Laczkovich Orsolya, **Mártha Csaba**, Szabóné Révész Piroska: Őrlés hatása a hatóanyag kristályosságára gyógyszertechnológiai szempontból. *Gyógyszerkémiai és Gyógyszertechnológiai Szimpózium '13 2013. 09. 30 – 10. 01.* — Herceghalom, Magyarország (előadás)

8. **Mártha Csaba**, Jójártné Laczkovich Orsolya: Együttőrlés hatása kémiailag hasonló anyagok kristályosságára *XI. Clauder Ottó Emlékverseny 2013. 10. 17-18.* Budapest, Magyarország (előadás)

9. Jójártné Laczkovich Orsolya, **Mártha Csaba**, Katona Gábor, Szabóné Révész Piroska: Gyógyszertechnológiai formulálások során alkalmazott cukror, cukoralkoholok amorfizálódási tulajdonságai *MKE Kristályosítási és Gyógyszerformulálási Szakosztály 7. Kerekasztal Konferencia 2014. 05. 16-17* Szeged Magyarország (előadás)

Other publications and presentations

1. **Csaba Mártha**, Sai H. S. Boddu, Mariann D. Churchwell: Physical compatibility of sodium citrate with alcohol and cefepime *American Journal of Health-System Pharmacy 2013. 06. 01. 70. 932-937*

2. **Mártha Csaba**, Doró Péter, Mártha Gabriella, Nagy Andrea, Németh Ákos, Soós Gyöngyvér: Patikaválasztás szempontjai. *Congressus Pharmaceuticus Hungaricus XIV. P-133. 2009. 11. 13-15.* Budapest, Magyarország (poszter)

1. List of abbreviations

API - active pharmaceutical ingredient
ATR - attenuated total reflectance
CLP - clopidogrel bisulphate
DSC - differential scanning calorimetry
DTA - differential thermal analysis
DVS - dynamic vapour sorption
EC - Ethyl cellulose
FT IR - Fourier transform infrared spectroscopy
HPC - Hydroxypropyl cellulose
HPMC - Hydroxypropyl methylcellulose
ICH - International Conference on Harmonisation
LOQ - Limit of Quantification
MX - Meloxicam
NIR - Near infrared
NMR - Nuclear magnetic resonance
PEG - polyethylene glycol
PVA - polyvinyl alcohol
PVP - polyvinylpyrrolidone
SEM - scanning electron microscopy
ss-NMR – solid state nuclear magnetic resonance
TEM - transmission electron microscopy
TG - thermo gravimetry
T_g - glass transition temperature
T_m - melting point
XRD - X-ray diffraction
XRPD - X-ray powder diffraction

2. Introduction

Investigation of the crystal structures of pharmaceutical materials is a continuously increasing interest. The variety of the order of molecules in the unit cell of an API can result differences in dissolution rate, wettability, solubility or bioavailability. Since it is essential to monitor these properties during development, methods for the investigation of crystal structure are increasingly in the focus.

Technological methods to obtain a product with more suitable properties (i.e. faster dissolution and complete distribution) or to achieve better flow, particle size reduction may be needed. The methods that are available to reach these goals are operate with high kinetic energy, especially if the required particle size interval is at the nano range. This energy can be enough to transform the crystal structure of the material and corrupt its pharmacokinetic properties.

A wide range of instruments are available to investigate even small changes in crystal structure of a material. The limits of quantification of these devices are sufficiently low to allow distinctions to be made between apparently identical materials. This has reached such a high level, that Walter McCrone stated that:

"…the number of (polymorphic) forms known for a given compound is proportional to the time and money spent in research on that compound."

3. Aims

In present study, our primary aim was to investigate the changes in crystallinity of selected materials, which differ in many aspects, especially in glass-forming properties. To achieve this, we compiled the following steps:

1. to establish the literature background of investigation methods which are suitable to follow changes in crystallinity of organic materials with small molecular weights.
2. to find an easy and rapid method, that is able to predict the glass-forming properties of given materials.
3. to select excipient pair, which are similar chemically, but differ in crystal structure; which are relatively inexpensive, widely used in pharmaceutics and have different glass-forming properties. Mannitol and sorbitol turned out to possess these properties.
4. to characterize the change in crystallinity of MX without any excipient and also with polymers (PEG, PVP) using different investigation methods.
5. to characterize the amorphization tendency of CLP by co-grinding with an inorganic silicon dioxide (Aerosil 200).

3. Literature background

3.1. The importance of the amorphous form in pharmaceuticals

Amorphous or glassy materials are in the solid phase, but unlike crystalline ones they lack long-range order (Yu, 2001). This means that the orders of the molecules are similarly random to each other as in the liquid phase. They may have short-range order, though they can exhibit this over merely a few molecules (Hancock, et al. 1997). The absence of well-defined molecular packing gives glassy materials different physical and physical-chemical properties, such as higher enthalpy and free energy, and a greater volume (Figure 1).

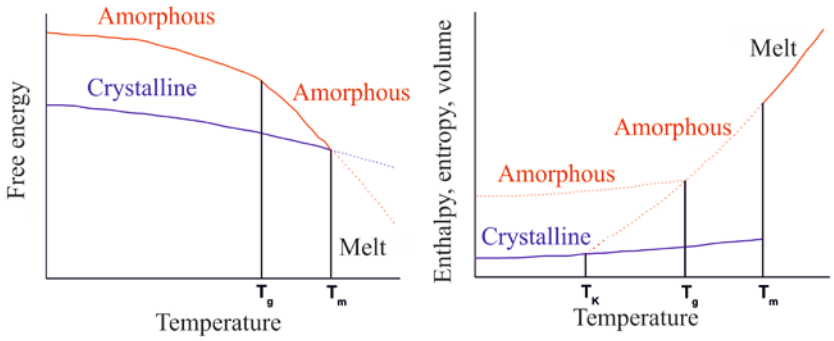

Figure 1 Temperature parameters of crystalline and amorphous forms. T_g: glass transition temperature; T_m: melting point. (Kauzmann, 1948)

Since amorphous materials do not possess a well-ordered crystal structure, their lattice energy is also at a minimum level. Consequently, they will not have a characteristic T_m, as crystalline materials do. They respond to heating from low temperature by softening at a specific point, which is called the glass transition temperature (T_g). Below T_g amorphous materials are generally brittle and rigid, while above it they are rubbery or viscous.

Due to these circumstances, the amorphous form will always be thermodynamically unstable and will tend to recrystallize, as demonstrated many times (Fukuoka et al. 1986; Yoshioka et al. 1994; Hancock et al. 1995). They have a high capacity to absorb water, they are extremely hygroscopic, and they display considerable chemical reactivity (Pikal et al. 1978).

In pharmaceutics most often organic materials with relatively small molecular weight are used. These materials, investigated from a structural view, normally feature complex

molecular geometry, high conformational flexibility, and extensive hydrogen bonding. Therefor pharmaceutical solids have high tendency to present in amorphous form. Amorphous form can appear through the following ways:

a) When the aim is to improve some disadvantageous properties of the drug, it can be prepared in an amorphous form. Through the destruction of the order of the molecules, the lattice energy, which is a thermodynamic barrier to dissolution, will remain at the minimum too. In that case the dissolution rate and water solubility can be enhanced (Hancock & Parks, 2000; Rodríguez-Spong et al., 2004; Takeuchi et al., 2005; Zhang et al, 2004).

b) When the formulation contains a partially amorphous form of the organic material at room or body temperature. This can occur when the substance is easy to amorphize or when one of the excipients of the formulation is able to bind the API molecularly (e. g. PVP, colloidal silicon dioxide). With these types of additives, the dosage form will be at least partially amorphous (Craig et al. 1999).

c) When the material is accidentally converted into an amorphous form by a pharmaceutical technique. The techniques, that are able to amorphize the material are those, which involve the use of the drug in the liquid phase (solvent techniques or hot-melt techniques) (Kumar et al. 2011; Carpentier et al. 2003; S. Qi et al. 2008) or are able to provide sufficiently high energy (e. g. milling) (Sharma et al. 2009).

The pharmaceutical industry has high interest in case **a)**, when an amorphous solid is made deliberately to avoid the disadvantageous properties of a given material. Three basic ways have been developed to amorphize the APIs:

- **Solvent methods:** The API is dissolved in a good solvent, then it is evaporated as fast as possible. This can be done by heating, pressure reduction or evaporation. This is one of the simplest processes developed for amorphization, although it has its weaknesses: as the materials usually have low water solubility, large amounts of organic solvents are needed. Some of these organic

solvents tend to make inclusions, or leave traceable solvent residuals (Kim et al. 2008; Takeuchi et al. 2005; Rossmann et al., 2012).

- **Hot-melt techniques:** The material is heated above its T_m and then immediately cooled down, or a suitable excipient is melted and the API is dissolved in the melt. This method appears easy, but it has its limitations. Though most materials have relatively low melting points, this is still an energy-intensive process. Furthermore it can be highly challenging to move and treat the material in the liquid phase (Pokharkar et al. 2006; Saerens et al., 2012).
- **Milling techniques:** The drug may be milled alone, or with an excipient in a co-milling or co-grinding method. Due to the impact of the balls or rods of the mill, the crystal structure of the material is destroyed, while the friction is able to melt it locally, which causes a further crystallinity decrease (Watanabe et al. 2003; Mallick et al. 2008).

Attention has nowadays started to turn to case **c)**, when the amorphous form is not a particular aim, but is a result of one of the techniques used during the formulation. These techniques are widely used in pharmaceutical technology since; the currently discovered effective molecules are mostly poorly water soluble. To launch them in an appropriate formulation is the task of pharmaceutical technology.

Popular methods such as the formulation of salts (Tarsa et al. 2010), complexes (Dai et al. 2013), or cyclodextrin-inclusions (Aigner et al., 2012) usually require solvent evaporation or crystallization from the melt, and there is therefore a high possibility of obtaining an amorphous final product. Freeze-drying methods are widely used to make parenteral dosage forms, but the amorphization of lyophilized product must be reconed with, since the solvent, which is generally water, evaporates rapidly (Kumar et al. 2011).

Another way can that be chosen to improve the dissolution rate of a poorly water-soluble drug: is to reduce the particle size to the micro- or the nano range (Ambrus et al. 2013; Chen et al. 2011). These processes demand high energy input, which again readily allows the material to be present in amorphous state: the impact of balls or rods, or the destructive effect of ultrasound or cavitation is capable of destroying the molecular structure of any material. Spray-drying can also be an effective method of adjusting the particle size to the required

range. Needless to say, the rapid solvent evaporation leads to a high chance of amorphization (Pomázi et al. 2011; Takeuchi et al. 2004).

Tableting, a process initiating high pressure and friction can also be the source of accidental amorphization (Bozic et al. 2008).

3.2. Prediction of amorphization

In view of the circumstances detailed above the possibility of predicting of the amorphization or glass-forming properties of any given material is essential. From the aspect of whether a material is easy to amorphize or not two groups can be distinguised: poor and good glass-formers. Most authors calculate with the ratio of T_g and T_m. Kerč & Srčič, (1995) classified poor glass-formers as those with $\frac{Tg}{Tm} < 0.7$; while for good glass-formers is $\frac{Tg}{Tm} > 0.7$. Although this is widely accepted, the ratio for poor glass-formers in other publications is: $\frac{Tg}{Tm} > 1.5$; while that for good glass-formers is: $\frac{Tg}{Tm} < 1.5$ (Craig et al., 1999, Hancock & Zografi, 1997.)

Obviously the values of T_g and T_m must first be determined. For this, the most suitable method is DSC. Observations indicate that T_g is usually between 65% and 80% of T_m (expressed in K) (Yu, 2001). If the investigated sample is a multicomponent system containing several amorphous units, the Gordon-Taylor equation could give a sufficient approximation of the value of T_g (Gordon & Taylor, 1952).

3.3. The factor of excipients in an amorphous system

When the aim is the preparation of amorphous solid, suitable excipients can be extremely helpful. In fact their usage may even be essential to reach the required goal.

When a **solvent technique** is planned the most challenging problem is to dissolve the drug in some cheap, non-toxic, and if possible inorganic solvent. To achieve this, a co-solvent excipient is often needed, which enhances the wetting or the solubility of the drug in the main solvent (Teagarden et al. 2002; Miller et al. 2012). Carrier excipients may also be needed, e. g. during a spray-drying process (Chauhan et al., 2005; Takeuchi et al., 2005).

Hot-melt technologies, can be performed in two ways: the API is melted alone above its T_m and then cooled down rapidly (Qi et al. 2008) or it is dissolved in a suitable melted excipient, which has an appropriate low T_m.

The amorphization of materials by **grinding** has a high energy demand. This energy can be reduced by adding a suitable excipient and performing a co-grinding procedure (Choi et al. 2009; Kürti et al. 2011; Merisko-Liversidge 2008). An appropriate additive also helps to prevent the aggregation of nanoparticles, lubricates the system, and increases the water solubility of the API.

Since materials in the amorphous phase are less stable than crystalline substances and have a high tendency to return to a crystalline form, stabilization can be needed, so as to prevent the product from recrystallization during subsequent formulation, packaging, storage and usage. An ideal stabilization additive also prevents the amorphous material from undergoing chemical degradation. The stabilizing action of these crystallization inhibitors depends on different mechanisms:

- **Vitrification**-based stabilizers immobilize and isolate substances in rigid glasses of inert stabilizer molecules. This reduces the potential of aggregation and diffusion of molecules.

- **Direct drug-excipient interactions** (e. g. hydrogen-bonding) can maintain the material practically molecularly bonded to the stabilizer, thereby preventing it from undergoing recrystallization.

- **Molecular encapsulation** can also be used for stabilization, as the API inside the “capsule” is practically amorphous.

- **Storage temperature:** On the basis of previous studies (Hatley 1997; Hancock 1997) Yu (2001) proposed the rule, that the storage temperature should be approximately 50 K below T_g. T_g can be set with the aid of suitable additives, since the binary mixture has a lower T_g.

Pharmaceutical excipients include several materials which meet the requirements, but most of them are polymers. The most widely used as grinding materials are the different types of PEG, PVP, PVA, cellulose ethers and esters (e.g. HPC, HPMC, EC).

When certain excipients are used to formulate a partially amorphous form of the material, additives can facilitate the amorphization. The problem of undesirable amorphization chiefly appears in dosage forms where the API is in the solid phase. This can occur in solid, semi-solid, or liquid formulations too, such as powders, granules, tablets, suppositories, ointments or suspensions too.

These products nearly always involve **filler agents**. Most commonly, starch, microcrystalline cellulose, sugar-alcohols or lactose is used. Numerous literature examples refer to the glass-forming properties of these additives (Bialleck. et al. 2011; Sato. et al. 2012; Reitz et al. 2013; Vollenbroek et al. 2010).

Binders are indispensable in a well-formulated granule or tablet. They also may cause difficulties as they readily bind other materials, turning them into amorphous form. The widely used binders, such as different celluloses, acrylic acid copolymers, PVP are able to amorphize the API (Kotiyan et al. 2001; Watanabe et al. 2003; Mura et al. 2002).

Similar characteristics may be displayed by **disintegrant** agents. They must have a high water absorption capacity to burst the particles of granules or tablets physically. Such properties are possessed by polymeric materials e. g. starches, crosspovidones or sodium hydrogen carbonate. These materials are also capable of decreasing the crystallinity of any active agent (Lin et al. 2012; Martini et al. 1991).

To increase the solubility of the API **solubility-enhancing agents** may be used. They can operate with different mechanisms such as the inclusion formulation property of cyclodextrins (Al-Marzouqi et al. 2007; Sangwai & Vavia 2013), solubilizing with polysorbates (Zhang et al. 2012), or the ability of PEGs of making solid solutions (Papadimitriou et al. 2012; Yam et al. 2011).

Colloidal silicon dioxide (Aerosil) is widely used as an **adsorbent** because of its large surface area, or as an **antistatic additive,** because of its ability to discharge the formulated system. It is well known that colloidal silicon dioxide is an agent, with a high ability to turn materials into amorphous form (Chauhan et al. 2005; Takeuchi et al. 2005).

Aerosil is also used as a **glidant** and **lubricant**. For this, magnesium stearate, talc, stearic acid and different hydrogenated vegetable oils are also used. These materials may further cause a crystallinity decrease of the active agent (Watanabe T. et al. 2002).

Moisture retention additives such as glycerol or sorbitol, which can also be **sweeteners,** can reduce the crystallinity of the API (Tee S. K. et al. 2000).

Further groups of additives include many other excipients, which can induce the amorphization of a drug, e. g. **coating agents** (different celluloses, acrylic acid copolymers) or **viscosity increasing agents** (different celluloses, gelatine, alginates) or **ointments** and **suppository bases** (vaselins, PEGs or fatty glycerides).

4. Method applied for investigation of the amorphous form

The methods for the investigation of amorphous materials are based on the various physical and physico-chemical properties: as they can differ in appearance, molecular structure, intra-molecular interactions and hygroscopicity, they can be investigated with a broad number of devices. Since the amorphous and crystalline forms are chemically equivalent, the amorphous form can only be measured in the solid state. Depending on the detection and quantification limit of the device two or more complementary methods are advised (Aaltonen et al., 2009).

The choice of the most suitable and reliable investigation device and method is a real challenge for a pharmaceutical scientist. The requirements it has to meet are cited in the ICH (1996) Guidelines of Quality. During the validation of such a method, the following properties are monitored and validated: Accuracy, Precision, Repeatability, Intermediate Precision, Specificity, Detection Limit, Quantitation Limit, Linearity, and Range of the instrument.

Those instruments and methods will next be demonstrated which are applied most frequently in the pharmaceutical industry to investigate the amorphous form, with special attention to those used during our investigations.

4.1. X-ray crystallography

XRD methods are the most commonly used to investigate the crystallinity of any solid material (Uvarov & Popov 2008; Li, et al. 2000; Kim et al. 2008). The theory of XRD is that X-ray beams are diffracted at specific angles from the electron cloud of the molecules. The 3-dimensional structure of the crystal can therefore be observed in a 2-dimensional diffractogram. The equation of diffraction was described by Henry and Lawrence Bragg: $\lambda = 2\ d\ sin\ \theta$, where d is the spacing between diffracting planes, θ is the incident angle, n is any integer, and λ is the wavelength of the beam (Figure 2) (Jauncey 1924). The X-ray beam arriving from a certain angle is scattered by the molecules and produces secondary circular waves emanating from the electron cloud. A regular array of scatters produces a regular array of spherical waves, but these waves cancel one another out in most directions through destructive interference, they add constructively in a few specific directions.

These intensifications and attenuations can be plotted in a 2-dimensional X-ray diffractogram, where the shot angle of the beam (2θ) is plotted on the x axis and the intensity of the reflected or transmitted beam on the y axis.

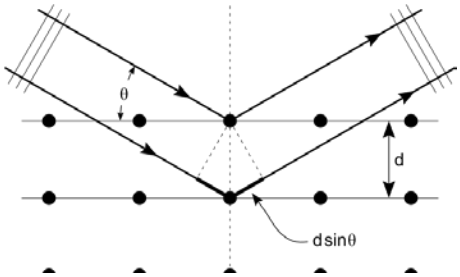

Figure 2 The Bragg's diffraction

By means of this phenomenon, single-crystals, powders or powder mixtures can be observed. As the amorphous form can only exist in a solid phase mass, XRPD devices can be used.

The main task for operation with an XRPD device is the sample preparation: to avoid non-preferred orientation and to obtain a homogeneous powder sample, particle size setting is usually needed. Through this physical activation, although XRPD is a non-destructive method, the amorphous product can be destroyed by recrystallization (Moore et al. 2009).

An XRPD measurement can yield quantitative and qualitative information (Tian et al. 2007). To improve the applicability of the XRPD devices, they can be equipped with hot-

humidity chamber, so that the crystallinity can be measured at different temperatures and humidity values (Guguta C. et al. 2008).

4.2. Thermal analysis

With thermal analytical instruments all the changes, which occur on temperature change can be measured. As the amorphous form exhibits different thermal behaviour as the crystalline form, these methods can be suitable to investigate and characterize the glassy form. The main analytical methods are: TG, DTA and DSC.

TG involves a use of an instrument which records the mass change of a sample in response to temperature change (Wyttenbach et al. 2013). As it gives only partial information about the crystal structure of the material, it is often utilized as an additional analytical method during investigations of amorphous forms.

DTA and **DSC** measure the heat flow of a sample in response to temperature change, but DTA is not capable of giving accurate calorimetric information and its usage has started to decline. DSC measures the amount of heat required to increase the temperature of a sample in proportion to a reference sample with a recording as a function of temperature. The measured signal stems from the difference in temperature of the sample and the reference. As the ending temperature is usually high enough to ignite the sample, a protective gas is used, which can be any noble gas (normally argon), or nitrogen. Sample preparation is important, as is the correct choice of sample holder: there are different holders on the market, which can protect the sample, or give a faster heat change, depending on what is needed.

For the investigation of an amorphous material, DSC is the most common analytical method used (Jójárt-Laczkovich & Szabó-Révész, 2011; Qi et al., 2008; Sonje et al. 2011; Royall, 1999).

4.3. Vibrational spectroscopy

Vibrational spectroscopic devices operate in the infrared region of the electromagnetic spectrum. This part of the electromagnetic spectrum is divided into 3 sub-regions: the near-infrared (approximately 14000-4000 cm^{-1}); the mid-infrared (approximately 4000–400 cm^{-1}); and the far-infrared (approximately 400-10 cm^{-1}).

The theory of infrared spectroscopy is based on the fact that the frequency of electromagnetic radiation is the same range as the frequency of the vibrations of the bonds between the atoms of the molecules. Thus, the molecules being measured will absorb, reflect or transmit the infrared beam. The intensity of the absorbed, reflected or transmitted photons can be measured and this can give qualitative or quantitative information. The most current methods are the FT IR, Raman and NIR.

The **FT IR** method measures the vibrational modes, which can change the dipole (they are IR-active modes). These are: symmetric and asymmetric stretching, scissoring, rocking, wagging and twisting. In practice this means that the CH_2X_2 groups, (where X can represent any other atom) can be investigated. Consequently in the case of amorphous systems, FT IR can provide only chemical information (Priemel, 2012; Ambike, et al. 2004). For the investigation of amorphous systems FT IR with an ATR accessory is the best choice, as it does not need difficult sample preparation (Schönbichler et al., 2013).

Qualitative and quantitative information on amorphous systems can be obtained by a complementary method of FT IR: **Raman** spectroscopy (Hédoux et al., 2009). This is based on Raman scattering, when the light beam suffers inelastic scattering on the electron cloud of the molecule. In this case, the reflected beam contains photons with both higher and lower frequencies. In practice it is widely used, as the vibrational information it gives is specific for the chemical bonds and the symmetry of the molecules.

NIR spectroscopy is widely used in pharmaceutics, because the near infrared beam penetrates much further into the sample than the mid-infrared beam and can provide valuable chemical information, especially about C-OH groups (which is suitable to characterize hydrogen bonding). This makes it a good analytical method for in-line use (Saerens et al., 2012).

4.4. Other methods

Besides optical microscopy, other more advanced microscopy techniques are also suitable to investigate the appearance of amorphous form: **SEM** and **TEM** can provide a good visual view of the sample (Karavas E. et al. 2007). The SEM method produces images of a sample by scanning it with a focused beam of electrons; consequently it gives information

about the surface, while TEM visualizes the particle shape: it measures the beam of electrons transmitted through an ultra-thin specimen, interacting with the specimen as it passes through (Priemel et al., 2013; Shah et al., 2012).

Some techniques take advantage of special properties of the amorphous material. One such method is **DVS** which measures the changes in mass at different relative humidity values. The theory behind this is that the amorphous material can absorb more water, than the crystalline material, so that even the crystallinity degree can be calculated after a calibration (Shah et al., 2006; Vollenbroek et al., 2010).

NMR can also give valuable information about the crystallinity of a material, but only in the solid state: solid-state NMR (**ss-NMR**) permits the observation of specific quantum-mechanical magnetic properties of the atomic nucleus. The asymmetric broadening of the NMR line observed in the amorphous state is due to an inhomogeneous distribution of isotropic chemical shifts, which can be assigned to static fluctuations of bond or torsion angles (Shah et al., 2006; Lefort et al., 2004).

5. Materials and Methods

5.1. Model materials of the crystallinity decrease

5.1.1. Finding the model materials

To choose the most suitable model materials for our study 30 possible materials, commonly used in pharmaceutics were investigated. Melting points (T_m), glass transition (T_g) and their ratio were measured with DSC equipment. 5 mg (± 10%) of each pure crystalline form of the materials was measured into Al chambers. Heating was first applied up to slightly over the melting point. This determined the T_m. After the whole amount of the sample had melted it was cooled down to below the T_g as fast as the device allowed (approximately 45 °C/min), measurement was then repeated. If the crystalline form of the material emerged, it was considered as poor glass-former. If the amorphous form appeared, the ratio T_g/T_m was calculated and the glass-forming properties were concluded on this basis. The results to be seen in Table 1.

For further investigations, we chose materials from the groups of poor and good glass-formers. Two similar sugar-alcohols with dissimilar glass-forming properties were also chosen.

Table 1 Measured T_g/T_m ratios of model materials and the glass-forming properties

Material	(T_m;°C)	(T_g;°C)	T_g/T_m (K/K)	Amorphous	Glass forming poroperties
Tenoxicam	226	-	-	No	poor
Mannitol	*166.9*	-	-	*No*	*poor*
Niflumic-acid	205.4	-	-	No	poor
Teophylline	271.6	-	-	No	poor
Lidocaine	70.1	-	-	No	poor
Naproxen	156.4	-	-	No	poor
Sulfametoxazol	169.53	-	-	No	poor
Trimetoprime	200.64	-	-	No	poor
Econazol-nitrate	165.71	-	-	No	poor
Sertakonazol	160.3	-	-	No	poor
Etacrin-acid	124.7	-	-	Yes	poor
Meloxicam	*264*	*63.5*	*0.63*	*Yes*	*poor*
Ibuprofen	77.4	-42.5	0.66	Yes	poor
Diclofenac	177.0	34.24	0.68	Yes	poor
Carbamazepine	191.6	51	**0.70**	Yes	good
Piroxicam	203.1	58.1	**0.70**	Yes	good
Proranolol HCl	165.2	37.8	**0.71**	Yes	good
Lacidipine	184.8	54.4	**0.71**	Yes	good
Gemfibrozil	61.5	-29.2	**0.73**	Yes	good
Sulfadimidin	196.7	76.5	**0.74**	Yes	good
Sorbitol	*91.4*	*0.77*	***0.75***	*Yes*	*good*
Loratadine	137.6	40.4	**0.76**	Yes	good
Clopidogrel HSO_4	*181.2*	*88.9*	***0.80***	*Yes*	*good*
Chlorhexidine	140.3	61.7	**0.81**	Yes	good

5.1.2. Mannitol and sorbitol

We first investigated the crystallinity changes of β-D-mannitol ((2R,3R,4R,5R)-Hexan-1,2,3,4,5,6-hexol) and D-sorbitol ((2S,3R,4R,5R)-hexane-1,2,3,4,5,6-hexol). Both materials were purchased from Hungaropharma (Budapest, Hungary) and met the quality requirements of Ph.Eur.8 (Figure 3).

Both are widely used in pharmaceutics as sweeteners, bulking agents or moisture stabilizers (Kim et al., 1998; Maury et al., 2005). Both are stable and inert compounds, properties which make them a good choice as excipients during tableting, freeze-drying, capsulizing, granulating or grinding (Tee et al., 2000; Gombás et al., 2003). They are often used together as carrier additives usually in pulmonary delivery systems (Hamishehkar H. et al. 2010). Both can exist in many polymorphic, solvate, hydrate and amorphous forms (mannitol has 3 stable polymorphs and sorbitol has 5) (Cavatur et al., 2002; Nezzal et al., 2009).

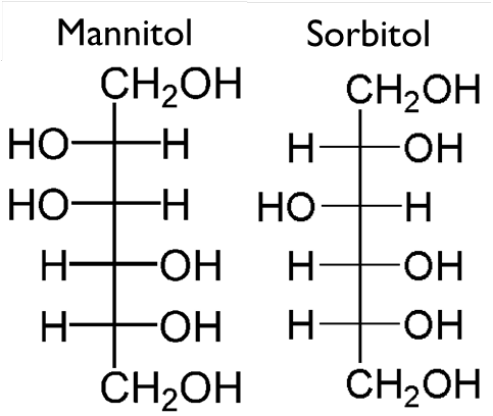

Figure 3 Chemical structure of mannitol and sorbitol

5.1.3. Meloxicam

Pure crystalline MX (4-hydroxy-2-methyl-*N*-(5-methyl-2-thiazolyl)-2*H*-benzothiazine-3-carboxamide-1,1-dioxide) was purchased from EGIS Ltd. Budapest, Hungary (Figure 4).

MX is a non-steroidal anti-inflammatory drug that is mainly applied in therapy as an anti-inflammatory and strong analgetic agent (Hanft et al., 2001). MX is practically insoluble in water, while it displays a relatively high permeability through cell membranes. It was chosen as model compound because it is capable of hydrogen-bond to other materials.

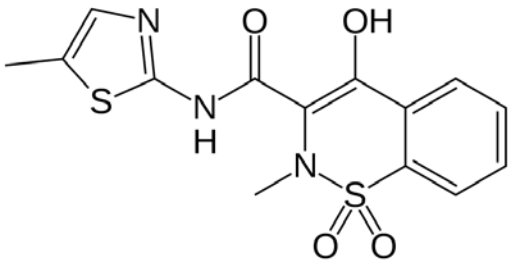

Figure 4 Chemical structure of meloxicam

5.1.4. Clopidogrel bisulphate

Pure polymorphic form II CLP (methyl (+)-(*S*)-alpha-(2-chlorophenyl)-6,7-dihydrothieno[3,2-c]pyridine-5(*4H*)-acetate sulphate) was obtained from EGIS Ltd., Budapest, Hungary (Figure 4).

CLP is an oral antiplatelet drug, which is often used in the treatment of coronary artery disease, peripheral vascular disease and cerebrovascular disease. The amorphous and polymorphic forms of CLP has been prepared and described in the literature (Német et al., 2009; Jójárt-Laczkovich & Szabó-Révész, 2010).

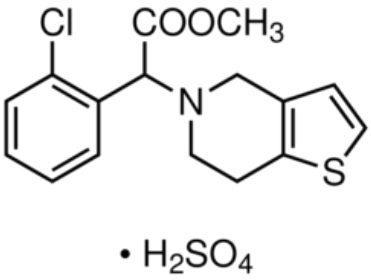

Figure 5 Chemical structure of clopidogrel bisulphate

5.1.5. Additives

PVP C30 (with a molecular weight of 58,000), obtained from BASF (Ludwigshafen, Germany) and PEG 6,000 from Sigma-Aldrich Chemie GmbH, (München, Germany), were used as grinding excipients. Aerosil 200 (colloidal SiO_2, with hydrophilic properties) was purchased from Nippon Aerosil Co., (Japan).

The various PEGs are used in the pharmaceutical industry as binders, carriers, lubricants, etc., thanks to their advantageous properties: PEGs are completely biocompatible, they can exhibit a combination of hydrophilic and lipophilic properties and they are

commercially available in various molecular weights. As semicrystalline materials, they have melting points in the range from 3 to 68 °C, depending on the molecular weight (Yam et al., 2011). Their importance in pharmaceutical research is increasing, in consequence of their ability to enhance the dissolution rate of numerous poorly water-soluble drugs (Leuner et al., 2000).

PVP is also produced in various molecular weights and particle sizes. These materials are mostly used as binders, matrix polymers, disintegrants, crystallization inhibitors and stabilizers. In the literature, PVP has often been used as an additive during co-grinding, serving as a carrier or to prevent aggregation (Martini et al., 1991). It has also been demonstrated that it can decrease the crystallinity of API during methods providing high energy (Mura et al., 2002).

We earlier verified that PEG and PVP can be applied as suitable additives to decrease the energy requirements of grinding, to help reduce the particle size to the nano range, to prevent the aggregation of nanoparticles and to increase solubility (Kürti et al., 2011).

5.2.Methods of sample preparation

Physical mixtures of the crystalline sugar-alcohols (mannitol and sorbitol) and stabilizer polymer additives (PVP C30 and PEG 6,000) were prepared and charged into a hard polyamide mortar. Equal amounts of agate balls were also placed into the chamber. The mass ratio of the mixtures was in all cases 1:1. The grinding processes were carried out with a Fritsch - Pulverisette® planetary ball mill. Mixtures were ground at 120 min on 400 rpm. Samples were withdrawn for investigation after 20, 40, 60, 80, 100 and 120 min.

Physical mixtures of MX, as API, and the grinding (stabilizer) polymer (PEG 6 000 or PVP C30) were prepared and charged into the stainless steel jar of a planetary ball mill containing 10 stainless steel balls (Retsch PM 100, Retsch GmbH & Co., Haan, Germany). The mass ratios were based on previous work (Kürti et al., 2011), so as to give nanoparticles (200-600 nm). For the PVPs, the drug-excipient mass ratio was 1:1, while for the PEGs it was 1:2. Mixtures were ground for 140 min, samples being withdrawn for investigation after 20, 40, 60, 80, 100, 120 and 140 min. During the grinding process, the temperature of the mortar

was measured with an infrared thermometer immediately before sample withdrawal. The temperature of the mortar was not higher than 56 °C throughout milling.

The co-grinding of the mixture of CLP and Aerosil 200 was performed in a planetary ball mill (Retsch PM 100, Retsch GmbH & Co., Germany). The mass ratio of CLP and Aerosil 200 was 7:3. This ratio was based on a previous work by our team (Jójárt-Laczkovich & Szabó-Révész, 2011). The maximum grinding time was 240 min. Samples were withdrawn for investigation after 15, 30, 45, 60, 90, 120, 150, 180 and 240 min.

5.3.Methods of investigation

5.3.1. X-ray powder diffraction (XRPD)

XRPD analysis was performed with Bruker D4 and Bruker D8 Advance diffractometer (Bruker AXS GmbH, Karlsruhe, Germany) systems with Cu K λI radiation (λ = 1.5406 Å). The samples were scanned at 40 kV and 40 mA from 3° to 40° 2θ, at a scanning speed of 0.05°s^{-1} and a step size of 0.010°. The crystallinity of the mannitol and sorbitol samples was determined as ratio of the areas beneath characteristic and separate peaks of physical mixtures and samples and was expressed as percentage (%). These peaks are specific for each material; none of them is a double peak, or covered by the peak of the semicrystalline PEG. The crystallinity of the MX and CLP samples were determined via the total area beneath the curve between 12° and 30° 2θ. All manipulations of diffractograms and the calculation of area under curves were performed with DIFFRACTplus EVA software.

In the case of MX samples, we used an internal standard method to avoid the problems caused by the particle size reduction and randomly oriented particles. This technique is widely applied for quantitative XRPD. As internal standard, we mixed 20% (w/w) of pure crystalline NaCl into the binary mixtures. Before its application, the particle size of the NaCl was set into the similar range as that of the MX (2643.6 ± 2629.1 nm). After Kα_2-stripping, background removal and smoothing of the areas under the peaks, the area under the peak of MX was proportioned to the area under the peak of NaCl (31°-32.5° 2θ).

5.3.2. Differential scanning calorimetry (DSC)

DSC data were recorded with a Netzsch STA-409 (Selb, Germany) and a Mettler-Toledo DSC 821e instruments with intercoolers. 4.5-5.5 mg samples were crimped in aluminium pans with two holes and were examined in temperature interval 25-200 °C under an argon gas flow at 100-150 ml min^{-1}, at heating rates of 10 and 20 °C min^{-1}.

5.3.3. Thermogravimetry (TG)

TG curves were obtained with a TGA/DSC1 (Mettler-Toledo, Switzerland). 4.5-5.5 mg of the samples were crimped in aluminium pans with two holes and were examined in the temperature interval 25-200 °C. Heating rate was 20 °C min^{-1}.

5.3.4. Fourier transform infrared (FT IR) spectroscopy

FT IR spectra were recorded with a Bio-Rad Digilab Division FTS-65A/896 FT IR spectrometer (Bio-Rad Digilab Division FTS-65A/869, Philadelphia, USA) between 4000 and 400 cm^{-1}, at an optical resolution of 4 cm^{-1}; operating conditions: Harrick's Meridian SplitPea single reflection, diamond, ATR accessory. Thermo Scientific GRAMS/AI Suite software (Thermo Fisher Sciencific Inc., Waltham, USA) was used for the spectral analysis.

For FT IR determinations, the ATR method was chosen, because with this there is no need for sample preparation, such as particle size reduction or KBr tableting, which would expose the samples to further physical stress.

5.3.5. Scanning electron microscopy (SEM)

The morphology of the MX particles was examined by SEM (Hitachi S4700, Hitachi Scientific Ltd., Tokyo, Japan). A sputter coating apparatus (Bio-Rad SC 502, VG Microtech, Uckfield, UK) was applied to induce electric conductivity on the surface of the samples. The air pressure was 1.3-13.0 mPa. Briefly, the samples were sputter-coated with gold–palladium under an argon atmosphere, using a gold sputter module in a high-vacuum evaporator and the samples were examined at 10 kV and 10 μA. MX particle diameter distributions were obtained by analysing several SEM images with the ImageJ software environment.

6. Results

6.1. Investigation of sugar-alcohols

6.1.1. Determination of crystallinity of mannitol

The DSC measurements indicated that the ratio T_g/T_m (K/K) for pure β-D-mannitol (T_g: 285.75 K T_m: 440.05 K) is lower than 0.7, suggesting that this compound has only a low tendency to exist in amorphous form. β-D-mannitol has linear molecules and an orthorhombic crystal structure, which is preferable for the development of strong long-range order among the molecules.

Thermoanalytical techniques such as DSC or DTA are suitable methods for investigation of the crystallinity of samples. From the areas under the peaks of melting of the samples can be concluded. DSC measurements demonstrated that the raw mannitol did not suffer any loss in crystallinity during the grinding process, and it exhibited a similar characteristic melting peak at the same temperature (440.05 K ± 3.1 K), with identical enthalpy (ΔH= 41.02 Jg^{-1} ± 1.13 Jg^{-1}) as for raw mannitol itself. The mannitol samples made with polymer additives behaved similarly to pure mannitol: the amorphous PVP has no peak in the DSC curve, while the semi-crystalline PEG had a broad melting peak at around 338 K; the mannitol in the mixtures displayed identical melting action to that without polymers. Specific peaks relating to the melting point of mannitol appeared in the curves with slightly varying enthalpy (ΔH= 22.04 J g^{-1} ± 0.83 J g^{-1}) indicating that the mannitol maintained its well-defined long-range order in the crystal structure.

XRPD measurements can also be used to investigate the crystal structure of ingredients. LOQ of XRPD methods is low enough for them to be used for quantitative measurements. In case of clopidogrel bisulfate polymorphs and olanzapine polymorphs the LOQ were 1.0–1.5 % (w/w) and 1.22% (w/w) respectively. The areas under diffraction peaks are related to the crystallinity and the decrease in crystallinity can be calculated from the changes in the independent characteristic peaks.

XRPD measurements were performed on each of the raw materials and samples. Amorphous PVP exhibited a halo with no specific peaks in the diffractogram, while PEG, as a semicrystalline polymer gave a few broad peaks in the investigated range (Figure 6). Pure

mannitol displayed peaks characteristic of the β-D form (sharp peaks at the following *2θ* values: 10.441°, 14.572°, 18.722°, 21.019°, 23.374°, 28.282°, 29.444°, 31.728°, 38.645° and 44.052°). After 120 min of grinding, the same peaks were found in the curve. No shifts were observed, no peaks disappeared and no new peaks appeared. The areas under peaks at 9.5-11° 2θ; 13.7-15.5° 2θ and 17.7-19.9 ° 2θ were calculated for each sample that was withdrawn. This revealed that, although some peaks decreased to an irrelevant extent, no fundamental change in crystallinity occurred during grinding (Figure 7).

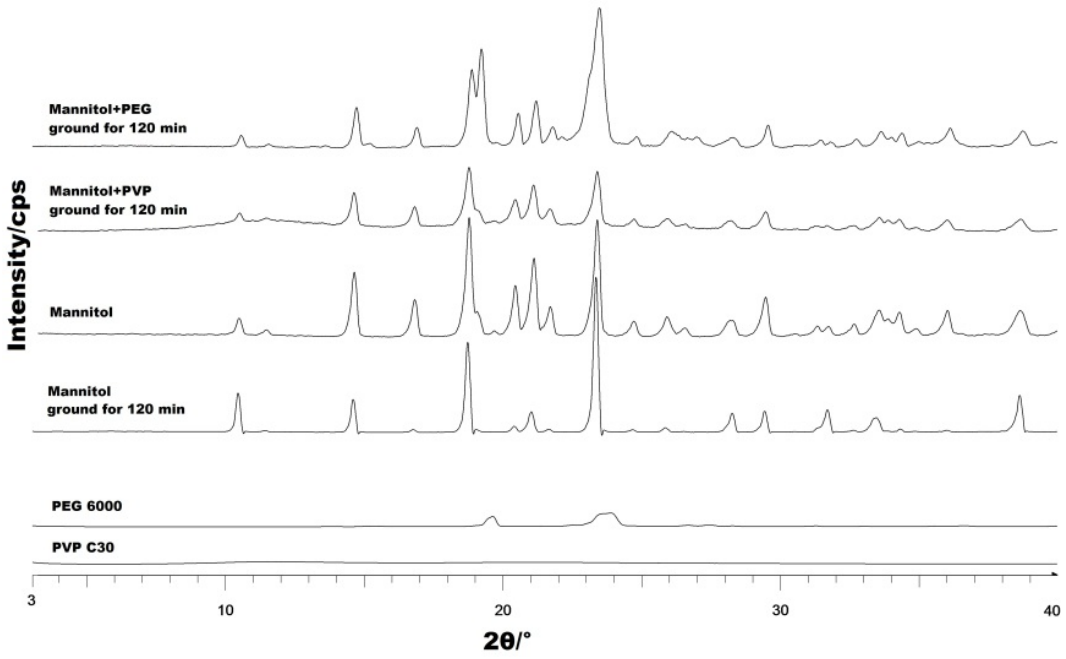

Figure 6 X-ray diffractograms of pure PVP C30, PEG 6000, and mannitol; and mannitol samples ground for 120 min with PVP C30 and PEG 6000.

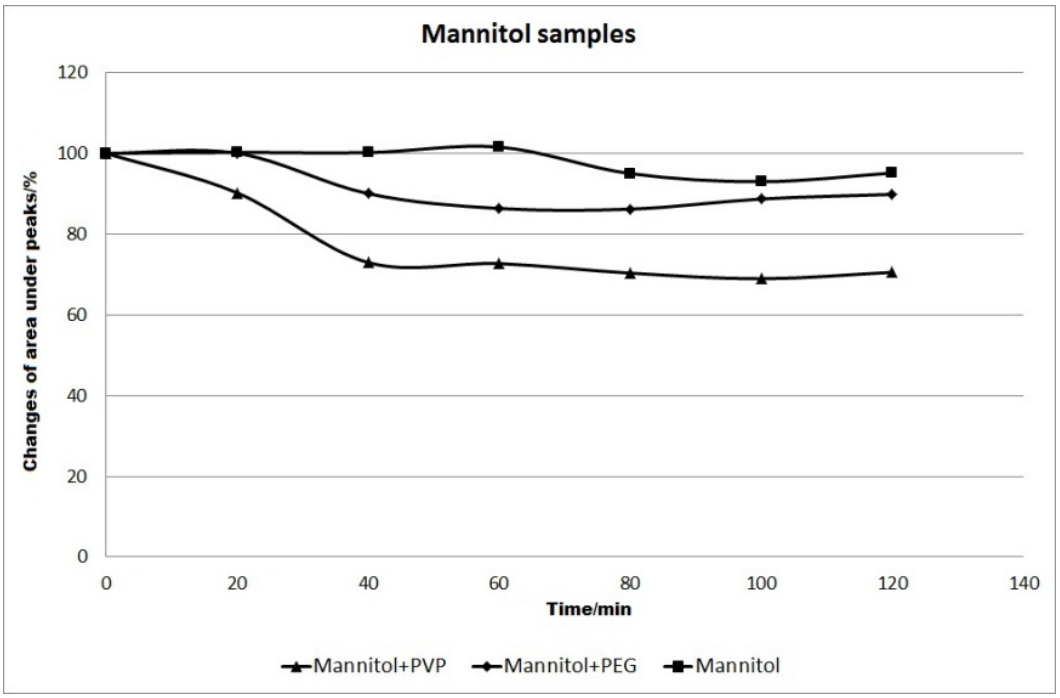

Figure 7 Crystallinity change of mannitol and mannitol ground with polymer additives (PVP and PEG) as a function of the milling time.

Same grinding and investigation method was applied in the presence of the polymer additives. The samples containing PEG gave the peaks characteristic of mannitol and the broad peak relating to PEG at around 22-24° 2θ. Crystallinity determination (based on the same peaks as utilized in the case of raw mannitol) proved that minor amorphization took place after 40 min of milling. No polymorph transition was observed: no peaks underwent a shift or disappeared and no new peaks were detected. Slightly different behaviour was observed for the samples containing PVP. The peaks were specific for mannitol, but the areas under the curves decreased with increasing grinding duration. The degree of this decrease exceeded the LOQ and could not be interpreted in terms of a decrease in particle size. The change in crystallinity during the milling did not exceed 70%. After 40 min of grinding an apparent equilibrium set between the crystalline and amorphous phases.

6.1.2. Crystallinity determination of sorbitol

The ratio T_g/T_m (T_g and T_m in K) measured for D-sorbitol was 0.75 (T_g: 273.92 K T_m: 364.55 K), which predicted this material is a good glass-former.

The DSC measurements showed that the sorbitol used was a mixture of the epsilon (T_m: 364.55 K) and gamma (372.05 K) polymorphs. During the grinding process the proportions of the polymorphs changed. The pure material contained a predominance of the epsilon form. The milling led to a decrease in the amount of the epsilon form, while the amount of the gamma polymorph slightly increased (Figure 8). This means that the mechanical energy broke down the crystal structure of the crystalline epsilon sorbitol. Some of the amorphous material recrystallized due to the mechanical impact.

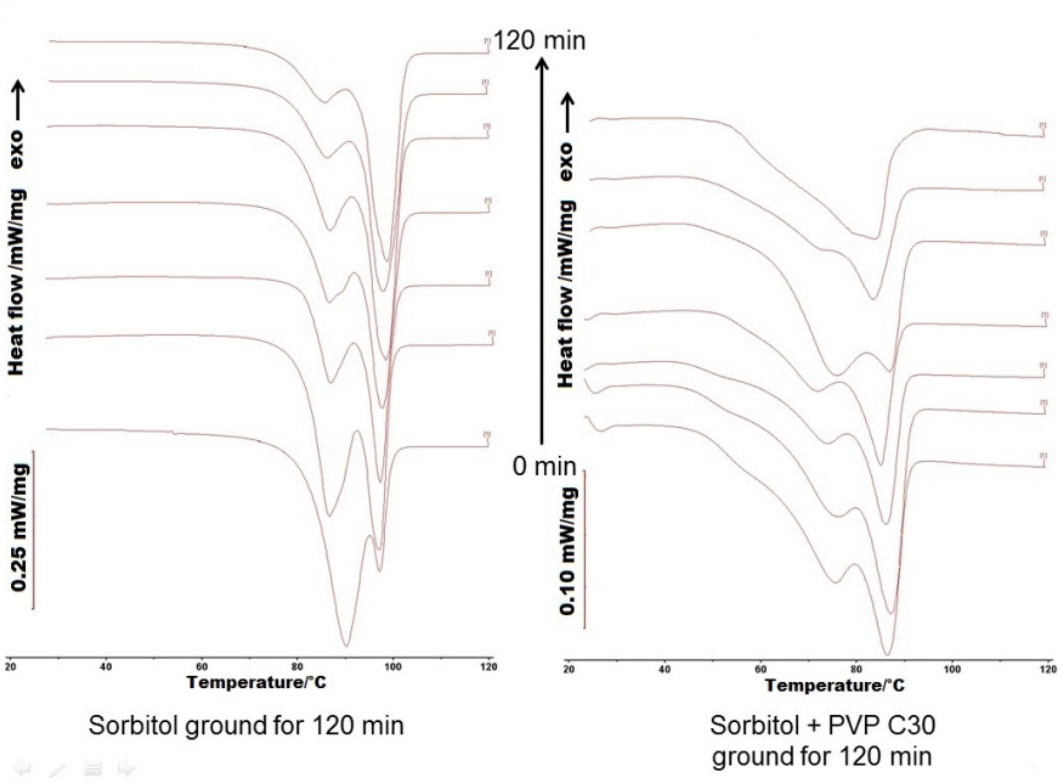

Figure 8 DSC curves of pure sorbitol grinding, and sorbitol ground with PVP C30

A similar phenomenon was observed in the DSC curves of sorbitol co-ground with PVP. The melting point of the sorbitol was lowered by the polymer excipient. Both polymorphs gave characteristic DSC curve. Similarly as when no additive was present, the epsilon polymorph amount decreased during the milling. In this case, the content of gamma polymorph also decreased, as demonstrated by the decrease of the area under the curve. The bulk part of the system lost its well-defined long-range order of the crystal structure.

The DSC investigation of sorbitol samples containing PEG did not show any significant change in crystallinity. The melting point of the semicrystalline polymer and the melting of sorbitol were to be seen in the curves. The areas under the melting peak of sorbitol varied only slightly during the milling (ΔH= 25.04 J g^{-1} ± 1.25 J g^{-1}), within the error of the measurement. No amorphization or polymorphic alteration was noted during the milling of these two materials.

To investigate the change in crystallinity of the co-ground sorbitol and to calculate the extent of amorphization, XRPD method was also carried out on the samples (Figure 9).

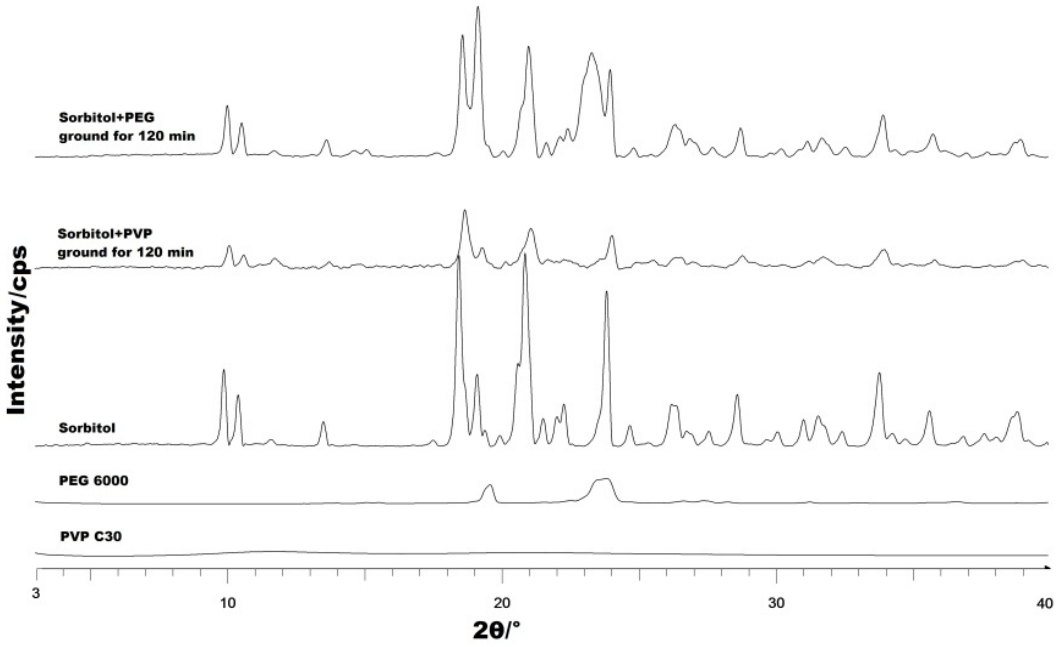

Figure 9 X-ray diffractograms of pure PVP C30, PEG 6000, and sorbitol; and sorbitol samples ground for 120 min with PVP C30 and PEG 6000.

The peaks of X-ray diffractograms of pure sorbitol were mostly characteristic of the epsilon form, though the peaks of the gamma form were also present. The determination of the polymorphs was based on the calculated X-ray powder diffractograms obtained from the Cambridge Crystallographic Data Centre (CCDC). During the milling process the areas under the peaks relating to the epsilon form noticeably decreased with milling time. In parallel the peaks of the gamma polymorph became slightly larger at a similar rate. This phenomenon which affected slightly more than 20% of the ground sorbitol could occur in two ways:

mechanical energy converted some of the material into the amorphous phase and the gamma form recrystallized from this; or the epsilon form was transformed directly to the gamma form.

A similar polymorph transition took place during the grinding of sorbitol with PVP: peaks relating to both polymorph forms were found in the diffractogram of the physical mixture. During the milling process, the areas under the peaks characteristic of the epsilon form decreased markedly (Figure 10).

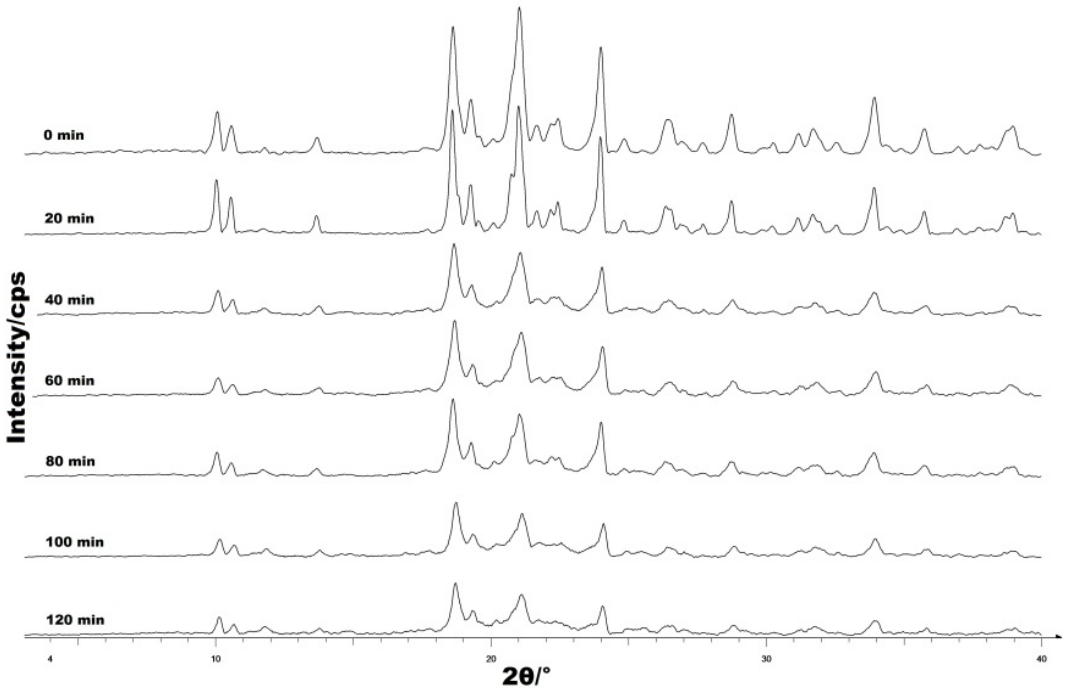

Figure 10 X-ray diffractograms of sorbitol samples ground with PVP (withdrawn every 20 min).

From the areas under the peaks of the epsilon form at 9.5-11° *2θ*, 23.15-24.53° *2θ* and 28.2-29.6° *2θ*, the degree of reduction in crystallinity was measured (Figure 11). During the first 40 min, the system lost about 50% of its well-defined crystal structure. After 40 min there was an apparent lag phase. At the end of the milling, slightly more than 30% of the sorbitol remained in the epsilon polymorph form. Most of the remaining 70% had lost its well-defined order of molecular packing and a minor part had been transformed into the gamma polymorph (Figure 12).

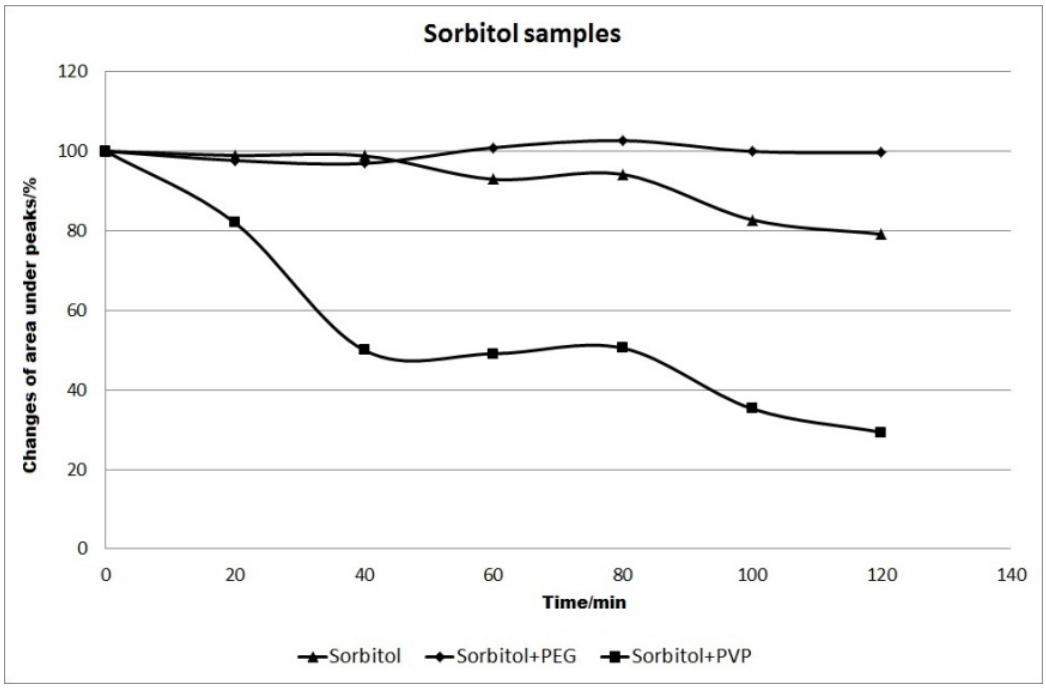

Figure 11 Crystallinity change of sorbitol and sorbitol ground with polymer additives as a function of milling time.

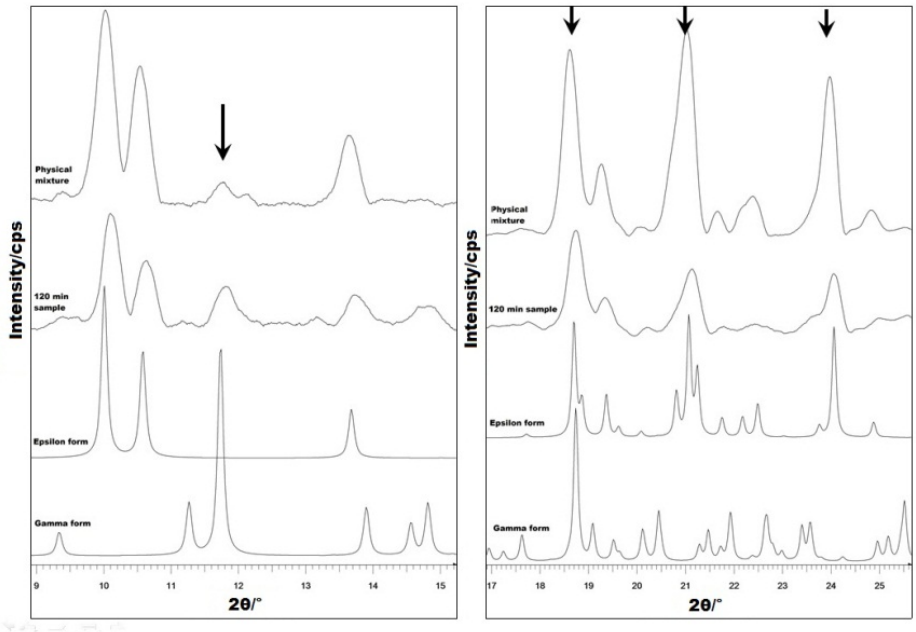

Figure 12 Polymorphic transition of sorbitol during milling with PVP excipient. While the amount of the epsilon form decreases with the milling time, the amount of the gamma form increased. Diffractograms of epsilon and gamma forms were acquired from the Cambridge Crystallographic Data Centre

Only the peak at 11.5-12.1° 2θ is clearly related to the gamma form. All the other peaks were characteristic either of epsilon form or of both polymorphs. This gamma sorbitol peak was used to evaluate the polymorphic transition. Figure 13 illustrates the decrease in the epsilon form and the increase in the gamma form with the increasing milling time. The figure has two "y" axes scaled differently to demonstrate the similar courses of the changes in proportions of the two polymorphs. There was a strong decrease in epsilon form initially, which was accompanied by a comparable rapid increase in the gamma form. After an apparent lag phase between 40 and 80 min both changes (increase in the gamma and decrease in the epsilon) continued similarly. This polymorph alteration was confirmed by the changes in the other peaks. Whereas the peaks clearly relating to the epsilon form (for example those at 23.15-24.53° *2θ* and 28.2-29.6° *2θ*) decreased continuously with increasing grinding time, the common peaks (at 18.1-19.1° *2θ*) diminished only slightly. All the changes observed are indicative of a constant crystallinity decrease as the milling time becomes longer, some of the sorbitol recrystallizing and changing into the gamma polymorphic form during the process.

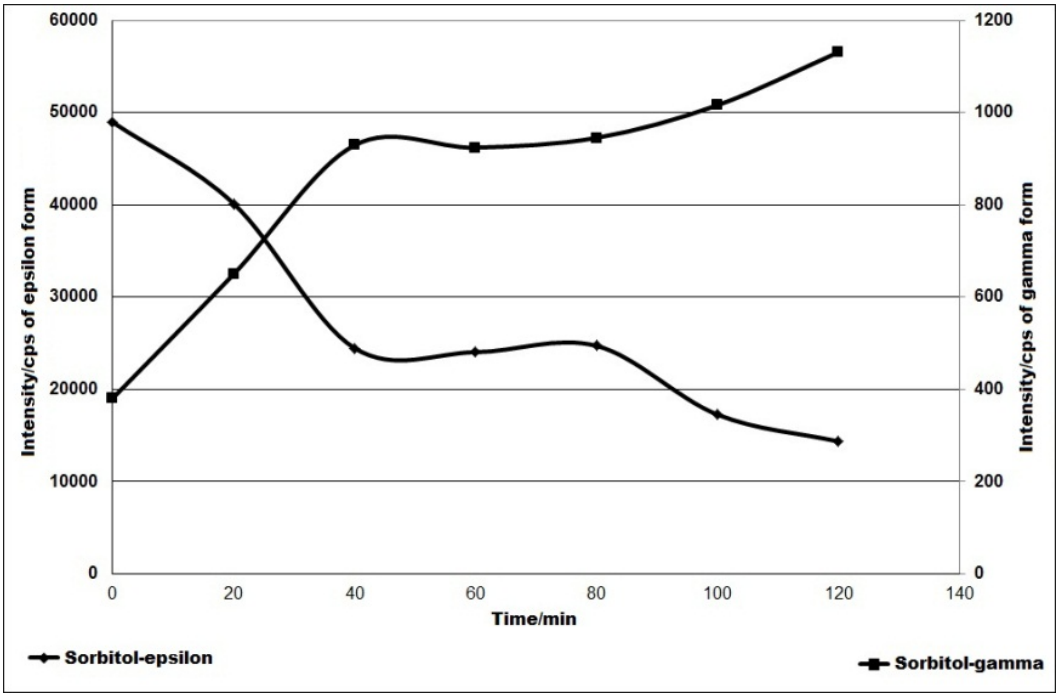

Figure 13 Crystallinity change of different sorbitol polymorphs. The left "y" axis is for the epsilon form, the right one is for the gamma form. The diagram shows the similar course of the decrease of the epsilon and the increase of the gamma form.

The samples containing PEG displayed different behaviour during mechanical activation. The degree of crystallinity changed by around 100% during the overall procedure. The sorbitol did not suffer any loss in crystal structure. As the sorbitol itself did lose its crystallinity noticeably in the absence of excipient, it can be concluded, that PEG stabilized the crystal structure of this sugar alcohol and helped it maintain its crystallinity. No polymorphic transformation was detected in the X-ray pattern.

6.2. Investigation of crystallinity changes of MX

MX was selected as model API because it has only a low tendency to occur in amorphous phase: T_g/T_m (K/K) is 0.63. The polymers were PVP and PEG. We set out to quantify the decrease in crystallinity in time and to detect any bonding formed between the MX and the polymers.

6.2.1. X-ray diffraction

Figures 14 shows the diffractograms of the samples prepared. In each graph, the characteristic peaks of MX can be observed. As PEG is semi-crystalline, it gives a large peak, with a considerable full width at half-maximum, while PVP is fully amorphous, so it does not yield any signal in the diffractograms. At 31.6° 2θ, the specific peak relating to NaCl appears. Figure 14a (PEG 6 000) demonstrates that no amorphization occurred during the co-grinding process: the areas under the peaks did not decrease radically. The samples prepared with the PVPs behaved differently: the areas under the peaks continuously decreased as the grinding time was lengthened (Figure 14b (PVP C30)). Although the drugs were not converted completely into the amorphous form, because the diffractograms exhibited small peaks in the amorphous halo, the change in crystallinity was drastic. During the co-grinding process, no other polymorphic form of MX appeared: no shift in the peaks and no new peaks were observed in the pattern.

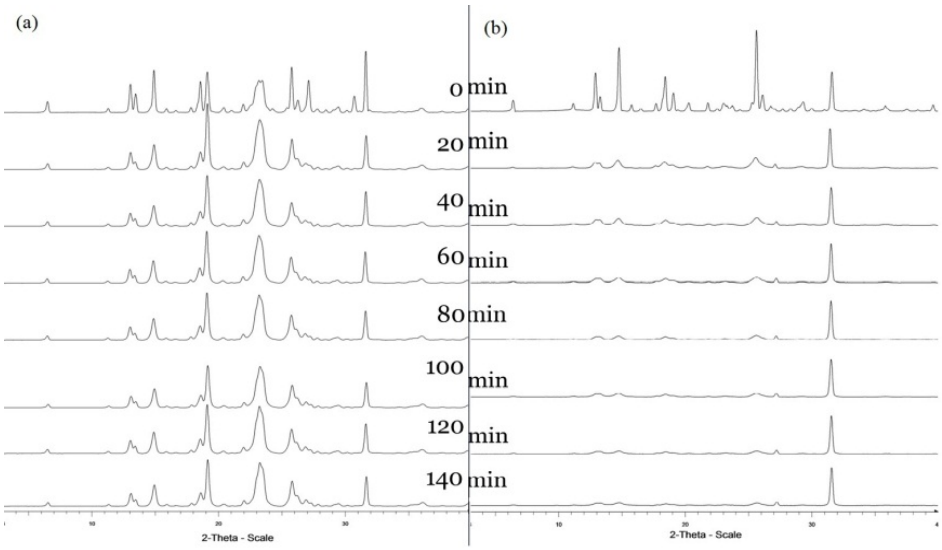

Figure 14 XRPD diffractograms of MX mixed with PEG 6000 (a) and PVP C30 (b).

To quantify the changes in time, the areas underneath the diffractograms were determined between 12° and 30° *2θ* after Kα2-stripping, background removal and curve smoothing. The areas under the peaks relating to MX were divided by the areas under the peaks of NaCl. These values are illustrated in Figure 15, which shows the crystallinity changes based on the areas under the peaks. The samples made with PEG did not undergo any amorphization. The long-range order of molecular packing remained. The diversity of the values may be caused by the variation in particle size, and the orientation of the larger particles. Samples involving the use of PVP as grinding material lost their well-defined molecular conformation. The areas under the peaks decreased on increase of the grinding time. For PVP C30 12.23% of the MX remained in crystalline form at the end of the grinding process.

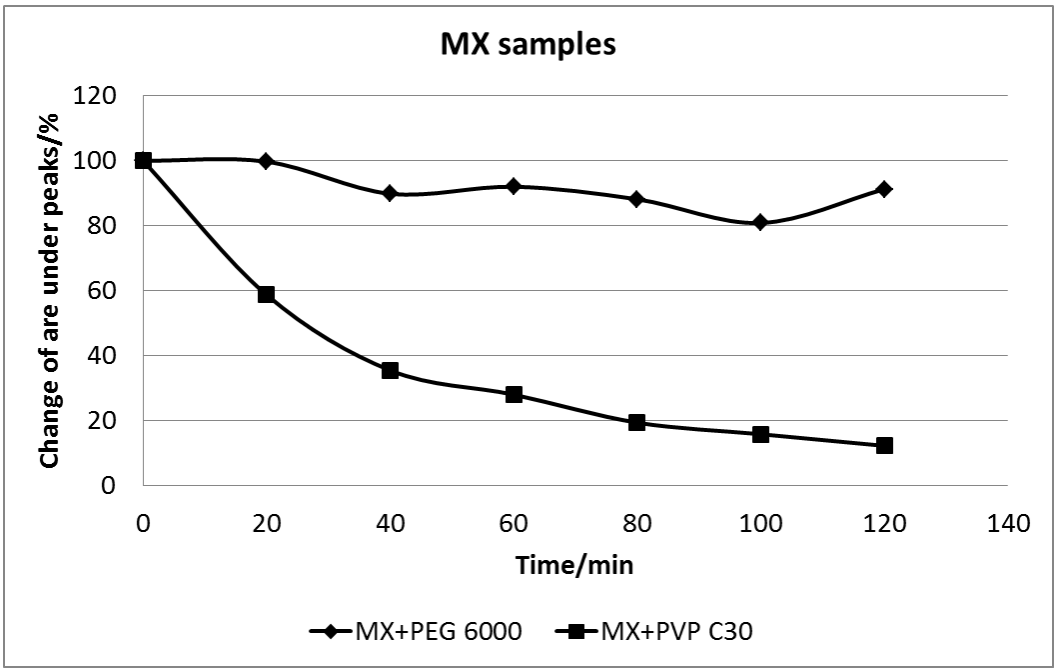

Figure 15 Crystallinity changes of the samples

6.2.2. FT-IR spectroscopy

To determine whether any decomposition occurred during the grinding process and to search for any possible bonding between the API and the polymers, FT-IR spectroscopy was carried out. This proved that no disintegration took place in any of the samples. The characteristic bands of MX were seen in all of the curves.

No measurable changes were observed in the case of the products made with the PEGs. No shifts, no changes in band shape and no new bands were detected in the curves. This means that bonds between the materials were not created by grinding. Changes in the intensities of the peaks can be explained by the decreasing particle size of the products.

The samples made with the PVP polymers exhibited several changes in the spectra during the grinding process (Figure 16), most significantly in the interval 3725-2600 cm^{-1}. At 3400-3500 cm^{-1}, the intensity of the associated ν*OH* mode increased with increasing grinding time. A similar increase was observed in the range of CH and NH valence vibrations, between 3000 and 2800 cm^{-1}. The separation of the two ranges is impracticable.

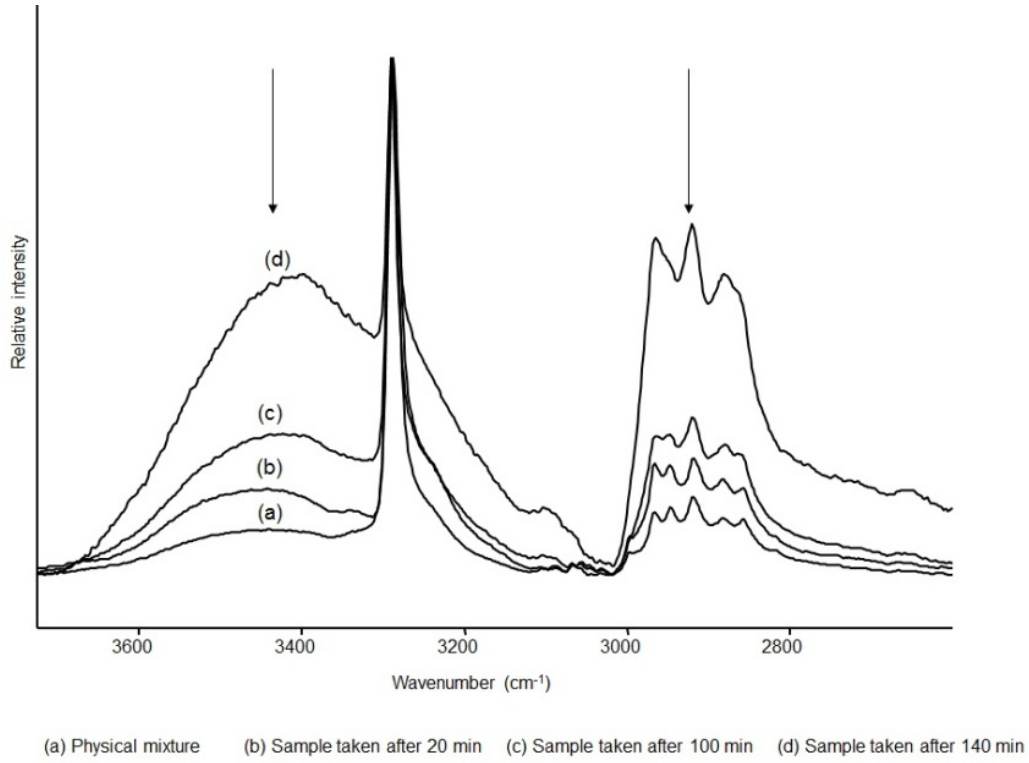

Figure 16 FI IR spectra of samples made with PVP C30. The arrows show increasing intensity at 3400-3500 cm^{-1} and between 3000 and 2800 cm^{-1}.

The most significant changes for both excipients are related to the secondary amide group of MX. Increases in intensity can be observed at around 1620 cm^{-1} (νCONH) and between 1550 cm^{-1} and 1530 cm^{-1} (νNH). Further, the intensity relating to a hybrid stretching mode at around 1440 cm^{-1} is increased and a shoulder grows around 1390 cm^{-1} (Figure 17).

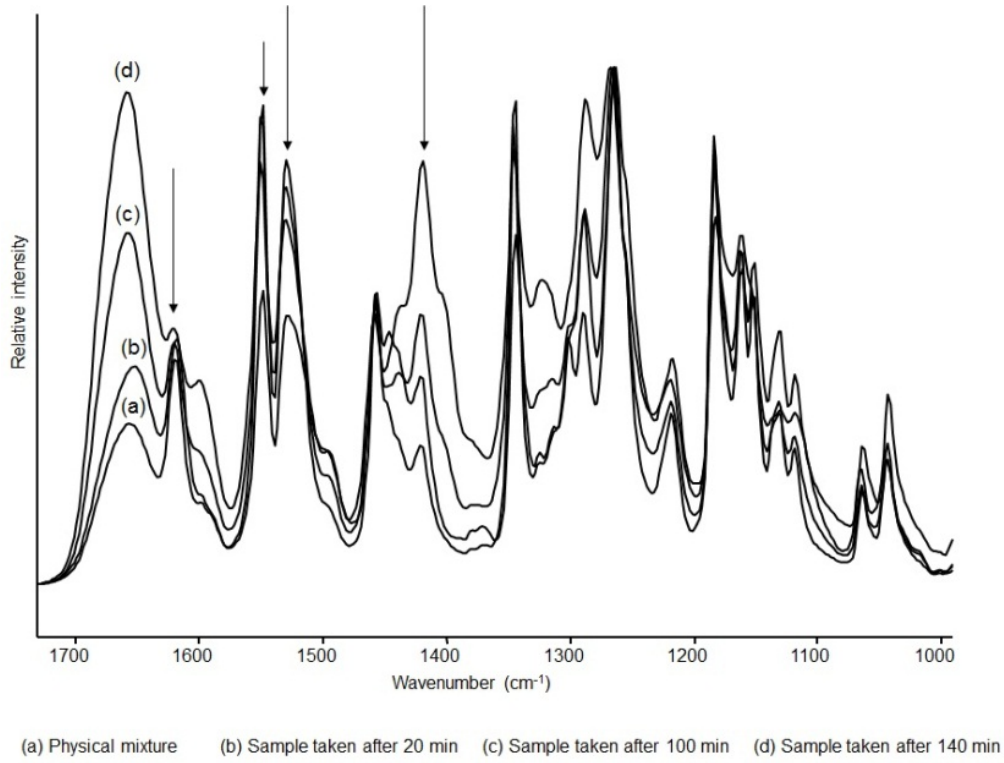

Figure 17 FI-IR spectras of the samples made with PVP C30. The arrows indicate changes related to secondary amide groups. Increasing intensities can be observed around 1620 cm^{-1} (vCONH) and between 1550 cm^{-1} and 1530 cm^{-1} (vNH).

All these alterations point to the presence of weak bonding between the carboxyl group of MX and the polymers, which is able to help the molecules to separate from each other and keep them in this (not well-defined) conformation.

6.2.3. SEM

Differences between the abilities of the polymers to decrease the crystallinity of MX can also be seen in the SEM photomicrographs. Figure 18 presents SEM pictures of physical mixtures and samples (ground for 140 min) made with PEG 6000 and PVP C30. PEG has relatively low melting points, which were exceeded during the co-grinding process (the temperature of the mortar was not higher than 55 °C). The polymers are locally melted by the impact and friction of the balls in the mortar. Reduced-sized MX particles can be observed in the melt of the polymer. These particles are in the nano range.

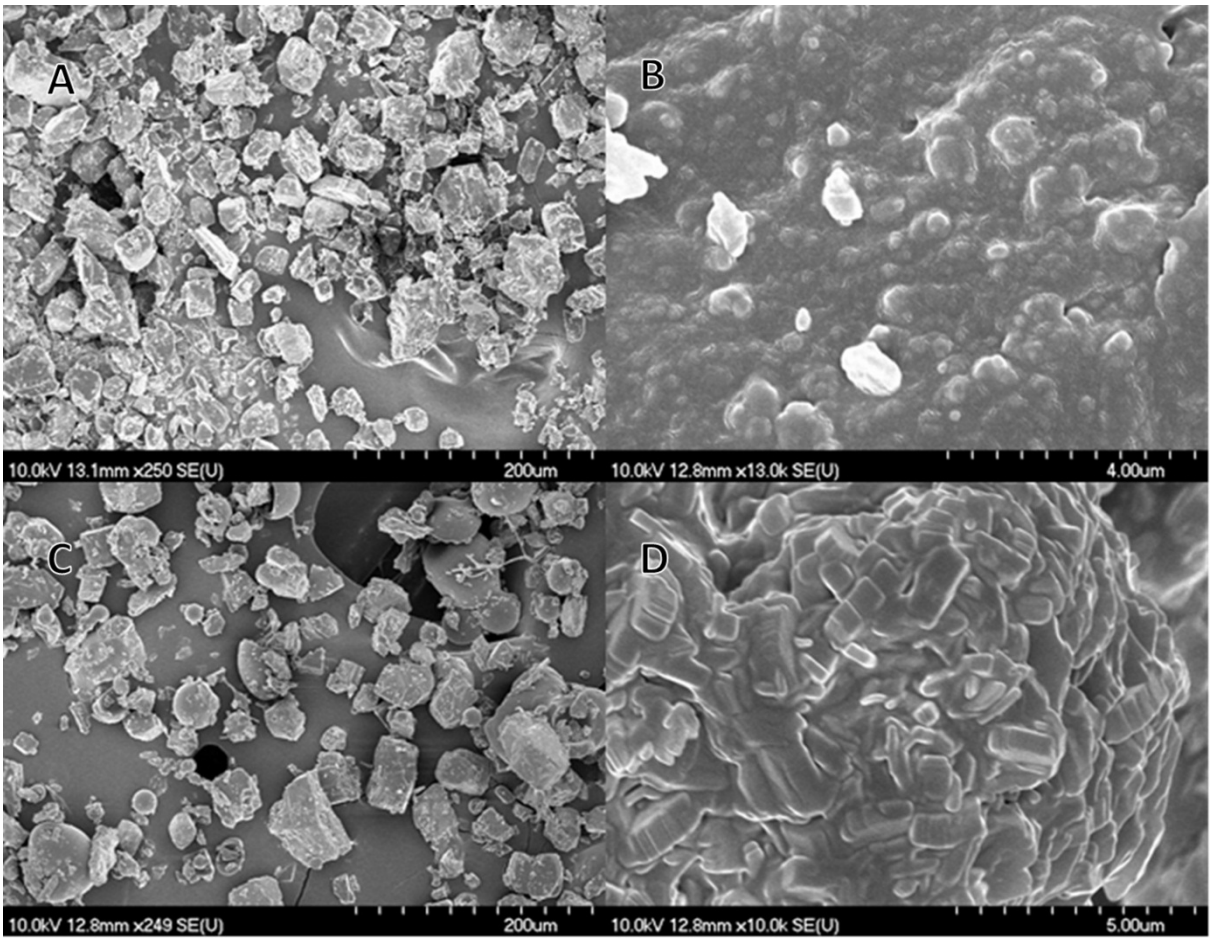

Figure 18 SEM photomicrographs of samples made with PEG 6000 (A: physical mixture, B: sample ground for 140 min) and PVP C30 (C: physical mixture, D: sample ground for 140 min)

PVPs are amorphous polymers, and did not melt during the milling process. The temperature was locally higher than the T_g of the excipients, so the polymers softened and coated the amorphized MX. These MX particles more or less preserved their contour while they were decreased to the nano level.

To identify the habit of the MX particles formed by the co-grinding with the polymers, the water-soluble excipients were extracted from the system by washing-out with cold distilled water, and the material was centrifuged three times. By this method, the water-insoluble MX [the solubility of MX is 4.4 ± 0.7 μg mL^{-1} (Ambrus et al., 2009)] can be observed individually. The SEM images of the samples made with PEG (Figure 19A) revealed well-formed crystalline MX particles with sharp edges. The shape and position of the particles indicate recrystallization. The MX molecules could dissolve in the melted PEG

polymer, but immediately following the decrease of temperature, the MX precipitated out from the dispersion, forming crystalline particles. The samples made with the PVPs did not give sharp lines, but formed a shapeless amorphous mass (Figure 19B).

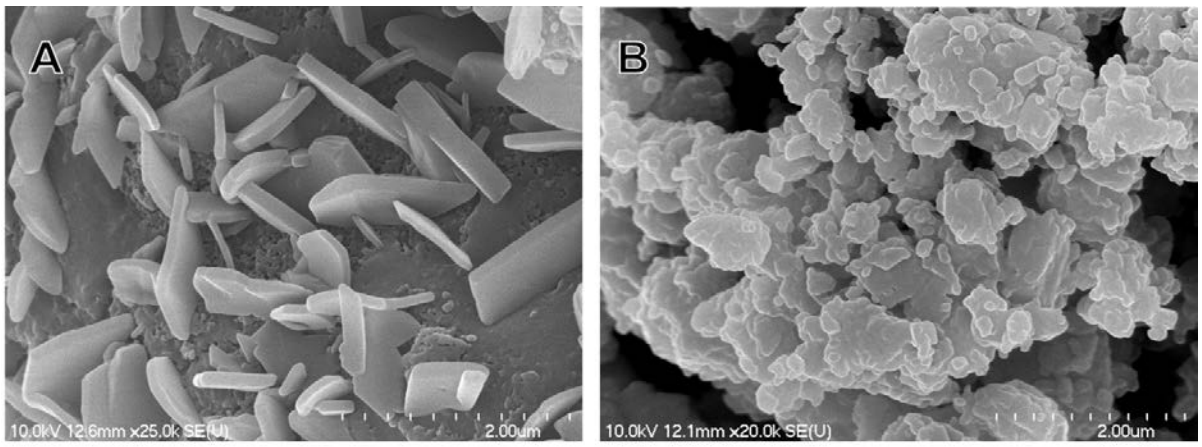

Figure 19 MX particles, water-soluble polymer additives: PEG 6000 A; and PVP C30 B removed.

6.3. Investigation of crystallinity change of CLP

CLP was chosen as a model API, as it has a relatively high melting point, and did not melt in the milling chamber and it has a really high tendency to exist in amorphous form. Its T_g/T_m (K/K) ratio is 0.80. Aerosil 200 was used as carrier because of its amorphous properties, with neither any thermal sign, nor any peak in the XRPD diffractograms and its excellent properties as a crystallization inhibitor was cited (Chauhan et al., 2005; Watanabe et al., 2001).

6.3.1. DSC determination

As thermal analysis techniques are widely used in the characterization of the amorphous form, the intact CLP, Aerosil 200 and the prepared samples were investigated by DSC. The curve of the raw CLP gave a characteristic sharp peak at 181.20 °C, corresponding to the melting point of the material. No other changes were observed on the curve, which means that the CLP contained no moisture or any residual solvent. The Aerosil 200 (as an amorphous additive) did not exhibit any thermal signal so it was practically amorphous and contained no moisture or any r residual est solvent either.

The curves of the samples indicated the endothermic peak of the melting point of CLP in each case, except that at 240 min (Figure 20). The area of the peak decreased with

increasing grinding time until it practically disappeared after 240 min of grinding. The peak of the physical mixture was similar to the peak of the raw CLP, but with a smaller area. This indicates the decreasing crystallinity of the CLP, which was finally converted into the amorphous phase. The peaks are shifted slightly to lower temperatures during the grinding while a peak was observed at 80 °C after 120 min of grinding.

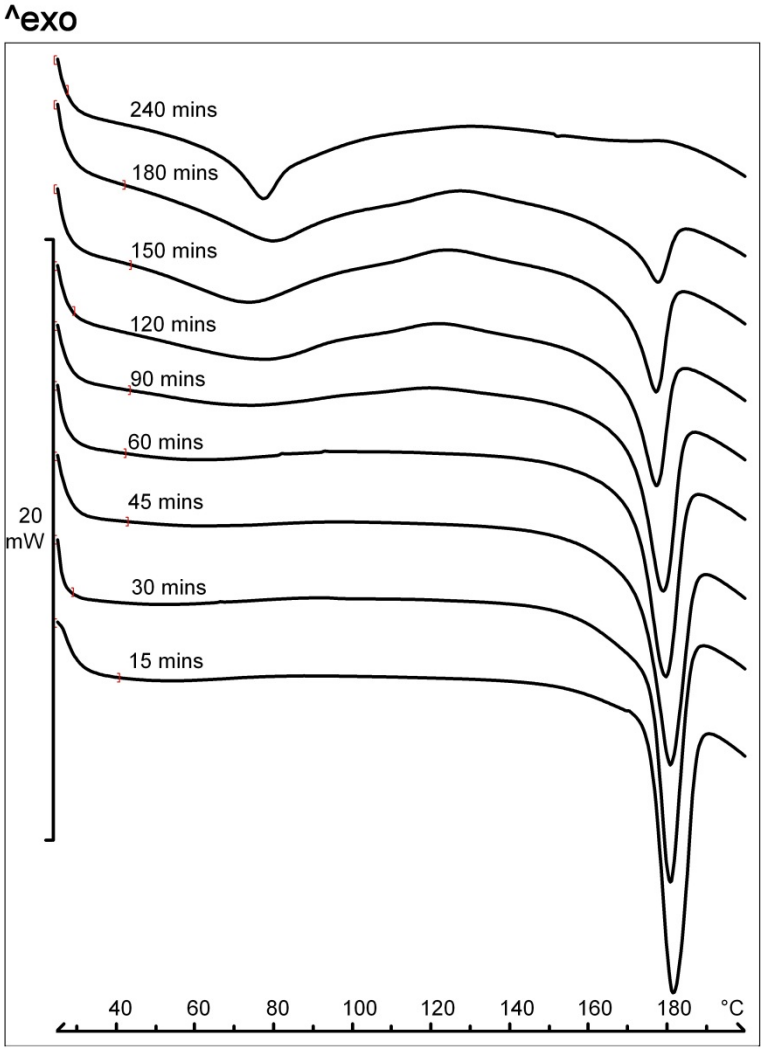

Figure 20 DSC determination of samples. The endothermic peak of CLP appears in each curve, and the areas under the peaks decreased with the grinding time.

It was impossible to determine the accurate area under each curves because of the imprecise pre- and post-baseline fittings of the melting peaks. The DSC method was not applicable for further semiquantitative determination.

6.3.2. X-ray diffraction

XRPD is an appropriate method with which to determine the crystallinity of materials. The X-ray pattern of the raw CLP exhibits characteristic high-intensity diffraction peaks, which demonstrates the crystalline nature of the unprocessed API. Comparison of the results on the CLP used and the data recieved from the Cambridge Crystallographic Data Centre (CCDC ID: AI631510) proved, that our API was in polymorphic form II. The pattern of the Aerosil 200 does not show any peaks in the measured interval, which means that the excipient was practically amorphous.

The typical peaks of the CLP emerged clearly in the diffractograms of the ground products (Figure 21). The intensities of these peaks were lower than those of the peaks for the raw API, corresponding to the concentrations of the materials in the samples. The amorphous Aerosil 200 did not exhibit any further reflection. The intensities of these peaks decreased with increasing grinding time and practically disappeared after co-grinding for 240 min. The diffractogram of the last sample displayed the amorphous halo. During the co-grinding process, no other polymorphic form of the CLP appeared, no shifting of the peaks occurred, and no any new peaks were observed in the pattern.

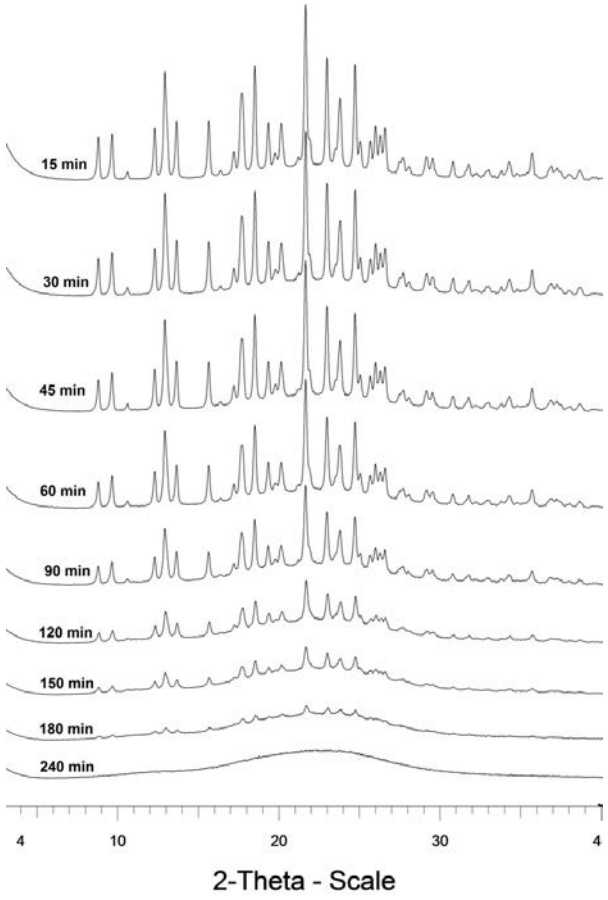

Figure 21 XRPD diffractograms of samples. The characteristic peaks of CLP decrease with the increasing grinding time. The last sample (240 min) shows no peaks, so it is practically amorphous.

Quantification of the crystallinity decrease is illustrated in Figure 22 which shows that of the crystallinity decreased sigmoidally with increase of the grinding time. The rise in the fitted trendline relates to the rate coefficient of formation of the amorphous product (the regression line equation is $y = -0.0233x + 1.619$ $R^2 = 0.9935$).

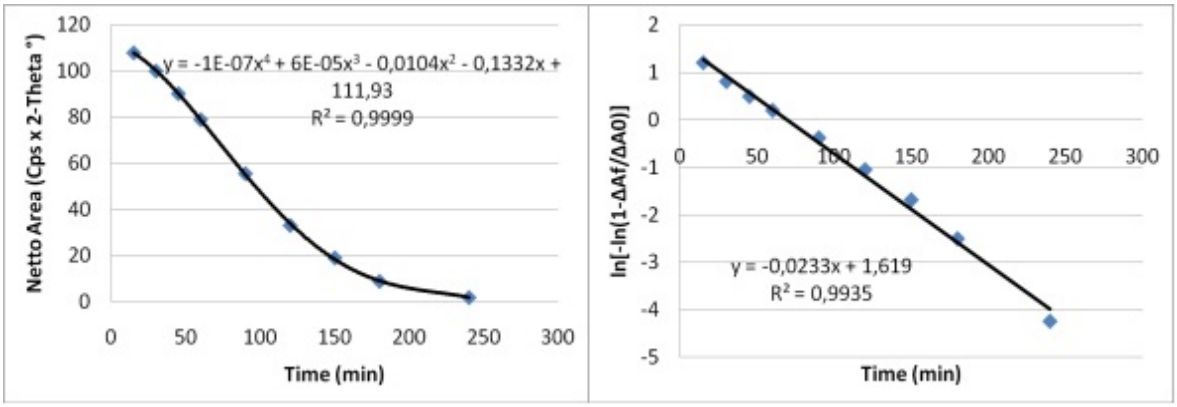

Figure 22 Crystallinity changes during grinding. First function shows the area under the curves decreasing with increasing grinding time; the second function is the linearization of the first.

This phenomenon revealed that the crystallinity of the products started to decrease slowly. After a certain time had elapsed, the decrease became faster, and at the end of the procedure the curve of the amorphization flattened. This phenomenon can be caused by in-process secondary bonding formation between the API and the excipient, because the formation of the bond is an energy-intensive process.

6.3.3. TG and hot-humidity stage XRPD

The curves of the samples ground for more than 120 min demonstrated an endothermic peak at 80 °C. The area under this peak increased and sharpened with increasing grinding time. To identify the source of the peaks, the last sample (ground for 240 min) was investigated by TG and hot-humidity stage XRPD.

The TG curve revealed, that the product was thermodynamically stable and a mass decrease of only 3,33% was detected up to the melting point of the CLP (Figure 23). At 80 °C, the determination did not show a salient mass decrease, which means that the peak observed in the DSC pattern did not involve dissolution or solvent evaporation. Neither was any major decrease observed at 100 °C, which means that the sample was sufficiently dry.

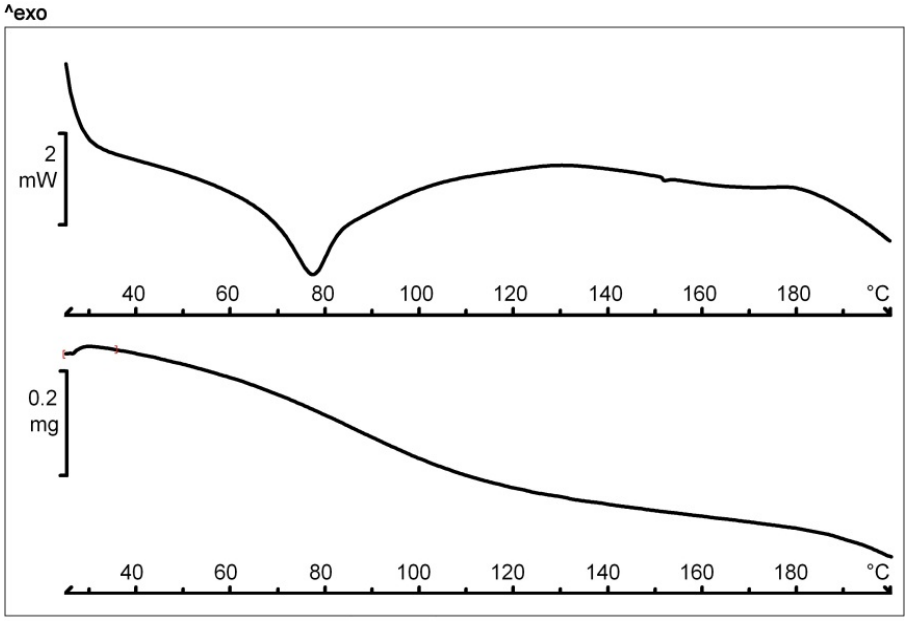

Figure 23 DSC and TG determination of sample ground for 240 min. No major mass decrease is detected at 80 °C, or at 100 °C.

The last sample (ground for 240 min) was determined by XRPD, using the hot-humidity chamber at room temperature (25 °C), at the temperature of the peak (80 °C) and at a

temperature higher than the peak (95 °C). The diffractograms showed an amorphous halo in all three cases, so this peak did not relate to any change in crystallinity (Figure 24).

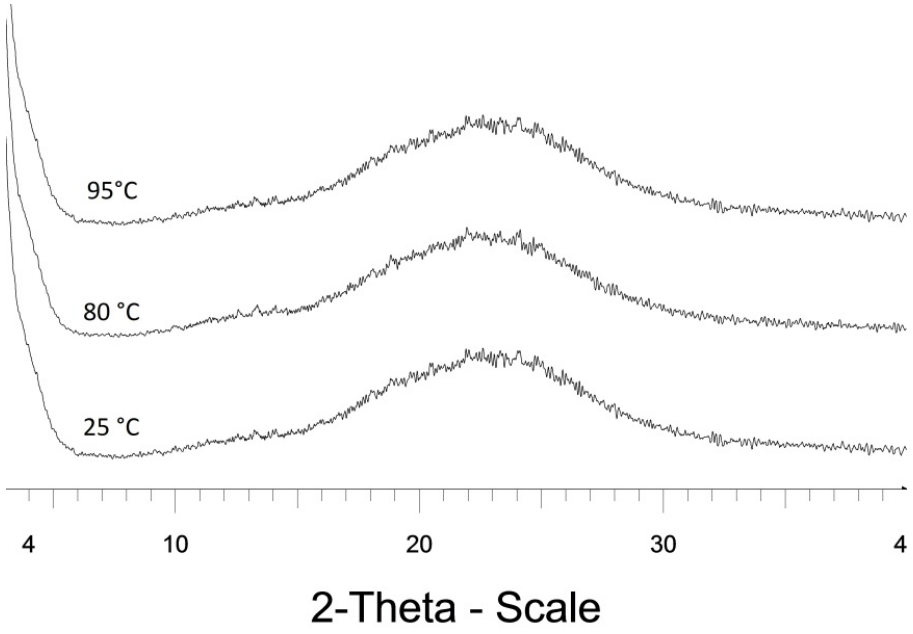

Figure 24 Hot-XRPD diffractograms of samples ground for 240 min at 25°C, 80 °C or 95°C. Each diffractogram shows the amorphous halo. No changes in the crystallinity occured at these temperatures.

The outlined phenomenon could be emerging secondary bonding between the API and the additive. The endothermic peak detected at 80 °C indicated the spliting of the bond. At higher temperature the CLP-Aerosil 200 complex broke down, giving a solid dispersion of the two independent materials.

6.3.4. FT-IR spectroscopy

FT IR spectroscopy is a suitable method for the investigation of interactions between pharmaceutical materials and polymers. For FT IR determination the ATR method was chosen, because sample preparation, such as particle size reduction or KBr tableting, which would expose the samples to further physical stress, is unnecessary.

FT IR determination showed that the grinding process caused several small changes in the spectra of the samples. One of the most spectacular changes was seen at 1752 cm^{-1}, the region of the νC=O valence vibration of CLP. These peaks of the samples ground for more than 120 min expanded, shifted to lower wavenumbers, and slightly increased in intensity with increase of the grinding time (Figure 25).

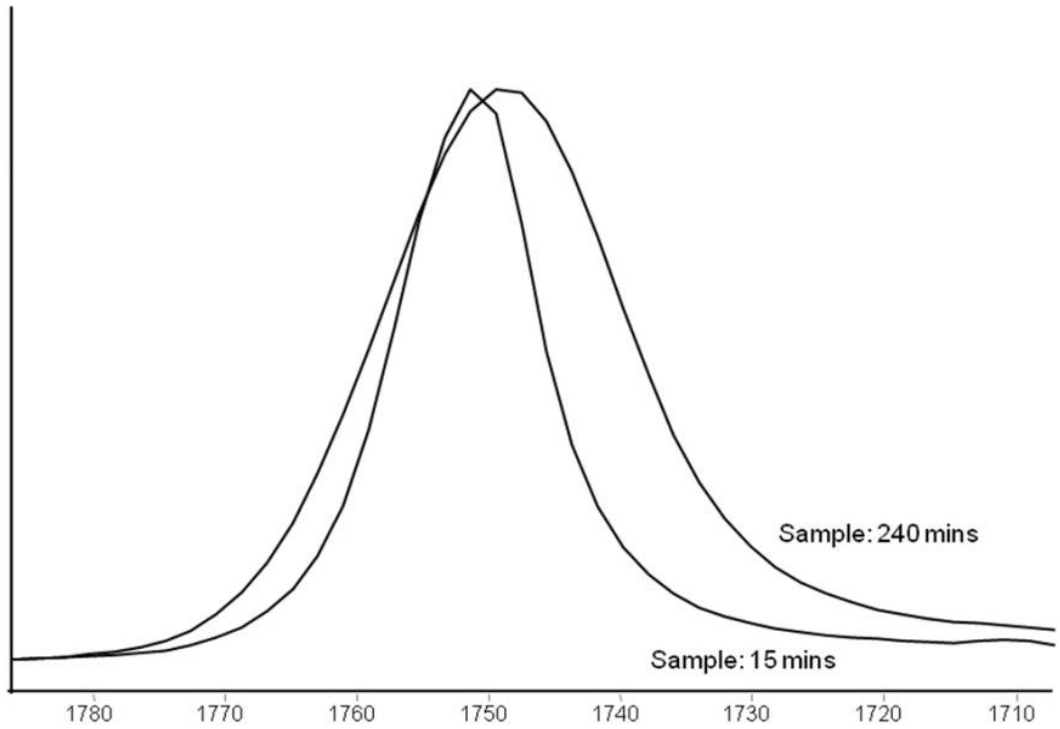

Figure 25 FT-IR investigation of samples ground for 15 min or 240 min. The area under the peak at 1750 cm^{-1} increased, and the peak shifted to lower wavenumbers.

Another change was observed at 865 cm^{-1} where a band with high intensity started to decrease after 120 min of grinding, while a double peak at 858 cm^{-1} and 838 cm^{-1} fused into one peak with a higher intensity (Figure 26). These changes proportionally followed the changes at 1752 cm^{-1}. The same phenomenon was observed between 1200 cm^{-1} and 1135 cm^{-1}: the peak at 1188 cm^{-1} decrease, while the peak at 1150 cm^{-1} slightly increased parallel after 120 min of co-grinding.

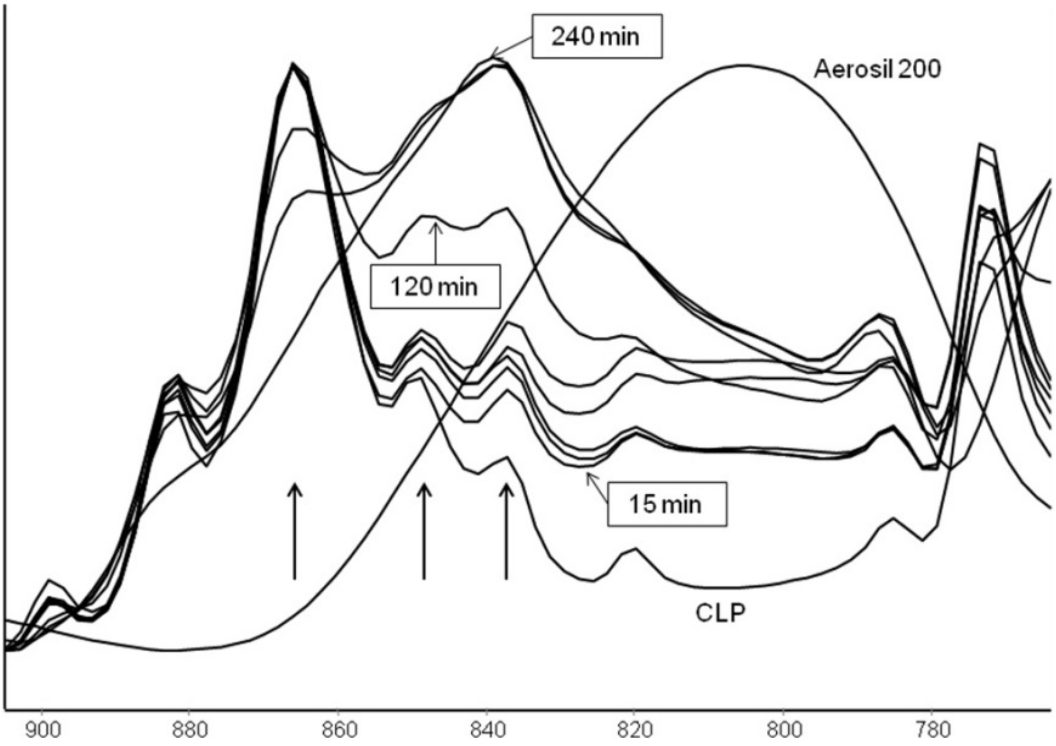

Figure 26 The bands of Aerosil 200, CLP and 9 samples ground for from 15 min to 240 min. The area under the peak at 865 cm^{-1} decreased after 120 min of grinding, while the double peak at 858 cm^{-1} and 838 cm^{-1} fuse into one peak with a higher intensity.

The described changes can refer to the following processes: the CLP first temporarily melts forming a molecularly disperse system. After 120 min of grinding, a weak secondary bond appears between CLP and the silanol groups of the CLP. This bond is strong enough to keep the CLP in amorphous phase. The work of our team (Jójárt-Laczkovich & Szabó-Révész, 2011), demonstrated that this secondary bond is a hydrogen-bond.

7. Summary, novelty and practical relevance

1. Our first aim, to establish the literature background of investigation methods which are suitable to follow changes in crystallinity of organic materials with small molecule weights was accomplished: all of the widely used investigation methods were learnt and practiced. Those that were most suitable for our aims were chosen and used.

2. An easy and rapid method, which is able to predict the glass-forming properties of given materials were applied: DSC method was carried out, with only a small amount of material and two heatings were needed to determine the glass-forming properties of each material. It was therefore quite simple to choose between the possible substances: two sugar-alcohols, which are widely used in pharmaceutics, were selected: although they are chemically equivalent, they have different tendencies to exist in amorphous form. Interesting APIs were investigated: MX, although considered poor glass-former readily occurs in amorphous form, and CLP with its relatively high T_g/T_m ratio needed a long-term grinding with Aerosil to amorphize completely. The method used, which was suitable to decrease the degree of crystallinity of the chosen materials was relatively cheap. Its most important advantage was it repeatability and feasibility.

3. First, two chemically equivalent sugar-alcohols (mannitol and sorbitol) as model materials were subjected to milling both alone and in the presence of polymer excipients (PVP C30 and PEG 6000) to accentuate the differences in behavior of analogous materials. As a poor glass-former, mannitol did not exhibit any decrease in crystallinity when it was milled alone or together with PEG. In the presence of PVP, the crystal structure of mannitol was slightly lost. When ground alone or together with PVP, sorbitol suffered amorphization and it underwent polymorph transformation when co-ground: the initial, mostly epsilon form was transformed continuously into the gamma form, while parallel lost more than 70% of its crystallinity. PEG preserved the well-ordered molecular packing of sorbitol and stabilized the crystal structure so that the sorbitol could not amorphize. It can be concluded that these sugar alcohols, which have the same chemical structure, demonstrated different rates of crystallinity loss.

4. A similar effect of polymers was proved by the grinding of MX: the work demonstrated that the polymers used to reduce the grinding energy during co-grinding to nanoparticles can decrease the crystallinity of MX. These polymers have different abilities to convert the drug into amorphous form. XRPD measurements confirmed that the PEG did not have a significant effect on the crystallinity of MX, while the PVP decreased it drastically. Weak secondary bonding between MX and the PVPs was found by FT IR. The SEM images confirmed the major particle size decrease and the differences in crystal behaviour of the samples made with the different polymers.

5. Finally, raw, crystalline CLP was amorphized by co-grinding. It was found that the crystallinity decreased sigmoidally with increasing co-grinding time. XRPD and DSC examinations confirmed that the product had become totally amorphous after a relatively long time, 240 min of grinding. No polymorphic conversion was observed in the samples. TG proved that no major mass reduction occurred during the procedure. FT IR changes indicated the formation of a secondary bond between CLP and Aerosil 200, which is able to keep the drug in the amorphous phase.

Finally it can be concluded, that so similar molecules as two chemically equivalent sugar-alcohols can behave completely different on effect of grinding. The study also revealed the possibility of polymorph transition, which can lead to issues in physical appearance, dissolution or stability.

It was proven, that organic APIs, which amorphization inclination were predicted as different, can react similarly to a high energy intake: two material with dissimilar tendency to present in amorphous form exhibited comparable reaction to the co-grinding process.

Important properties of excipients used as co-grinder additives were revealed too. Some of the materials can support amorphization by decreasing the energy devoted to grinding or stabilizing the molded amorphous dispersion. Meanwhile some of them can prevent the API from crystallinity loss by coating the particles and protect their structure from breaking down.

References

Aaltonen J., Allesø M., Mirza S., Koradia V., Gordon K. C., Rantanen J. Solid form screening - A review. *Eur. J. Pharm. Biopharm*. (2009) 71, 23-37.

Aigner Z., Berkesi O., Farkas G., Szabó-Révész P. DSC, X-ray and FTIR studies of a gemfibrozil/dimethyl-β-cyclodextrin inclusion complex produced by co-grinding *J. Pharm. Biomed. Anal.* (2012) 57, 62–67.

Al-Marzouqi A. H., Jobe B., Dowaidar A., Maestrelli F., Mura P. Evaluation of supercritical fluid technology as preparative technique of benzocaine-cyclodextrin complexes--comparison with conventional methods. *J Pharm Biomed Anal*. (2007) Jan 17;43(2):566-74.

Ambike A. A., Mahadik K. R., Paradkar A. Stability study of amorphous valecoxib. *Int. J. Pharm*. (2004) 282, 151-162.

Ambrus R., Kocbek P., Kristl J., Sibanc R., Rajkó R., Szabó-Révész P. Investigation of preparation parameters to improve the dissolution of poorly water-soluble meloxicam. *Int. J. Pharm.* (2009) 381(2), 153-159.

Ambrus R., Radacsi N., Szunyogh T., E.D.M. van der Heijden A., J. H. ter Horst, Szabó-Révész P., Analysis of submicron-sized niflumic acid crystals prepared by electrospray crystallization *J. Pharm. Biomed. Anal.* (2013) 76, 1–7.

Bialleck S., Rein H. Preparation of starch-based pellets by hot-melt extrusion. *Eur. J. Pharm. Biopharm.* (2011) 79(2), 440-8.

Bozic D. Z., Dreu R., Vrecer F. Influence of dry granulation on compactibility and capping tendency of macrolide antibiotic formulation. *Int. J. Pharm.*, (2008) 357, 44–54.

Carpentier L., Desprez S., Descamps M., Crystallization and glass properties of pentitols. Xylitol, adonitol, arabitols. *J. Therm. Anal. Calorim.* Vol. (2003) 73, 577-586.

Cavatur R. K., Vemuri N. M., Pyne A., Chrzan Z., Toledo-Velasquez D., Suryanarayanan R., Crystallization Behavior of Mannitol in Frozen Aqueous Solutions. *Pharm. Res.* (2002) 19:6.

Chauhan B., Shimpi S., Paradkar A. Preparation and evaluation of glibenclamide-polyglycolized glycerides solid dispersions with silicon dioxide by spray drying technique. *Eur. J. Pharm. Sci.* (2005) 2, 219-230.

Chen H., Khemtong C., Yang X., Chang X., Gao J., Nanoization strategies for poorly-water soluble drugs. *Drug Discov. Today*, (2011) 16, 354–360.

Choi H, Lee W, Kim S. Effect of grinding aids on the kinetics of fine grinding energy consumed of calcite powders by a stirred ball mill. *Adv. Powder. Technol.* (2009) 20, 350–354.

Craig D. Q.M., Royall P. G., Kett V. L., Hopton M. L., The relevance of the amorphous state to pharmaceutical dosage forms: glassy drugs and freeze dried systems. *Int. J. Pharm.* (1999) 179, 179–207.

Dai W. G., Dong L. C., Song Y., Enhanced bioavailability of poorly absorbed hydrophilic compounds through drug complex/in situ gelling formulation. *Int. J. Pharm.* (2013) 457, 63–70.

Fukuoka E., Makita M., Yamamura S., Some physicochemical properties of glassy indomethacin. *Chem. Pharm. Bull.* (1986) 34, 4314–4321.

G. E. M. Jauncey The Scattering of X-rays and Bragg's Law *Proc. Natl. Acad. Sci. USA.* (1924) 10, 57–60.

Gombás Á., Szabó-Révész P., Regdon G. jr., Erős I, Study of thermal behaviour of sugar alcohols. *J. Therm. Anal. Calorim.* (2003) 73, 615-621.

Gordon M., Taylor J. S. Ideal copolymers and the second-order transitions of synthetic rubbers. *J. Appl. Chem*. (1952). 2, 493-500.

Guguta C., Meekes H., de Gelder R. The hydration/dehydration behavior of aspartame revisited. *J. Pharm. Biomed. Anal*. (2008) 46, 617-24.

Hamishehkar H., Emami J., Najafabadi A. R., Gilani K., Minaiyan M., Mahdavi H., Nokhodchi A. Effect of carrier morphology and surface characteristics on the development of respirable PLGA microcapsules for sustained-release pulmonary delivery of insulin. *Int. J. Pharm.* (2010) 389, 74-85.

Hancock B.C., Shamblin S.L., Zografi G., Molecular mobility of amorphous pharmaceutical solids below their glass transition temperatures. *Pharm. Res.* (1995) 12, 799–806.

Hancock B.C., Zografi G. Characteristics and significance of the amorphous state in pharmaceutical systems. *J. Pharm. Sci.* (1997) 86, 1-12.

Hancock B. C., Parks M. What is the True Solubility Advantage for Amorphous Pharmaceuticals? *Pharm. Res*. (2000) 17, 397-403.

Hanft G., Türck D., Scheuerer S., Sigmund R. Meloxicam oral suspension: a treatment alternative to solid meloxicam formulations. *Inflamm. Res.* (2001) 50, S35-S37.

Hatley R.H.M., Glass fragility and the stability of pharmaceutical preparations – excipients selection. Pharm. Dev. Technol. (1997) 2, 257–264.

Hédoux A., Paccou L., Guinet Y., Willart J. F., Descamps M. Using the low-frequency Raman spectroscopy to analyze the crystallization of amorphous indomethacin. *Eur. J. Pharm. Sci*. (2009) 38, 156-64.

International Conference on Harmonization, Technical Requirements for Registration of Pharmaceuticals for Human Use. Validation of Analytical Procedures: Text and Methodology. Analytical Validation Q2/R1 December (1996), issued as CPMP/ICH281/95.

Jójárt-Laczkovich O., Szabó-Révész P., Amorphization of a crystalline activepharmaceutical ingredient and thermoanalytical measurements on this glassy form. J. *Therm. Anal. Calorim.* (2010) 102, 243–247.

Jójárt-Laczkovich O., Szabó-Révész P. Formulation of tablets containing an 'in-process' amorphized active pharmaceutical ingredient. *Drug Dev. Ind. Pharm.* (2011), 37, 1272-1281.

Karavas E., Georgarakis M., Docoslis A., Bikiaris D. Combining SEM, TEM, and micro-Raman techniques to differentiate between the amorphous molecular level dispersions and nanodispersions of a poorly water-soluble drug within a polymer matrix. *Int. J. Pharm*. (2007) 340, 76-83.

Kauzmann W. The nature of glassy state and the behavior of liquids at low temperatures. *Chem. Rew*. (1948) 43, 219-256.

Kerč J., Srčič S. Thermal analysis of glassy pharmaceuticals. *Thermochim. Acta*, (1995) 248, 81-95.

Kim A. I., Akers M. J., Nail S. L. The physical state of mannitol after freeze-drying: Effects of mannitol concentration, freezing rate, and a noncrystallizing cosolute. *J. Pharm. Sci.* (1998) 87, 931–935.

Kim M. S., Jin S. J., Kim J. S., Park H. J., Song H. S., Neubert R. H., Hwang S. J. Preparation, characterization and in vivo evaluation of amorphous atorvastatin calcium nanoparticles using supercritical antisolvent (SAS) process. *Eur. J. Pharm. Biopharm.* (2008) 69, 454-65.

Kim J.-S., Kim M.-S., Park H. J., Jin S.-J., Lee S., Hwang S.-J. (2008). Physicochemical properties and oral bioavailability of amorphous atrovastatin hemi-calcium using spry-drying and SAS process. *Int. J. Pharm*., 359, 211-219.

Kotiyan P. N., Vavia P. R. Eudragits: role as crystallization inhibitors in drug-in-adhesive transdermal systems of estradiol. *Eur. J. Pharm. Biopharm.* (2001) 52, 173-80.

Kumar L., Baheti A., Mokashi A., Bansal A.K. Effect of counterion on the phase behaviour during lyophilization of indomethacin salt forms. *Eur. J. Pharm. Sci*. (2011) 44, 1-2, 136-41.

Kurti L., Kukovecz A., Kozma G., Ambrus R., Deli M., Szabó-Révész P. Study of the parameters influencing the co-grinding process for the production of meloxicam nanoparticles. *Powder Technol.* (2011) 212, 210–217.

Kürti L., Kukovecz Á., Kozma G., Ambrus, R., Deli, M. A., Szabó-Révész, P. Study of the parameters influencing the co-grinding process for the production of meloxicam nanoparticles. *Powder Technol.* (2011) 212, 210-217.

Latsch S., Selzer T., Fink L., Kreuter J. Crystallisation of estradiol containing TDDS determined by isothermal microcalorimetry, X-ray diffraction, and optical microscopy. *Eur. J. Pharm. Biopharm.* (2003) 56,43-52.

Lefort L., De Gusseme A., Willart J.-F., Danéde F., Descamps M. Solid state NMR and DSC methods for quantifying the amorphous content in solid dosage forms: an application to ball-milling of trehalose. *Int. J. Pharm.* (2004) 280, 209-219.

Leuner C., Dressman J.. Improving drug solubility for oral delivery using solid dispersions. *Eur. J. Pharm. Biopharm.* (2000) 50, 47-60.

Li Y., Han J., Zhang G. G. Z., Grant D. J. W., Suryanarayanan, R. In situ dehydration of carbamazepine dehydrate: a novel technique to prepare amorphous anhydrous carbamazepine. *Pharm. Dev. Technol.* (2000). 5 257-266.

Lin X., Gao W., Li C., Chen J., Yang C., Wu H. Nano-sized flake carboxymethyl cassava starch as excipient for solid dispersions. *Int. J. Pharm.* (2012) 423, 435-9.

Mallick, S., Pattnaik, S., Swain, K., Saha, P. K. De A., Ghoshal, G., Mondal, A. Formation of physically stable amorphous phase of ibuprofen by solid state milling with kaolin. *Eur. J. Pharm. Biopharm.* (2008) 68, 346-351.

Martini A. Torricelli C. De Ponti R. Physico-pharmaceutical characteristics of steroid/crosslinked polyvinylpyrrolidone coground systems. *Int. J. Pharm.* (1991) 75, 141-146.

Maury M., Murphy K., Kumar S., Mauerer A., Lee G, Spray-drying of proteins: effects of sorbitol and trehalose on aggregation and FT-IR amide I spectrum of an immunoglobulin G. *Eur. J. Pharm. Biopharm* (2005) 59, 251–261.

McCrone W. C., Fox D., Labes M. M.,Weissberger A. Physics and Chemistry of the Organic Solid State. *Interscience Publishers*, (1965) 2, 725-767

Merisko-Liversidge E. M., Liversidge G. G. Drug nanoparticles: formulating poorly water-soluble compounds. *Toxicol. Pathol.* (2008) 36, 43–48.

Miller J.M., Beig A., Carr R.A., Spence J.K., Dahan A. A Win-Win Solution in Oral Delivery of Lipophilic Drugs: Supersaturation via Amorphous Solid Dispersions Increases Apparent Solubility without Sacrifice of Intestinal Membrane Permeability. *Mol Pharm*. (2012) 5 20.

Moore M. D., Cogdill R. P., Wildfong P. L. Evaluation of chemometric algorithms in quantitative X-ray powder diffraction (XRPD) of intact multi-component consolidated samples. *J. Pharm. Biomed. Anal.* (2009) 49, 619-26.

Mura P., Cirri M., Faucci M. T., Ginès-Dorado J. M., Bettinetti G. P. Investigation of the effects of grinding and co-grinding on physicochemical properties of glisentide. *J. Pharm. Biomed. Anal*. (2002) 30, 227-37.

Német Z., Demeter A., Pokol G. Quantifying low levels of polymorphic impurity in clopidogrel bisulphate by vibrational spectroscopy and chemometrics. *J. Pharm. Biomed. Anal.* (2009) 49, 32–41.

Nezzal A., Aerts L., Verspaille M., Henderickx G., Redl A., Polymorphism of sorbitol. *J. Cryst. Growth.* (2009) 311, 3863–3870.

Papadimitriou S. A., Barmpalexis P., Karavas E., Bikiaris D. N. Optimizing the ability of PVP/PEG mixtures to be used as appropriate carriers for the preparation of drug solid dispersions by melt mixing technique using artificial neural networks: I. *Eur. J. Pharm. Biopharm.* (2012) 82, 175-86.

Pikal M.J., Lukes A.L., Lang J.E., Gaines K., Quantitative crystallinity determinations for b-lactam antibiotics by solution calorimetry: correlation with stability. *J. Pharm. Sci* (1978) 67, 767–772.

Pokharkar V. B., Mandpe L. P., Padamwar M. N., Ambike A. A., Mahadik K. R., Paradkar A. Development, characterization and stabilization of amorphous form of a low Tg drug. *Powder Technol.* (2006) 167, 20-25.

Pomázi A., Ambrus R., Sipos P., Szabó-Révész P. Analysis of co-spray-dried meloxicam-mannitol systems containing crystalline microcomposites. *J. Pharm. Biomed. Anal.* (2011) 56, 183-90.

Priemel P. A., Grohganz H., Gordon K. C., Rades T., Strachan C. J. The impact of surface- and nano-crystallisation on the detected amorphous content and the dissolution behaviour of amorphous indomethacin. *Eur. J. Pharm. Biopharm.* (2012) 82, 187-93.

Priemel P. A., Laitinen R., Barthold S., Grohganz H., Lehto V. P., Rades T., Strachan C. J. Inhibition of surface crystallisation of amorphous indomethacin particles in physical drug-polymer mixtures. *Int. J. Pharm.* (2013) 456, 301-6.

Qi S, Avalle P, Saklatvala R, Craig DQ. An investigation into the effects of thermal history on the crystallisation behaviour of amorphous paracetamol. *Eur. J. Pharm. Biopharm*. (2008), 69, 364-71.

Qi S., Avalle P., Saklatvala R., Craig D. Q. An investigation into the effects of thermal history on the crystallisation behaviour of amorphous paracetamol. *Eur. J. Pharm. Biopharm*. (2008) 69(1), 364-71.

Reitz E., Vervaet C., Neubert R. H., Thommes M. Solid crystal suspensions containing griseofulvin - Preparation and bioavailability testing. *Eur. J. Pharm. Biopharm*. (2013) 83, 193–202.

Rodríguez-Spong B., Price C. P., Jayasankar A., Matzger A. J., Rodríguez-Hornedo N. General principles of pharmaceutical solid polymorphism: a supramolecular perspective. *Adv. Drug Deliver. Rev*. (2004) 56, 241-274.

Rossmann M., Braeuer A., Dowy S., Gottfried Gallinger T., Leipertz A., Schluecker E. Solute solubility as criterion fort he appearance of amorphous particle precipitation or crystallization in the supercritical antisolvent (SAS) process. *J. of Supercritical Fluids*, (2012) 66, 350-358.

Royall P. G., Craig D. Q., Doherty C. Characterisation of moisture uptake effects on the glass transitional behaviour of an amorphous drug using modulated temperature DSC. *Int. J. Pharm.* (1999) 192, 39-46.

Saerens L., Dierickx L., Quinten T., Adriaensens P., Carleer R., Vervaet C., Remon J. P., De Beer T. In-line NIR spectroscopy for the understanding of polymer-drug interaction during pharmaceutical hot-melt extrusion. *Eur. J. Pharm. Biopharm.* (2012) 81, 230-7.

Saerens L., Dierickx L., Quinten T., Adriaensens P., Carleer R., Vervaet C., Remon J. P., De Beer T. In-line NIR spectroscopy for the understanding of polymer-drug interaction during pharmaceutical hot-melt extrusion. *Eur. J. Pharm. Biopharm*. (2012) 81, 230-237.

Sangwai M., Vavia P. Amorphous ternary cyclodextrin nanocomposites of telmisartan for oral drug delivery: improved solubility and reduced pharmacokinetic variability. *Int. J. Pharm.* (2013) 453, 423-32.

Sato H., Kawabata Y., Yuminoki K., Hashimoto N., Yamauchi Y, Ogawa K, Mizumoto T, Yamada S, Onoue S. Comparative studies on physicochemical stability of cyclosporine A-loaded amorphous solid dispersions. *Int. J. Pharm.* (2012) 426, 302-6.

Schönbichler S. A., Bittner L. K., Weiss A. K., Griesser U. J., Pallua J. D., Huck C. W. Comparison of NIR chemical imaging with conventional NIR, Raman and ATR-IR spectroscopy for quantification of furosemide crystal polymorphs in ternary powder mixtures. *Eur. J. Pharm. Biopharm.* (2013) 84, 616-25.

Shah B., Kakumanu V. K., Bansal A. K. Analytical techniques for quantification of amorphous/crystalline phases in pharmaceutical solids. *J. Pharm. Sci*. (2006) 95, 1641-65.

Shah M., Ullah N., Choi M. H., Kim M. O., Yoon S. C. Amorphous amphiphilic P(3HV-co-4HB)-b-mPEG block copolymer synthesized from bacterial copolyester via melt transesterification: nanoparticle preparation, cisplatin-loading for cancer therapy and in vitro evaluation. *Eur. J. Pharm. Biopharm.* (2012) 80, 518-27.

Sharma P, Denny W A, Garg S, Effect of wet milling process on the solid state of indomethacin and simvastatin. *Int. J. Pharm.* (2009) 380, 40–48.

Sonje V. M., Kumar L., Puri V., Kohli G., Kaushal A. M., Bansal A. K. Effect of counterions on the properties of amorphous atorvastatin salts. *Eur. J. Pharm. Sci*. (2011) 44, 462-70.

Takeuchi H., Nagira S., Yamamoto H., Kawashima Y. Solid dispersion particles of amorphous indomethacin with fine porous silica particles by using spray-drying method. *Int. J. Pharm.* (2005) 293, 155-64.

Takeuchi H., Nagira S., Yamamoto H., Kawashima Y. Solid dispersion particles of tolbutamide prepared with fine silica particles by the spray-drying method. *Powder Technol*., (2004) 141, 187-195.

Takeuchi H., Nagira S., Yamamoto H., Kawashima Y. Solid dispersion particles of amorphous indomethacin with fine porous silica particles by using spray-drying method. *Int. J. Pharm.* (2005) 293, 155-164.

Takeuchi H., Nagira S., Yamamoto H., Kawashima Y. Solid dispersion particles of amorphous indomethacin with fine porous silica particles by using spray-drying method. *Int. J. Pharm.* (2005) 293, 155-164.

Tarsa P.B., Towlerb C. S., Woollamb G., Berghausen J. The influence of aqueous content in small scale salt screening—Improving hit rate for weakly basic, low solubility drugs *Eur. J. Pharm. Sci.* (2010), 41, 23–30.

Teagarden D.L., Baker D.S. Practical aspects of lyophilization using non-aqueous co-solvent systems. *Eur. J. Pharm. Sci*. (2002), 115-33.

Tee S. K., Marriot C., Zeng X. M., Martin G. P., The use of different sugars as fine and coarse carriers for aerosolised salbutamol sulphate. *Int. J. Pharm*. (2000) 208, 111–123.

Tee S. K., Marriott C., Zeng X. M., Martin G. P. The use of different sugars as fine and coarse carriers for aerosolised salbutamol sulphate. *Int. J. Pharm*. (2000) 208, 111-23.

Tian F., Zhang F., Sandler N., Gordon K. C., McGoverin C. M., Strachan C. J., Saville D. J., Rades T. Influence of sample characteristics on quantification of carbamazepine hydrate formation by X-ray powder diffraction and Raman spectroscopy. *Eur. J. Pharm. Biopharm*. (2007) 66, 466-74.

Uvarov V., Popov I. Development and metrological characterization of quantitative X-ray diffraction phase analysis for the mixtures of clopidogrel bisulphate polymorphs. *J. Pharm. Biomed. Anal.* (2008) 46, 676-82.

Vollenbroek J., Hebbink G. A., Ziffels S., Steckel H. Determination of low levels of amorphous content in inhalation grade lactose by moisture sorption isotherms. *Int. J. Pharm*. (2010) 395, 62-70.

Vollenbroek J., Hebbink G. A., Ziffels S., Steckel H.. Determination of low levels of amorphous content in inhalation grade lactose by moisture sorption isotherms. *Int. J. Pharm.* (2010) 395, 62-70.

Watanabe T., Hasegawa S., Wakiyama N., Kusai A., Senna M. Comparison between polyvinylpyrrolidone and silica nanoparticles as carriers for indomethacin in a solid state dispersion. *Int. J. Pharm*. (2003) 250, 283-6.

Watanabe T., Ohno I., Wakiyama N., Kusai A., Senna M. Stabilization of amorphous indomethacin by co-grinding in a ternary mixture. *Int. J. Pharm*. (2002) 241, 103-11.

Watanabe T., Wakiyama N., Usui F., Ikeda M., Isobe T., Senna M. Stability of amorphous indomethacin compounded with silica. *Int. J. Pharm.* (2001) 226, 81-91.

Wyttenbach N., Janas C., Siam M., Lauer M. E., Jacob L., Scheubel E, Page S. Miniaturized screening of polymers for amorphous drug stabilization (SPADS): rapid assessment of solid dispersion systems. *Eur J Pharm Biopharm*. (2013) 84, 583-98.

Yam N., Li X., Jasti B. R. Interactions of topiramate with polyethylene glycol 8000 in solid state with formation of new polymorph. *Int. J. Pharm*. (2011) 411, 86-91.

Yoshioka M., Hancock B.C., Zografi G.,. Crystallisation of indomethacin from the amorphous state below and above its glass transition temperature. *J. Pharm. Sci*. (1994) 83, 1700–1705.

Yu L., Amorphous pharmaceutical solids: preparation, characterization and stabilization. *Adv. Drug Deliver. Rev.* (2001) 48, 27–42.

Zhang M., Li H., Lang B., O'Donnell K., Zhang H., Wang Z., Dong Y., Wu C., Williams R. O. III. Formulation and delivery of improved amorphous fenofibrate solid dispersions prepared by thin film freezing. *Eur. J. Pharm. Biopharm.* (2012) 82, 534-44.

Zhang G. G. Z., Law D., Schmitt E. A., Qiu Y. Phase transformation consideration during process development and manufacture of solid oral dosage forms. *Adv. Drug Deliver. Rev.*, (2004) 56, 371-390.

ACKNOWLEDGEMENTS

First of all, I would like to express my warmest thanks to my supervisor, the head of the Department of Pharmaceutical Technology and the head of PhD Programme Pharmaceutical Technology, **Prof. Dr. Piroska Szabó-Révész DSc**, for her generous help and advice in my scientific work, and for critically reviewing my manuscript. I am deeply grateful to her, for her kindness and support from my first steps in the scientific field of pharmaceutical technology.

The great help, support and enormous patience of **Dr. Orsolya Jójárt-Laczkovich PhD**, the experimental supervisor of my work, is also greatly acknowledged.

I would like to phrase my deep appreciation to **Prof. Dr. Joachim Ulrich** his great help and supervision.

My thanks are also due to all of my **colleagues in the Department of Pharmaceutical Technology** for providing such a favourable atmosphere.

I am deeply grateful to **my family** for their patience and love.

Annex

I

Acta Pharmaceutica Hungarica 81. 1-6 2011.

Amorf forma a gyógyszertechnológiai kutatásokban

MÁRTHA CSABA, JÓJÁRTNÉ LACZKOVICH ORSOLYA, SZABÓNÉ RÉVÉSZ PIROSKA*

Szegedi Tudományegyetem, Gyógyszertechnológiai Intézet, Szeged, Eötvös u. 6. – 6720
**Levelezési cím: revesz@pharm.u-szeged.hu*

Summary

Mártha, Cs., Jójárt-Laczkovich O., Szabó-Révész P.: *Amorphous form in pharmaceutical technological research*

Detecting and analysing of the amorphous phase are increasingly important in pharmaceutical technology. The amorphous or glassy state has a several advantages and disadvantages. The amorphous form can be applied in deliberate amorphization, when active pharmaceutical ingredient (API) is formulated in glassy state, or this form can appear accidentally during formulation or storage. The aim of this study was to characterize glass-forming properties of 13 different materials. Differential Scanning Calorimetry (DSC) was used as an analytical technique and T_g and T_m values were determined. The equation of T_g/T_m (K/K) was applied to determine the glass-forming tendencies. We made 2 groups of investigated substances. The first group was that we could not amorphized: tenoxicam, mannitol, niflumic acid, theophyllin and lidocain. The second group contains materials, which could be prepared in glassy form. This group can be divided into 2 sub-groups: poor-glass formers and good-glass formers. Poor-glass formers are following: meloxicam, ibuprofen and piroxicam. Good-glass formers are lacidipine, gemfibrosil, sorbitol, loratadine, chlorhexidine and clopidogrel hydrogensulfate.

Keywords: amorphous, amorphization, accidentally amorfization, glass *transition, DSC.*

Összefoglalás

Az amorf forma kimutatása, vizsgálata és a különböző anyagok amorfizálhatósági tulajdonságainak meghatározása egyre inkább előtérbe kerül a gyógyszertechnológiában. Az amorf fázis számos előnyös és hátrányos tulajdonsággal rendelkezik a kristályos fázishoz képest. Előnyös tulajdonságai miatt amorfizálhatjuk közvetlenül a hatóanyagokat, vagy keletkezhet véletlenszerűen is különböző behatások miatt. Munkánk során 13 ható- illetve segédanyag amorfizálhatóságát vizsgáltuk egy termoanalitikai gyorsteszttel, amelyhez DSC készüléket használtunk. Meghatároztuk az egyes anyagok olvadáspontját (T_m) és üvegesedési hőmérsékletét (T_g). A T_g/T_m (K/K) arány segítségével meghatároztuk az anyagok amorfizálhatóságát. A kapott eredmények alapján két csoportba soroltuk az anyagokat: az első csoport anyagait nem tudtuk amorfizálni. Ezek voltak: a tenoxikám, a mannit, a niflumínsav, a teofillin és a lidokain. A második csoport anyagait üveges állapotba tudtuk vinni. Ezt a csoportot két alcsoportra osztottuk: az első alcsoportba a rosszul amorfizálható anyagok tartoznak, amelyek a következőek: ibuprofén, meloxikám és piroxikám. A második alcsoport anyagai jól amorfizálhatóak. Ezek a következők: lacidipin, gemfibrozil, szorbit, loratadin, klórhexidin, és a klopidogrel hidrogén-szulfát.

Kulcsszavak: amorf, amorfizálás, véletlenszerű amorfizálódás, üvegesedési hőmérséklet, DSC.

Bevezetés

Az amorf fázis, a szilárd fázis egyik alfázisa a kristályos alfázis mellett [1]. Az amorf kifejezés alaktalan, formátlan, rendezetlen állapotot jelent. Ez utal arra, hogy egy amorf anyag kristályrácsában csak rövid távú rendezettség alakul ki. Az ipar számos területén alkalmaznak különböző amorf anyagokat: az üveggyártásban, ahol a szilícium-dioxid, mint kis molekulájú szervetlen anyag kerül felhasználásra, a műanyagiparban, ahol makromolekulás szerves anyagokat használnak, például a polietilént, illetve a gyógyszergyártásban, ahol főleg kis molekulatömegű szerves anyagokat formulálnak.

Célkitűzés

Munkánk során célunk volt áttekintést adni az amorf formáról gyógyszer-technológiai szempontból, illetve kristályos anyagok amorfizálódását vizsgálni, egy egyszerűen és gyorsan elvégezhető gyorsteszt segítségével, amely alkalmas az amorf forma keletkezését szimulálni. Meghatároztuk az anyagok olvadáspontját (T_m), üvegesedési hőmérsékletét (T_g), valamint a kettő arányából következtetést vontunk le azok amorfizálhatóságra. További célunk volt annak az ellenőrzése, hogy az irodalmi közlésnek megfelelően a T_g valóban a T_m 2/3-a illetve 4/5-e közé várható-e [1].

Az amorf forma jellemzése

Az amorf (üveges) forma jelenléte és vizsgálata a gyógyszeriparban fokozott, hiszen az amorf fázis viselkedése merőben eltér a kristályos anyagétól, tulajdonságai lehetnek hátrányosak, de előnyösek is. Az amorf anyag szabadenergiája, entalpiája,

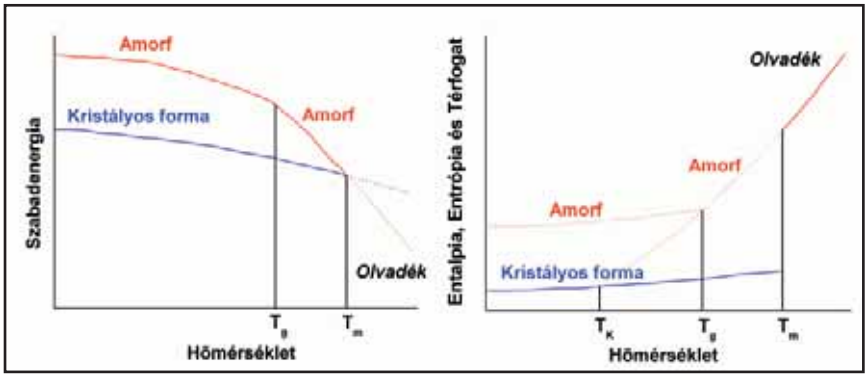

1. ábra: Az amorf és a kristályos forma összehasonlítása szabadenergiájuk, entalpiájuk, entrópiájuk és térfogatuk hőmérséklet-függésében. T_g: üvegesedési hőmérséklet, T_m: olvadáspont, T_K: Kauzmann hőmérséklet [2].

entrópiája és térfogata is nagyobb, mint a kristályosé. A hőmérséklet emelésével viszont szabadenergiája csökken, entalpiája, entrópiája és térfogata növekszik (*1. ábra*). Az amorf anyag általában higroszkóposabb és nagyobb oldódási sebességgel rendelkezik, mint a kristályos, hiszen nem rendelkezik szabályos kristályráccsal, így rácsenergiával sem, amely az oldódás termodinamikai gátja. Az anyag üveges állapotában nem rendelkezik olvadásponttal (T_m), viszont jellemző rá az ún. üvegesedési hőmérséklet (T_g). Az amorf fázisra jellemző érték továbbá a Kauzmann hőmérséklet (T_K), amelyen az amorf és a kristályos anyag entrópiája megegyezik. E hőmérséklet alatt az amorf anyag stabilabbnak tekinthető a kristályosnál (Kauzmann paradox) [2].

A T_g alatt az anyag rideg, törékeny, nehezen alakítható, majd a hőmérséklet emelése és a T_g átlépését követően fokozatosan lágyul, és válik rugalmassá. Ezért fontos tudni, hogy adott anyag T_g értéke szobahőmérséklet alatt vagy felett található-e. Tapasztalatok szerint a T_g az olvadáspont 2/3-a, 4/5-e között várható Kelvinben számolva. A T_g és T_m arányából következtethetünk az adott anyag amorfizálhatósági tulajdonságaira: ha a T_g/T_m aránya nagyobb, mint 0,7 akkor az anyag jól amorfizálható. Ha ez az arány kisebb, akkor a kristályos szerkezet letörése után a rendezetlen (amorf) forma szinte azonnal visszakristályosodik, tehát az anyag roszszul amorfizálható [1]. A hatóanyagok általában kis molekulájú szerves anyagok, amelyek a magas szerkezeti flexibilitásuk miatt, sok esetben sorolhatóak a jól amorfizálható csoportba.

Az amorf forma keletkezése

A gyógyszertechnológiai műveletek során két esetben számolhatunk az amorf forma jelenlétével: a formulálandó kristályos anyagot *közvetlenül amorf állapotba hozzuk*. Ebben az esetben amorf hatóanyag áll rendelkezésre a gyógyszerforma kialakításához. A másik esetben viszont a hatóanyag valamely gyártásközi művelet, esetleg a tárolás során, részben vagy akár egészében *véletlenszerűen amorfizálódik.*

A kristályos anyag amorfizálására hagyományosan három különböző eljárást alkalmazunk:

- *Oldószeres eljárás,* amely során feloldjuk az anyagot annak jó oldószerében, majd gyorsan eltávolítjuk azt, így a molekuláknak nincs elég idejük, hogy szabályos kristályrácsba rendeződjenek, tehát mindez rendezetlen, amorf formát eredményez [3]. Az oldószer eltávolítása történhet hőmérsékletemeléssel, nyomáscsökkentéssel, porlasztással [5], fagyasztva szárítással [10], vagy szuperkritikus technológiával [6].
- *Olvadék technológia (Hot-melt technology):* amelynek egyik módja, hogy az anyagot az olvadáspontja felé hevítjük, majd hirtelen visszahűtjük [7], vagy egy megfelelő segédanyagot olvasztunk meg, és az olvadékban diszpergáljuk a hatóanyagot.
- *Őrléssel,* amelynek során a hatóanyagot magában, vagy segédanyaggal őrölhetjük különböző malmokban szobahőmérsékleten, vagy akár hűtve [8]. Az őrlés során fellépő mechanikai erők, a nyomás és a súrlódás miatt keletkező hő okozta helyi olvadások amorfizálhatják az anyagot [11–13].

Az amorf forma véletlenszerű keletkezését számos technológiai folyamat eredményezheti. Az *oldószer eltávolítás* számos technológiai folyamat része és sok esetben eredményezhet amorf terméket. A napjainkban egyre gyakrabban alkalmazott *olvadék* technológiák is képesek az anyagot amorfizálni. Az olvadás során felbomlott kristályrács egyes esetekben nem nyeri vissza a rendezettségét a hűtést követően, amely így amorf formát eredményez [9]. Ugyancsak amorf terméket kaphatunk, ha egy segédanyagot, pl. filmképzőt (PEG) megolvasztunk, és az olvadékban a hatóanyag feloldódik [11]. Gyakran amorfizálódik a termék *szemcseméret csökkentés* közben is. Őrléses eljárás során golyósmalomban vagy hengermalomban végzett rövid ideig tartó őrlés is képes lehet rész-

ben, vagy egészében amorf formát létrehozni [11, 13], de olyan eszközök, amelyek kisebb szemcseméret elérésére alkalmasak, mint például a nagy nyomású homogenizátor [14] vagy a kolloid malom [15], nagyobb valószínűséggel amorfizálják a terméket. Leggyakrabban a préseléses eljárások, a tablettázás és száraz granulálás (brikettezés, kompaktálás), okoznak problémát: a művelet alatt fellépő nagy nyomás, és a súrlódás miatti hő okozta helyi olvadások amorfizálhatják a ható- vagy segédanyagokat [17].

Az amorf forma vizsgálata

Az előzőekből következik, hogy számos esetben szükség lehet olyan vizsgálatokra, amelyekkel igazolható a hatóanyag kristályos voltának teljes, vagy részleges hiánya, és a megjelenő amorf fázis kvantitatív meghatározása. Az amorf fázis detektálása, és további vizsgálata szerkezetéből adódóan számos problémát vet fel:

1. Mivel termodinamikailag instabil rendszerek, mindig számolnunk kell visszakristályosodással a vizsgálat egésze során. Már a minta vétele során alkalmazott fizikai behatás, az eltérő hőmérséklet, páratartalom vagy légnyomás is okozhat olyan változást, ami hamis eredményt adhat.
2. Sok esetben a terméknek csak egy része amorf, és a maradék kristályos rész sem feltétlenül csak egyféle polimorf módosulatot tartalmaz. Előfordulhat még, hogy a termékben az előállítás során keletkezett instabil amorf rész elbomlása során keletkező bomlástermék is kimutatható.
3. Problémás lehet még a termékben lévő különböző komponensek egymás mellett történő kimutatása.

Az amorf fázis kimutatására leggyakrabban a differenciális pásztázó kalorimetriát (DSC) alkalmazzák. A készülék entalpiaváltozást detektál a hőmérséklet függvényében. A T_m endoterm csúcsként jelenik meg a diffraktrogramon, amelynek görbe alatti területe arányos a mért anyag mennyiségével. A 100%-ban amorf anyag diffraktogramján nem láthatunk endoterm csúcsot. Ebből következik, hogy a csak részben amorfizálódott anyag T_m-nél jelentkező csúcs görbe alatti területe arányos a kristályos frakció mennyiségével. A készülék képes az üveges átmenet detektálására is, egy endoterm alapvonal eltolódás (ún. endoterm lépcső) formájában. Ezen tartomány inflexiós pontját tekinthetjük a T_g-nek. Ha ezt a lépcsőt egy másik entalpiaváltozással járó történés elfedné, a jelenségek szétválasztására használhatjuk a modulált fűtésű differenciális pásztázó kalorimetriát (MTDSC). A készülék képes elkülöníteni a reverzibilis változásokat az irreverzibilisektől. Az üvegesedési hőmérséklet, mint reverzibilis változás így elkülöníthető például az oldószer-vesztéstől, mint irreverzibilis változástól. Gondot okozhat még, ha kis mennyiségű amorf anyagot tartalmaz a kristályos minta. Ennek detektálására alkalmazhatunk gyors fűtésű differenciális pásztázó kalorimetriát (Hyper-DSC) [18]. A DSC módszer alkalmas kristályossági fok, illetve kristályosodási kinetika meghatározására is, hiszen a kristályos fázis olvadásakor jelentkező endoterm csúcs görbe alatti területe egyenesen arányos a kristályos rész mennyiségével.

Használatos még az amorf fázis kimutatására a porröntgen diffrakció (XRPD) is. Az atomi rácstávolságok nagyságrendjébe eső monokromatikus röntgensugár, az anyag periodikusan ismétlődő építőelemeinek elektronfelhőjéről szóródik. A sugarak különböző szögek alatt mérhető interferenciája (kölcsönös erősítése, illetve gyengítése) információt ad az anyag szerkezetéről. Amorf minta esetén eltűnnek a kristályos formára jellemző jellegzetes csúcsok, a görbe úgymond kisimul [19]. A röntgendiffrakció ugyancsak alkalmas kristályossági fok, illetve kristályosodási kinetika meghatározására, hiszen a különböző szögek alatt mért beütések száma attól függ, hogy mennyi kristályos anyagon haladt keresztül a röntgensugár.

Kristályossági fok, illetve kristályosodási kinetika meghatározására alkalmazhatjuk még a dinamikus gőzszorpciós (DVS) készüléket is. A mérések alapját az adja, hogy az anyag amorf állapotban higroszkóposabb, mint a kristályos [20]. Hátránya, hogy a kristályos formában is erősen higroszkópos anyagok amorf formája nem, vagy csak nehezen detektálható.

Használatos még az amorf forma vizsgálatára a Raman-, a Furier transzformációs infravörös- (FT-IR), a közeli infravörös- (NIR), a diffúz reflexiós Furier transzformációs infravörös- (DRIFT), és a molekula spektroszkópia; a szilárd fázisú NMR (ssNMR), a termogravimetria (TG), a derivatív termogravimetria (DTG), a dielektromos analízis (DEA), a denzitometria, és a viszkozimetria [1].

A vizsgáló módszereink mindegyikére meg kell adnunk egy ún. legkisebb detektálható (DL: Detection Limit) és legkisebb mérhető mennyiséget (QL: Quantitation Limit) százalékban. Mindkét adat kiszámolására többféle lehetőség adott, ame-

lyeket az ICH (International Conference on Harmonisation) iránymutatása határoz meg (Q2). Amorf tartalom meghatározásakor a legfontosabb módszer, amely szerint a standard deviáció és a kalibrációs görbe meredekségének a hányadosát 3,3-del szorozva a DL-et 10-zel szorozva pedig a QL-et határozhatjuk meg.

$$DL = 3{,}3\ \sigma / S,$$
$$QL = 10\ \sigma / S,$$

ahol a
σ = standard deviáció és az
S = a kalibrációs egyenes meredeksége.

Kísérleti rész

Anyagok

A felhasznált anyagok a következők voltak: klopidogrel hidrogén-szulfát, ibuprofen, meloxikám, piroxikám (EGIS, Budapest); gemfibrozil, lacidipin, loratadin (TEVA, Debrecen); nifluminsav (Richter Gedeon, Budapest); tenoxikám (Roche, Magyarország); lidokain és teofillin (Hungaropharma).

Módszer

Az amorf minták elkészítéséhez, és azok vizsgálatához DSC 821e (Mettler-Toledo, Svájc) készüléket használtunk, 4,8-5,2 mg tömegű mintákkal. A fűtési sebesség 10 °C/min volt. A mérés kezdeti és végső hőmérsékletének anyagonként különbözőt választottunk azok olvadáspontjától függően, úgy hogy az anyag minden esetben teljesen megolvadjon, de ne szenvedjen bomlást.

A kiindulási kristályos mintát fedett, lyukasztott standard alumínium tégelyekbe helyeztük. Az első fűtés során a mintát olvadáspontja felé hevítettük, majd a teljes olvadás után visszahűtöttük szobahőmérsékletre 45 ± 5 °C/min hűtési sebességgel. Ezután azonnal újra felfűtöttük, és a kapott eredményeket elemeztük. A második fűtés kezdeti hőmérsékletét úgy határoztuk meg, hogy a mérés a T_m Kelvinben mért 2/3-ánál kisebb értékről induljon.

Eredmények

A kapott eredmények alapján két csoportba sorolhatjuk a 13 vizsgált anyagot. Az első csoportba tartoznak azok az anyagok, amelyeknek amorf formáját nem sikerült előállítani. A második csoportba pedig azok az anyagok, amelyeknél el tudtuk érni az üveges állapotot. Az első csoportot a teofillin DSC diffraktogrammján keresztül mutatjuk be (*2. ábra*). Az ábrán a két fűtés során kapott görbék láthatóak. Az első fűtés során (A) kapott endoterm csúcs, amely az olvadást jelzi, a második fűtés (B) alkalmával is megjelent. Habár a görbe alatti terület a második fűtéskor némiképp csökkent, ami a szabályos kristályrács elvesztésére, tehát amorfizálódásra utalhat, tehát T_g-t nem tudtunk detektálni. Ezek alapján kijelenthető a T_g/T_m arányt alapul véve, hogy a teofillin rosszul amorfizálódik. A 13 vizsgált anyag közül a tenoxikám, a mannit, a nifluminsav, a teofillin és a lidokain került ebbe a csoportba. Az ilyen anyagok formulálása során nem számíthatunk számottevő amorfizálódásra.

A második csoport anyagait az általunk alkalmazott eljárással (olvadékhűtéssel) sikerült amorfizálni, a kapott eredmények alapján az anyagokat két alcsoportba sorolhatjuk. Az első alcsoportba azok az anyagok tartoznak, amelyek T_g/T_m aránya elmarad 0,7-től, tehát rosszul amorfizálódónak tekintjük őket. Ilyen volt az ibuprofen (*3. ábra*). A példaként bemutatott DSC görbén látható, hogy a kezdetben kristályos ibuprofent az első fűtés (A) amorfizálta, mivel a második fűtés (B) görbéjén nem látható az olvadás endoterm csúcsa. A második fűtést -60 °C-ról indítottuk, mivel a T_g a negatív hőmérsékleti intervallumban volt várható. Ebbe az alcsoportba sorolható továbbá a meloxikám és a határértéken fekvő piroxikám is. Az ilyen anyagok formulálásakor már a kevésbé agresszív behatások is amorfizálhatják az anyagot. Mindezek ellenére javasolható kristályos formában történő formulálásuk, hiszen ezeket az anyagokat csak nehezen, nagy energia befektetésével lehet amorf állapotba vinni. Kristályos formulá-

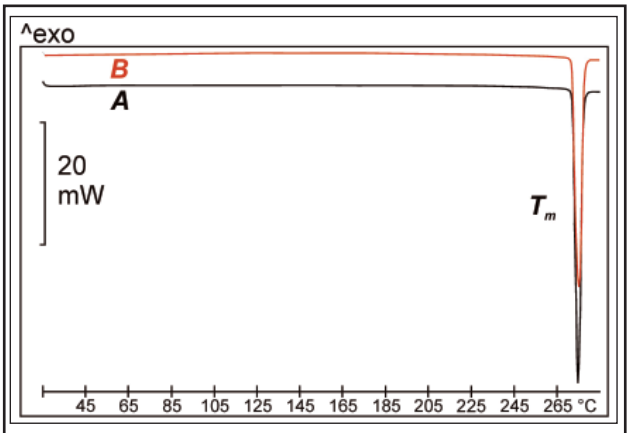

2. ábra: Teofillin DSC vizsgálata. A: az első fűtés során kapott görbe, T_m(A) = 274,7 °C. B: a második fűtés során kapott görbe, T_m(B) = 272,3 °C.

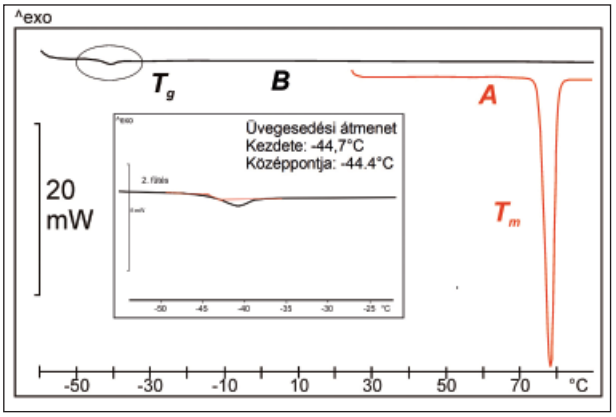

3. ábra: Ibuprofen DSC vizsgálata. A: az első fűtés során kapott görbe, T_m=77,4 °C. B: a második fűtés során kapott görbe, T_g=-44,4 °C.

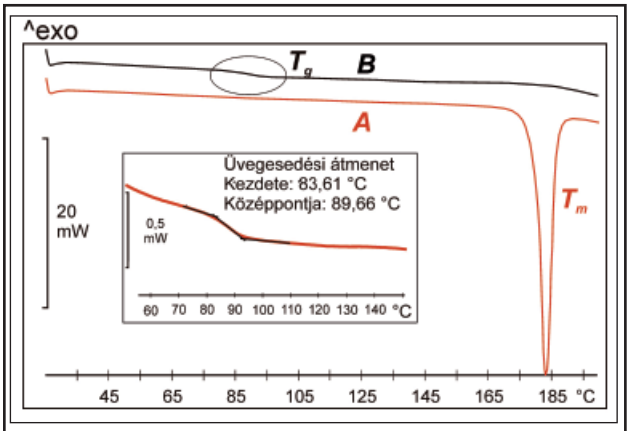

4. ábra: Klopidogrel hidrogén-szulfát DSC vizsgálata. A: az első fűtés során kapott görbe, T_m= 181,2 °C. B: a második fűtés során kapott görbe, T_g= 87,9 °C.

lásuk során kevésbé kell számolnunk az amorf forma megjelenésével.

A második alcsoport anyagainak a T_g/T_m aránya nagyobb, mint 0,7, így jól amorfizálódónak tekinthetjük őket. A klopidogrel hidrogén-szulfát DSC görbéjén látszik, hogy az első fűtés során (A) az anyag megolvadt, majd a visszahűtést követően, a második fűtéskor (B) eltűnt az olvadás endoterm csúcsa, és megjelent az üveges átmenet (*4. ábra*). Ha kristályos végtermék a cél, akkor a formulálás egésze során figyelemmel kell kísérnünk az anyag szerkezetét. Ugyanakkor az így viselkedő anyagok esetében javasolható az amorf formában való alkalmazás, hiszen könnyen üveges állapotba hozhatóak, és a megfelelő segédanyagokkal sokáig amorfak is maradnak. Ebbe a csoportba sorolható továbbá a lacidipin, a gemfibrozil, a szorbit, a loratadin és a klórhexidin is.

Az összes vizsgált anyag mérési eredményeit és amorfizálhatóságát az *I. táblázat* foglalja össze.

Megfigyelhető, hogy a hasonló molekulaszerkezetű anyagok, mint például az egyforma alapvázú oxikámok, vagy a szorbit és a mannit, melyek egymás diasztereomerei, teljesen eltérően amorfizálódnak.

Kijelenthető, hogy az esetek nagy részében a T_g *a* T_m *2/3-a illetve 4/5-e közé esett, tehát ezen értékek alkalmazhatóak a* T_g *előzetes megkeresésére.*

I. táblázat

A vizsgált anyagok T_m, T_g és T_g/T_m értékei

Hatóanyagok	Olvadáspont (T_m; °C)	Üvegesedési hőmérséklet (T_g; °C)	T_g/T_m (K/K)	Amorfizálhatóság	T_g a T_m 2/3-4/5-e között
Tenoxicam	226,0	-	-	rossz	-
Mannit	166,9	-	-	rossz	-
Niflumínsav	205,4	-	-	rossz	-
Teofillin	271,6	-	-	rossz	-
Lidokain	70,1	-	-	rossz	-
Meloxikám	264,0	63,5	0,63	rossz	nem
Ibuprofen	77,4	–42,5	0,66	rossz	nem
Piroxikám	203,1	58,1	**0,70**	határérték	igen
Lacidipin	184,8	54,4	**0,71**	jó	igen
Gemfibrozil	61,5	–29,2	**0,73**	jó	igen
Szorbit	91,4	0,77	**0,75**	jó	igen
Loratadin	137,6	40,4	**0,76**	jó	igen
Klopidogrel HSO_4	181,2	88,9	**0,80**	jó	igen
Klórhexidin	140,3	61,7	**0,81**	jó	nem

Összegzés

Végezetül kijelenthető, hogy az amorf forma jelenléte nagy figyelmet érdemel a gyógyszertechnológus részéről. Fontos amorfizálhatósági vizsgálatokat végezni a formulálni kívánt ható-, illetve segédanyagokon egyaránt, hiszen számos olyan technológiai folyamaton mennek keresztül, amelyek részben vagy teljesen amorfizálhatják az anyagot. Elvégeztünk egy termoanalitikai gyorstesztet 13 különböző anyagon, amellyel megállapítottuk az amorfizálhatóságukat. Az értékek tükrében kijelenthető, hogy az amorfizálhatósági vizsgálatokat minden egyes anyagnál egyedileg kell elvégezni, mert egymásra szerkezetileg hasonlító anyagoknál is jelentős eltérések adódhatnak.

Köszönetnyilvánítás

Ez a munka az Új Magyarország Fejlesztési Terv támogatásával valósult meg: *Keringési, anyagcsere és gyulladásos betegségek teranosztikájának fejlesztése* (TÁMOP-4.2.2-08/1-2008-0013).

IRODALOM

1. *Cui, Y.:* Int. J. Pharm. *339*, 3-18 (*2007*).
2. *Yu, L.*: Adv. Drug Deliver. Rev. *48*, 27-42 (*2001*).
3. *Kauzmann, W.*: Chem. Rew. *43*, 219-256 (*1948*).
4. *Laczkovich, O., Révész, P.*: Magyar Kémiai Folyóirat *116*, 102 (*2010*).
5. *Chieng, N., Rades, T., Saville, D.*: Eur. J. Pharm. Biopharm. *68* 771–780 (*2008*).
6. *Kim, J.-S., Kim, M.-S., Park, H. J., Jin, S.-J., Lee, S., Hwang, S.-J.*: Int. J. Pharm. *359* 211–219 (*2008*).
7. *Kim, M.-S., Jin, S.-J., Park, H. J., Song, H.-S., Hwang, S.-J.*: Eur. J. Pharm. Biopharm. *69*, 454–465 (*2008*).
8. *Zhang, F., Aaltonen, J., Tian, F., Saville, D. J., Rades, T.*: Eur. J. Pharm. Biopharm. *71*, 64–70 (*2009*).
9. *Chieng, N., Rades T., Saville D.*: Eur. J. Pharm. Biopharm. *68*, 771–780 (*2008*).
10. *DiNunzio J. C., Brough C., Hughey J. R., Miller D. A., Williams III R. O., McGinity J. W.*: Eur. J. Pharm. Biopharm. *74*, 340–351 (*2010*).
11. *Vollenbroek, J., Hebbink, G. A., Ziffels, S., Steckel, H.*: Int. J. Pharm. *395*, 62–70 (*2010*).
12. *Szűts A., Pallagi A., Regdon G. Jr., Aigner Z., Révész, P.*: Int. J. Pharm. *336*, 199–207 (*2007*).
13. *Mallick, S., Pattnaik, S., Swain, K., De, P. K., Saha, A., Ghoshal, G., Mondal, A.*: Eur. J. Pharm. Biopharm. *68*, 346–351 (*2008*).
14. *Mura, P., Cirri, M., Faucc,i M.T., Gine`s-Dorado, J.M., Bettinetti, G.P.*: J. Pharm. Biomed. Anal. *30*, 227–237 (*2002*).
15. *Sharma, P., Sharma, P., Denny, W. A., Garg, S.*: Int. J. Pharm. *380*, 40–48 (*2009*).
16. *Christensen, K.L., Pedersen, G.P., Kristensen, H.G.*: Eur. J. Pharm. Biopharm. *53*, 147–153 (*2002*).
17. *Porkharkar, V. B., Mandpe, L. P., Padamwar, M. N., Ambike, A. A., Mahandik, K. R., Paradkar, A.*: Powder Technol. *167*, 20-25 (*2006*).
18. *Bozic, D. Z., Dreu, R., Vrecer, F.*: Int. J. Pharm. *357*, 44–54 (*2008*).
19. *Saunders, M., Podluii, K., Shergill, S., Buckton, G., Royall, P.*: Int. J. Pharm. *274*, 35–40 (*2004*).
20. *Chen, X., Bates, S., Morris, K. R.*: J. Pharm. Biomed. Anal. *26*, 63–72 (*2001*).
21. *Mackin, L., Zanon, R., Park, J. M., Foster, K., Opalenik, H., Demonte, M.*: Int. J. Pharm. *231*, 227–236 (*2002*).

Érkezett: 2011. február 24.

II

European Polymer Journal xxx (2013) xxx–xxx

Contents lists available at SciVerse ScienceDirect

European Polymer Journal

journal homepage: www.elsevier.com/locate/europolj

Effects of polymers on the crystallinity of nanonized meloxicam during a co-grinding process

Csaba Mártha [a], Levente Kürti [a], Gabriella Farkas [a], Orsolya Jójárt-Laczkovich [a], Balázs Szalontai [b], Erik Glässer [b], Mária A. Deli [b], Piroska Szabó-Révész [a,*]

[a] Department of Pharmaceutical Technology, University of Szeged, Eötvös 6, H-6720 Szeged, Hungary
[b] Laboratory of Molecular Neurobiology, Institute of Biophysics, Biological Research Center, Hungarian Academy of Sciences, Szeged, Hungary

ARTICLE INFO

Article history:
Received 14 November 2012
Received in revised form 1 March 2013
Accepted 5 March 2013
Available online xxxx

Keywords:
Meloxicam
Polyethylene glycol
Polyvinylpyrrolidone
Crystallinity
Co-grinding

ABSTRACT

Particle size reduction to the submicron region in a grinding process demands a high energy input. This grinding energy requirement can be reduced by means of a suitable additive, e.g. polymer, and performing a co-grinding process. Although these excipients promote attainment of the nanoparticle size range, they can also decrease the crystallinity of the active pharmaceutical ingredient. Different types of polymers have different abilities to amorphize the active material. To demonstrate the amorphization effects of different polymers, meloxicam (MX) as a model drug was subjected to co-grinding in the presence of one or other of four different polymers (PEG 6000, PEG 20,000, PVP C30 and PVP K25) and the products were investigated by XRPD, FT-IR and SEM. Although the PEG materials slightly melted and covered the MX particles during the grinding, they did not cause any changes in crystallinity. The PVP polymers softened and covered the MX particles, but drastically reduced the crystallinity of the drug. FT-IR revealed a weak secondary bonding between MX and the PVP polymer chain.

1. Introduction

Grinding is a technique that is widely used to decrease the particle size of a solid material down to the nanorange, with the purpose of enhancing the solubility, the dissolution rate and the oral absorption of poorly water-soluble compounds [1,2]. To achieve the expected nano-sized particles, a high energy input is needed, which can be provided by various equipment, such as a ball-mill, cryo-mill, jet-mill, and colloidal mill. A common problem with these methods is the high energy requirement: the smaller the particles produced, the higher the energy needed. This energy requirement can be decreased by adding a suitable excipient and performing a co-grinding procedure [3,4]. An appropriate additive also helps to prevent the aggregation of nanoparticles, lubricates the system, and increases the water solubility of the active pharmaceutical ingredient (API). Pharmaceutical excipients include several materials which meet the requirements, but most of them are polymers. The most widely used as grinding materials are polyethylene glycol (PEG) and polyvinylpyrrolidone (PVP).

The various PEGs are used in the pharmaceutical industry as binders, carriers, lubricants, etc., thanks to their advantageous properties: PEGs are completely biocompatible, they can exhibit a combination of hydrophilic and lipophilic properties and they are commercially available in various molecular weights. As semi-crystalline materials, they have melting points in the range from 3 to 68 °C, depending on the molecular weight [5,6]. Their importance in pharmaceutical research is increasing, in consequence of their ability to enhance the dissolution rate of numerous poorly water-soluble drugs [7,8].

PVP is also produced in various molecular weights and particle sizes. These materials are mostly used as binders,

* Corresponding author. Tel.: +36 62 545572; fax: +36 62 545 571.
E-mail address: revesz@pharm.u-szeged.hu (P. Szabó-Révész).

0014-3057/$ - see front matter © 2013 Elsevier Ltd. All rights reserved.
http://dx.doi.org/10.1016/j.eurpolymj.2013.03.006

matrix polymers, desintegrant, crystallization inhibitors and stabilizers. In the literature PVP has often been used as an additive during co-grinding, serving as a carrier or to prevent aggregation [9,10]. It has also been demonstrated that it can decrease the crystallinity of API during methods providing high energy [11–13].

We earlier verified that PEG and PVP can be applied as suitable additives to decrease the energy requirements of grinding, to help reduce the particle size to the nanorange, to prevent the aggregation of nanoparticles and to increase solubility [14]. In that study, the API was ground in the presence of two types of PVPs and PEGs. All four additives helped to reduce the mean particle size to the nanorange. It was shown that the polymers exerted different influences on the crystallinity of the API, and the dissolution rate of the nano-sized API was also improved to different extents.

The aim of our present research work was to investigate the effects of different polymers on the crystallinity of a model material during co-grinding. MX was selected as model API, and the polymers were two types of PVP and two types of PEG. We set out to quantify the decrease in crystallinity in time and to detect any bonding formed between the MX and the polymers.

MX is a non-steroidal anti-inflammatory drug that is main by applied in therapy as an anti-inflammatory and strong analgetic agent [15]. MX is practically insoluble in water while it displays a relatively high permeability through cell membranes. It was chosen as model compound because it is capable of hydrogen-bond to other materials.

2. Materials and methods

2.1. Materials

Pure crystalline MX (4-hydroxy-2-methyl-N-(5-methyl-2-thiazolyl)-2H-benzothiazine-3-carboxamide-1,1-dioxide) was purchased from EGIS Ltd. (Budapest, Hungary). The polymer additives that were used as grinding excipients were PVP K25 with a molecular weight of 34,000 and PVP C30 with a molecular weight 58,000) from BASF (Ludwigshafen, Germany), and PEG with molecular weights of 6000 and 20,000 from Sigma–Aldrich Chemie GmbH, München, Germany.

2.2. Grinding process

Physical mixtures of MX, as active pharmaceutical ingredient, and the grinding (stabilizer) polymer (PEG 6000, PEG 20,000, PVP K25 or PVP C30) were prepared and charged into the stainless steel jar of a planetary ball mill containing 10 stainless steel balls (Retsch PM 100, Retsch GmbH & Co., Haan, Germany). The mass ratios were based on previous work [14], so as to give nanoparticles (200–600 nm). For the PVPs, the drug: excipient mass ratio was 1:1, while for the PEGs it was 1:2.

Mixtures were ground for 140 min, samples being withdrawn for investigation after 20, 40, 60, 80, 100, 120 and 140 min. During the grinding process, the temperature of the mortar was measured with an infrared thermometer right before sample withdrawal. The temperature of the mortar was not higher than 56 °C through milling.

2.3. X-ray powder diffraction (XRPD)

XRPD analysis was performed with a Bruker D8 Advance diffractometer (Bruker AXS GmbH, Karlsruhe, Germany) system with Cu K λI radiation (λ = 1.5406 Å). The samples were scanned at 40 kV and 40 mA from 3° to 40° 2θ, at a scanning speed of 0.05°/s and a step size of 0.010°. The crystallinity of the samples made with the PVPs as amorphous materials was determined via the total area beneath the curve between 12° and 30° 2θ, while the determinations of the samples made with the semicrystalline PEGs were based on the curves relating to MX alone. To avoid the problems caused by the particle size reduction and randomly oriented particles, we used an internal standard method. This technique is widely applied for quantitative XRPD. As internal standard, we mixed 20% (w/w) of pure crystalline NaCl into the binary mixtures. Before its application, the particle size of the NaCl was set into the similar range as that of the MX (2643.6 ± 2629.1 nm). After Kα2-stripping, background removal and smoothing of the areas under the peaks, the area under the peak of MX was proportioned to the area under the peak of NaCl (31–32.5° 2θ). All manipulations of diffractograms were performed with DIFFRACT^{plus} EVA software.

2.4. Fourier transform infrared (FT-IR) spectroscopy

FT-IR spectra were recorded with a Bio-Rad Digilab Division FTS- 65A/896 FTIR spectrometer (Bio-Rad Digilab Division FTS-65A/869, Philadelphia, USA) between 4000 and 400 cm^{-1}, at an optical resolution of 4 cm^{-1}; operating conditions: Harrick's Meridian SplitPea single reflection, diamond, ATR accessory. Thermo Scientific GRAMS/AI Suite software (Thermo Fisher Sciencific Inc., Waltham, USA) was used for the spectral analysis.

For FT-IR determinations, the ATR method was chosen, because with this there is no need for sample preparation, such as particle size reduction or KBr tableting, which would expose the samples to further physical stress.

2.5. Scanning electron microscopy (SEM)

The morphology of the particles was examined by SEM (Hitachi S4700, Hitachi Scientific Ltd., Tokyo, Japan). A sputter coating apparatus (Bio-Rad SC 502, VG Microtech, Uckfield, UK) was applied to induce electric conductivity on the surface of the samples. The air pressure was 1.3–13.0 MPa. Briefly, the samples were sputter-coated with gold–palladium under an argon atmosphere, using a gold sputter module in a high-vacuum evaporator and the samples were examined at 10 kV and 10 μA. Meloxicam particle diameter distributions were obtained by analyzing several SEM images with the ImageJ software environment.

2.6. Dissolution studies

The dissolution of physical mixtures and samples withdrawn after 140 min of grinding were determined

Please cite this article in press as: Mártha C et al. Effects of polymers on the crystallinity of nanonized meloxicam during a co-grinding process. Eur Polym J (2013), http://dx.doi.org/10.1016/j.eurpolymj.2013.03.006

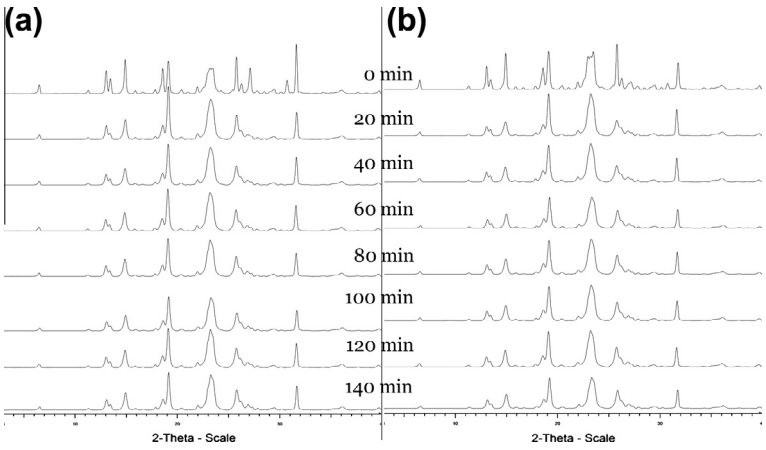

Fig. 1. XRPD diffractograms of MX made with PEGs; (a) MX:PEG 6000 (1:2); (b) MX:PEG 20,000 (1:2).

according to the European Pharmacopoeia (6th Edition) paddle method (Pharma test Heinburg, Germany), where a paddle was rotating in the dissolution vessel with speed of 100 rpm. All the samples contained 10 mg of the drug. The dissolution medium was 100.0 mL of phosphate buffer solution (pH 6.8 ± 0.1) at 37 ± 0.5 °C. 1 mL samples were withdrawn and immediately filtered (cut-off 0.2 μm, Minisart SRP 25, Sartorius, Germany) and the amount of dissolved drug was determined with spectrophotometrically (λ = 364 nm). Taken samples were replaced with 1 mL of fresh medium.

Drug content determination was carried out in 100.0 mL of phosphate buffer solution (pH 6.8 ± 0.1) at 37 ± 0.5 °C. Samples containing 10 mg of MX were stirred for 24 h. The solution was investigated by spectrophotometer (λ = 364 nm).

3. Results and discussion

3.1. X-ray diffraction

Figs. 1 and 2 show the diffractograms of the samples prepared. In each graph, the characteristic peaks of MX can be observed. As PEG is semi-crystalline, it gives a large peak, with a considerable full width at half-maximum, while PVP is fully amorphous, so it does not yield any signal in the diffractograms. At 31.6° 2θ, the specific peak relating to NaCl appears. Each figure shows the changes in crystallinity with time. Fig. 1a (PEG 6000) and b (PEG 20,000) demonstrate that no amorphization occurred during the co-grinding process: the areas under the peaks did not decrease radically. The samples prepared with the PVPs behaved differently: the areas under the peaks continuously decreased as the grinding time was lengthened (Fig. 2a (PVP C30) and b (PVP K25)). Although the drugs were not converted completely into the amorphous form, because the diffractograms exhibited small peaks in the amorphous halo, the change in crystallinity was drastic. During the co-grinding process, no other polymorphic form of MX appeared: no shift in the peaks and no new peaks were observed in the pattern.

To quantify the changes in time, the areas underneath the diffractograms were determined between 12° and 30° 2θ after Kα2-stripping, background removal and curve smoothing. The areas under the peaks relating to MX were divided by the areas under the peaks of NaCl. These values

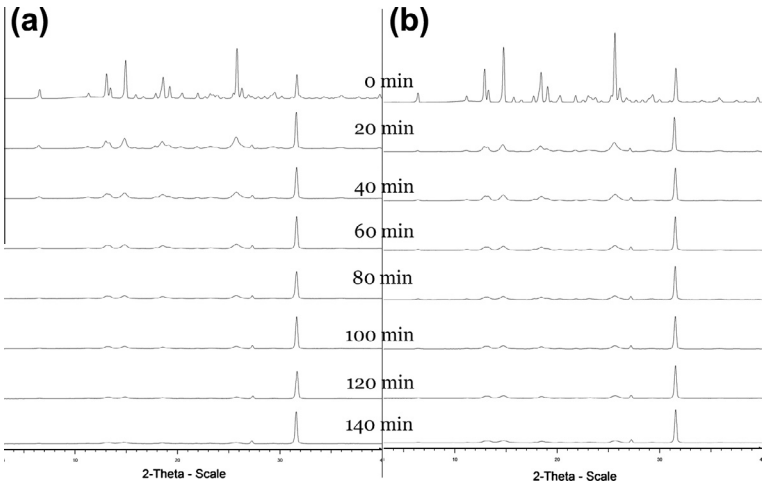

Fig. 2. XRPD diffractograms of MX made with PVPs; (a) MX:PVP K25 (1:1); (b) MX:PVP C30 (1:1).

Please cite this article in press as: Mártha C et al. Effects of polymers on the crystallinity of nanonized meloxicam during a co-grinding process. Eur Polym J (2013), http://dx.doi.org/10.1016/j.eurpolymj.2013.03.006

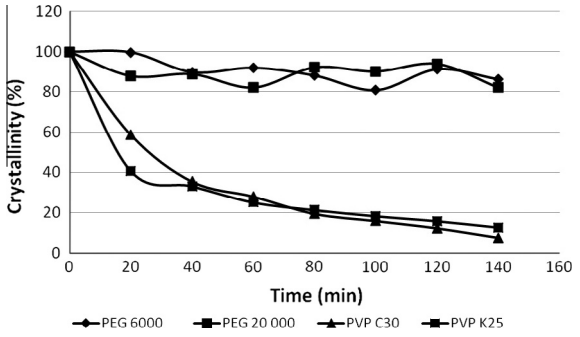

Fig. 3. Crystallinity changes of the samples.

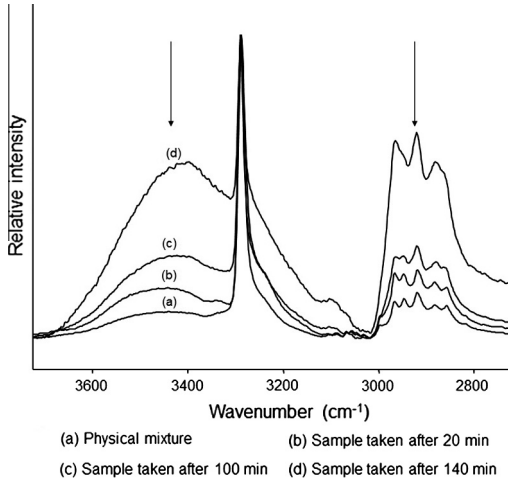

Fig. 4. FI-IR spectras of the samples made with PVP C30. Arrows show the increasing intensity at 3400–3500 cm^{-1} and between 3000 and 2800 cm^{-1}.

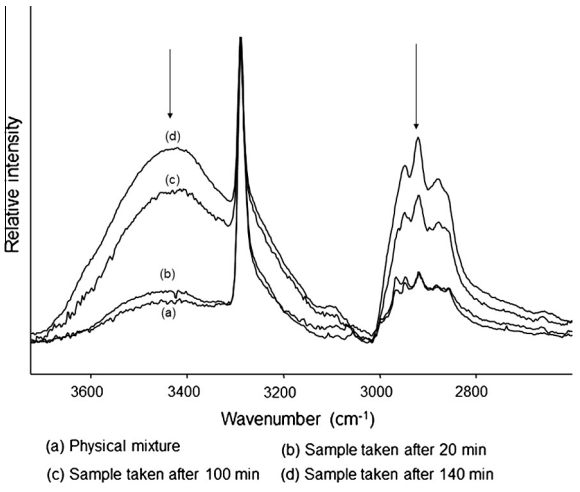

Fig. 5. FI-IR spectras of the samples made with PVP K25. Arrows show the same intensity changes as in case of PVP C30 at 3400–3500 cm^{-1} and between 3000 and 2800 cm^{-1}.

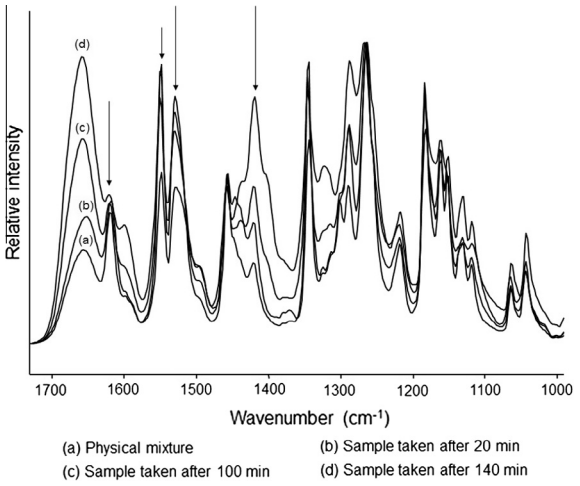

Fig. 6. FI-IR spectras of the samples made with PVP C30. The arrows point the changes related to secunder-amid groups. Increasing intensities can be observed around 1620 cm^{-1} (νCONH) and between 1550 cm^{-1} and 1530 cm^{-1} (νNH).

are illustrated in Fig. 2, which shows the crystallinity changes based on the areas under the peaks. The samples made with the PEGs did not undergo any amorphization. The long-range order of molecular packing remained. The diversity of the values may be caused by the variation in particle size, and the orientation of the larger particles. Samples involving the use of PVPs as grinding material lost their well-defined molecular conformation. The areas under the peaks decreased on increase of the grinding time. For PVP C30 and PVP K25, 12.23% and 15.66% of the MX remained in crystalline form at the end of the grinding process. To determine the difference between the rates of amorphization of the two different samples, logarithms were calculated (Fig. 3). The resulting plots were linear, and the diversity of the crystallinity could be observed

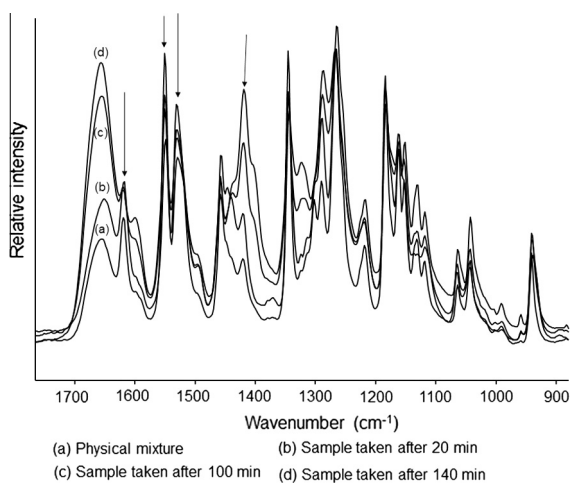

Fig. 7. FI-IR spectras of the samples made with PVP K25. Same changes can be observed as in case of PVP C30 at 1620 cm^{-1} and between 1550 cm^{-1} and 1530 cm^{-1}.

Please cite this article in press as: Mártha C et al. Effects of polymers on the crystallinity of nanonized meloxicam during a co-grinding process. Eur Polym J (2013), http://dx.doi.org/10.1016/j.eurpolymj.2013.03.006

via the slopes of the trend lines. The gradient of the equation relating to the samples made with PVP C30 was steeper (−0.0171) than that for those made with PVP K25 (−0.0127), which means that the use of PVP C30 as grinding material causes faster amorphization.

3.2. FT-IR spectroscopy

To determine whether any decomposition occurred during the grinding process and to search for any possible bonding between the API and the polymers, FT-IR spectroscopy was carried out. This proved that no disintegration took place in any of the samples. The characteristic bands of MX were seen in all of the curves.

No measurable changes were observed in the case of the products made with the PEGs. No shifts no changes in band shape and no new bands were detected in the curves. This means that bonds between the materials were not created by grinding. Changes in the intensities of the peaks can be explained by the decreasing particle size of the products.

The samples made with the PVP polymers exhibited several changes in the spectra during the grinding process (Figs. 4 and 5), most significantly in the interval 3725–2600 cm^{-1}. At 3400–3500 cm^{-1}, the intensity of the associated νOH mode increased with increasing grinding time. A similar increase was observed in the range of CH and NH valence vibrations, between 3000 and 2800 cm^{-1}. The separation of the two ranges is impracticable.

The most significant changes for both excipients are related to the secondary amide group of MX. Increases intensity can be observed at around 1620 cm^{-1} (νCONH) and between 1550 cm^{-1} and 1530 cm^{-1} (νNH). Further, the intensity relating to a hybrid stretching mode at around 1440 cm^{-1} is increased and a shoulder grows around 1390 cm^{-1} (Figs. 6 and 7).

All these alterations point to the presence of weak bonding between the carboxyl group of MX and the polymers, which is able to help the molecules to separate from each other and keep them in this (not well-defined) conformation.

3.3. SEM

Differences between the abilities of the polymers to decrease the crystallinity of MX can also be seen in the SEM photomicrographs. Fig. 8 presents SEM pictures of physical mixtures and samples (ground for 140 min) made with PEG 6000 and PVP C30. The PEGs have relatively low melting points, which were exceeded during the co-grinding process (the temperature of the mortar was not higher than 55 °C). The polymers are locally melted by the impact and friction of the balls in the mortar. Reduced-sized MX particles can be observed in the melt of the polymer. These particles are in the nanorange. The same phenomenon can be observed the samples made with PEG 20,000.

PVPs are amorphous polymers, and did not melt during the milling process. The temperature was locally higher than the T_g of the excipients, so the polymers softened and coated the amorphized MX. These MX particles more or less preserved their contour while they were decreased to the nanolevel.

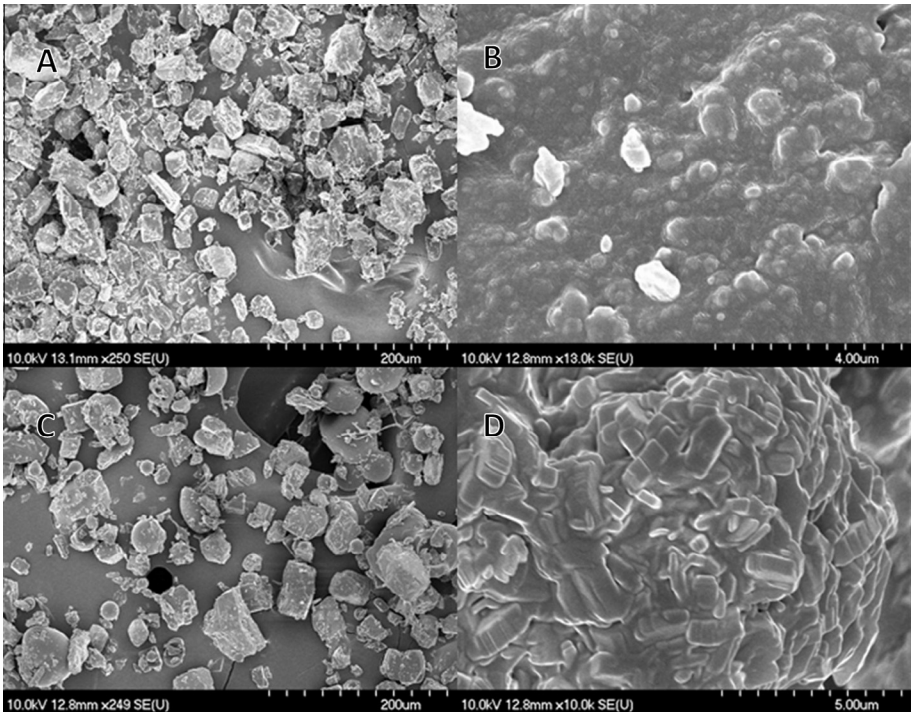

Fig. 8. SEM photomicrographs of samples made with PEG 6000 (“A” physical mixture, “B” sample ground for 140 min) and PVP C30 (“C” physical mixture, “D” sample ground for 140 min).

Please cite this article in press as: Mártha C et al. Effects of polymers on the crystallinity of nanonized meloxicam during a co-grinding process. Eur Polym J (2013), http://dx.doi.org/10.1016/j.eurpolymj.2013.03.006

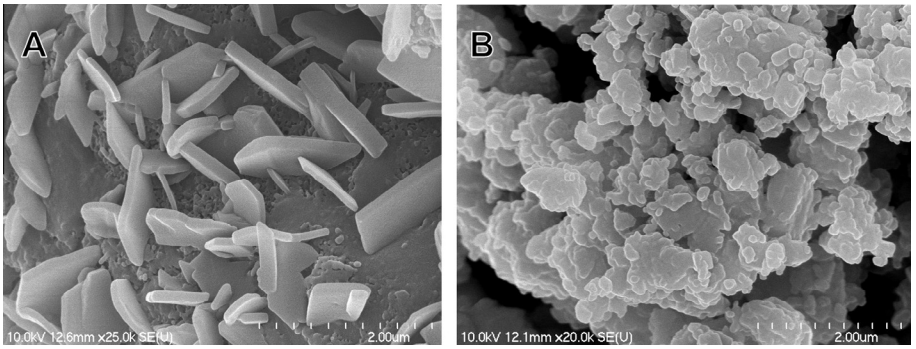

Fig. 9. MX particles, water soluble polymer additives: PEG 6000 "A"; and PVP C30 "B" removed.

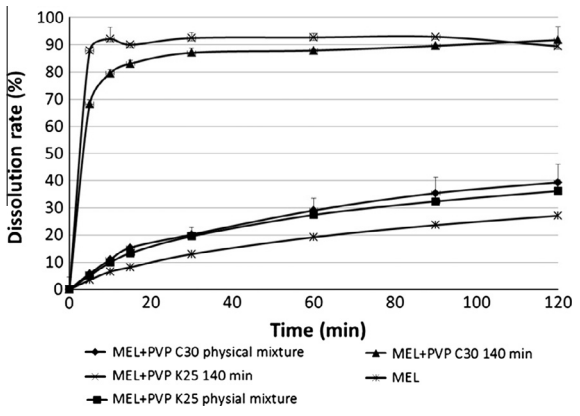

Fig. 10. Dissolution extents of pure MEL, physical mixtures and solid dispersions made with PVPs, withdrawn after 140 min of grinding.

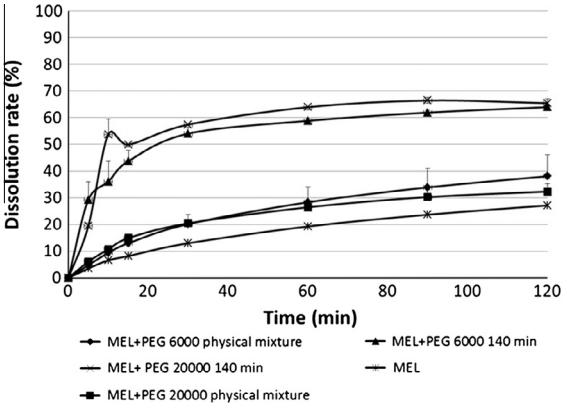

Fig. 11. Dissolution extents of pure MEL, physical mixtures and solid dispersions made with PEGs, withdrawn after 140 min of grinding.

To identify the habit of the MX particles formed by the co-grinding with the polymers, the water-soluble excipients were extracted from the system by washing-out with cold distilled water and the material was centrifuged three times. By this method, the water-insoluble MX (solubility meloxicam is 4.4 ± 0.7 μg/mL [16]) can be observed individually. The SEM images of the samples made with PEG (Fig. 9A) revealed well-formed crystalline MX particles with sharp edges. The shape and position of the particles indicate recrystallization. The MX molecules can dissolve into the melted PEG polymer, but immediately following the decrease of temperature, the MX precipitated out from the dispersion, forming crystalline particles. The samples made with the PVPs did not give sharp lines, but formed a shapeless amorphous mass.

3.4. Dissolution studies of prepared samples

Drug content determination showed, that actual drug content of each samples were 94.23% (±2.63%) of the theoretical drug content.

Dissolution studies of the samples showed that physical mixtures of MX and polymers have a similar dissolution profile as the pure MX (particle size of raw MX: d_{SEM}: 2643.6 ± 2629.1 nm). All mixtures made with PVPs and PEGs showed slightly higher and faster solubility. The dissolution of samples made with PVPs and ground for 140 min in the first 5 min was ~50 times greater than the dissolution of the corresponding physical mixtures. After 120 min more than 90% of the MX was dissolved in the media (Fig. 10). In case of samples with PEGs the dissolution was also higher, the extent of dissolution after 30 min was more than 60% (Fig. 11). The particle size of MX in the samples were: MX-PVP K25: d_{SEM}: 246.4 ± 108.5 nm; MX-PVP C30: d_{SEM}: 140.4 ± 69.2 nm; MX-PEG 6000: d_{SEM}: 229.5 ± 92.3 nm; MX-PEG 20000: d_{SEM}: 234.5 ± 122.9 nm. That means that the amount of released MX depends on the particle size of MX in the sample and also on the crystal structure, because the amorphous-nano-MX-PVP dispersions had a greater dissolution rate than the crystalline-nano MX-PEG compositions.

4. Discussion

The present work has demonstrated that the polymers used to reduce the grinding energy during co-grinding to nanoparticles can decrease the crystallinity of MX. These polymers have different abilities to convert the drug into amorphous form. XRPD measurements proved that the two different types of PEG did not have a significant effect

Please cite this article in press as: Mártha C et al. Effects of polymers on the crystallinity of nanonized meloxicam during a co-grinding process. Eur Polym J (2013), http://dx.doi.org/10.1016/j.eurpolymj.2013.03.006

on the crystallinity of MX, while the two different types of PVP decreased it drastically. Weak secondary bonding between MX and the PVPs was found by FT-IR and under these certain circumstances no degradation or decomposition occurred to MX. SEM images confirmed the major particle size decrease and the differences in crystal behavior of the samples made with the different polymers. All the ground samples exhibited a higher and faster dissolution rate, while the amorphous-nano-MX-PVP solid dispersions had an intense immediate dissolution.

Acknowledgements

The publication/presentation is supported by the European Union and co-funded by the European Social Fund. Project title: ''Broadening the knowledge base and supporting the long term professional sustainability of the Research University Centre of Excellence at the University of Szeged by ensuring the rising generation of excellent scientists.'' Project number: TÁMOP-4.2.2/B-10/1-2010-0012.

The help of Rita Ambrus and Ákos Kukovecz with the SEM measurements is gratefully acknowledged.

References

[1] Chen H, Khemtong C, Yang X, Chang X, Gao J. Nanoization strategies for poorly-water soluble drugs. Drug Discov Today 2011;16:354–60.
[2] Chen H, Khemtong C, Yang X, Chang X, Gao J. Nanonization strategies for poorly water-soluble drugs. Drug Discov Today 2011;16(7–8):1–7.
[3] Choi H, Lee W, Kim S. Effect of grinding aids on the kinetics of fine grinding energy consumed of calcite powders by a stirred ball mill. Adv Powder Technol 2009;20(4):350–4.
[4] Merisko-Liversidge EM, Liversidge GG. Drug nanoparticles: formulating poorly water-soluble compounds. Toxicol Pathol 2008;36(1):43–8.
[5] Yam N, Li X, Jasti BR. Interactions of topiramate with polyethylene glycol 8000 in solid state with formation of new polymorph. Int J Pharm 2011;411(1–2):86–91.
[6] Bailey FE, Koleske JV. Poly(ehtylene oxide). New York: Academic; 1976.
[7] Leuner C, Dressman J. Improving drug solubility for oral delivery using solid dispersions. Eur J Pharm Biopharm 2000;50(1):47–60.
[8] Sugimoto M, Okagi T, Narisawa S, Koida Y, Nakjima K. Improvement of dissolution characteristics and bioavailability of poorly water-soluble drugs by novel cogrinding method using water soluble-polymer. Int J Pharm 1998;160(1):11–9.
[9] Martini A, Torricelli C, De Ponti R. Physico-pharmaceutical characteristics of steroid-crosslinked polyvinylpyrrolidone coground systems. Int J Pharm 1991;75(2–3):141–6.
[10] Wu JZ, Ho PC. Evaluation of the in vitro activity and in vivo bioavailability of realgar nanoparticles prepared by cryo-grinding. Eur J Pharm Sci 2006;29(1):35–44.
[11] Mura P, Cirri M, Faucci MT, Ginès-Dorado JM, Bettinetti GP. Investigation of the effects of grinding and co-grinding on physicochemical properties of glisentide. J Pharm Biomed Anal 2002;30(2):227–37.
[12] Taylor LS, Zografi G. Spectroscopic characterization of interactions between PVP and indomethacin in amorphous molecular dispersions. Pharm Res 1997;14(12):1691–8.
[13] Watanabe T, Hasegawa S, Wakiyama N, Kusai A, Senna M. Comparison between polyvinylpyrrolidone and silica nanoparticles as carriers for indomethacin in a solid state dispersion. Int J Pharm 2003;250(1):283–6.
[14] Kurti L, Kukovecz A, Kozma G, Ambrus R, Deli M, Szabó-Révész P. Study of the parameters influencing the co-grinding process for the production of meloxicam nanoparticles. Powder Technol 2011;212(1):210–7.
[15] Hanft G, Türck D, Scheuerer S, Sigmund R. Meloxicam oral suspension: a treatment alternative to solid meloxicam formulations. Inflamm Res 2001;50(Suppl 1):S35–7.
[16] Ambrus R, Kocbek P, Kristl J, Sibanc R, Rajkó R, Szabó-Révész P. Investigation of preparation parameters to improve the dissolution of poorly water-soluble meloxicam. Int J Pharm 2009;381(2):153–9.

III

J Therm Anal Calorim (2014) 115:2479–2486
DOI 10.1007/s10973-013-3590-5

Investigation of the crystallinity of sugar alcohols co-ground with polymeric excipients

Csaba Mártha · Orsolya Jójárt-Laczkovich · Joachim Ulrich · Piroska Szabó-Révész

Received: 2 July 2013 / Accepted: 9 December 2013 / Published online: 22 December 2013

Abstract Particle size reducing methods demand high energy input, so during these procedures crystallinity change always can occur. These changes can be enhanced by additives, which are often used to improve the dissolution, the powder rheological properties or the processability of the API (active pharmaceutical ingredient), or to support the particle size reduction. Different materials act differently during these crystallinity changing methods: some materials are easy to amorphize, while some of them can be really resistant. In this work, two chemically equivalent sugar alcohols as model materials—β-D-mannitol as poor glass former and D-sorbitol as good glass former—were chosen to be co-ground with polymeric additives (PVP C30 and PEG 6000). During the 120 min milling process mannitol showed just minor change in crystallinity alone or with PEG. But milled with PVP some amorphization was found. Sorbitol suffered noteworthy changes in crystallinity: raw sorbitol lost its crystallinity during the milling, and also polymorphic transition was displayed. Same transition happened during the milling with PVP: the whole crystallinity of the sorbitol decreased, while the amount of gamma polymorph increased. During the co-grinding with PEG, the polymer prevented the amorphization of sorbitol and kept the well-ordered crystal structure of the material.

C. Mártha · O. Jójárt-Laczkovich · P. Szabó-Révész (✉)
Department of Pharmaceutical Technology, University of Szeged, Eötvös 6, Szeged 6720, Hungary
e-mail: revesz@pharm.u-szeged.hu

J. Ulrich
Center for Engineering Science, Process Technology, Martin Luther University Halle-Wittenberg, 06099 Halle, Germany

Keywords Mannitol · Sorbitol · Polyethylene glycol · Polyvinylpyrrolidone · Crystallinity · Co-grinding

Introduction

Grinding or milling is a technique that is widely used in pharmaceutical technology to increase the dissolution rate, the solubility, and the oral absorption of poorly water-soluble compounds [1–3]. Milling is also used to improve the processability and powder rheological properties of solid materials by formulating a spherical shape and enhancing the specific surface of the particles [4]. However, the accompanying high energy intake often causes major changes in the crystal structure of materials [5–7]. Mechanical activation can either break down the long-range order of the molecular packaging and turn the material into an amorphous form [8] or alter the order of the lattice structure and cause a polymorphic transition [9, 10]. This new arrangement is either stable or can recrystallize to the initial state during storage.

To reduce the high energy need, which is a general problem in particle size-reducing processes, suitable additives are used. These additives are able to reduce the friction between the particles and the milling device, and thereby they decrease the energy expended in grinding [11]. An appropriate additive can also avoid the aggregation of small particles by reducing the surface tension and the electrostatic charge. Moreover, the presence of these excipients can cause changes in crystallinity [12, 13]. For example polymers can adsorb drugs on their surface, or they can form co-crystals, eutectic mixtures or complexes.

To investigate the behaviour of organic drugs with low molecular mass during the milling process we chose simple and cheap sugar alcohols, β-D-mannitol and

D-sorbitol. Both are widely used in pharmaceutics as sweeteners, bulking agents or moisture stabilizers [14–16]. Both are stable and inert compounds, which are those properties that make them a good choice as excipients during tableting, freeze-drying, capsulizing, granulating or grinding [17–20]. They are often used together as carrier additives usually in pulmonary delivery systems [21]. Both can exist in many polymorphic-, solvate-, hydrate- and amorphous forms (mannitol has three stable polymorphs and sorbitol has 5) [22, 23].

Polyvinylpyrrolidone (PVP) is a fully amorphous polymer that is commercially available in various molecular masses and particle sizes. In pharmaceutics it is mostly used as binder, matrix polymer, disintegrant, crystallization inhibitor and stabilizer [24, 25]. It has been demonstrated that PVP is capable of decreasing the milling energy, while as a carrier it increases solubility in water [25, 26].

Polyethylene glycols (PEGs) are used in the pharmaceutical industry as binders, carriers, lubricants, etc. These semi crystalline excipients are water-soluble and completely biocompatible. They can be purchased in various molecular masses with different melting points [27, 28]. PEGs are able to reduce milling energy and enhance the water solubility of poor water-soluble drugs.

It has been reported that the ratio T_g/T_m *(K/K)* can serve as an appropriate value from which the glass-forming properties of materials can be inferred. If the value of this ratio is lower than 0.7 the given material is a poor glass-former, whereas if the value is higher than 0.7, the material is very likely a good glass-former [29–32].

In the present work, we investigated the influence of grinding and co-grinding with the polymer excipients, PVP and PEG, on crystallinity of the two common sugar alcohols, mannitol and sorbitol. These materials were chosen because they have similar chemical structures—they are diastereomers—but different glass-forming properties. In this relation, the investigated samples were monitored by XRPD and DSC techniques for the first time to our best knowledge.

Materials and methods

Materials

For our investigation two sugar alcohols were used: β-D-mannitol ((2*R*,3*R*,4*R*,5*R*)-Hexan-1,2,3,4,5,6-hexol) and D-sorbitol ((2*S*,3*R*,4*R*,5*R*)-Hexane-1,2,3,4,5,6-hexol). Both materials were purchased from Hungaropharma (Budapest, Hungary), which met the quality requirements of Ph.Eur.8.

PVP C30 (with a molecular mass of 58,000) which was obtained from BASF (Ludwigshafen, Germany) and PEG 6,000 from Sigma-Aldrich Chemie GmbH, München, Germany, were used as grinding excipients.

Grinding process

Physical mixtures of the crystalline sugar alcohols (mannitol and sorbitol) and stabilizer polymer additives (PVP C30 and PEG 6,000) were prepared and charged into a hard polyamide mortar. Equal amounts of agate balls were also placed into the chamber. The mass ratio of the mixtures was 1:1 in all cases. The grinding processes were carried out with a FRITSCH–Pulverisette® planetary ball mill.

Mixtures were ground for 120 min, samples being withdrawn for investigation after 20, 40, 60, 80, 100 and 120 min.

X-ray powder diffraction (XRPD)

XRPD analysis was performed with a Bruker D4 diffractometer (Bruker AXS GmbH, Karlsruhe, Germany) system with Cu K λI radiation ($\lambda = 1.5406$ Å). The samples were scanned at 40 kV and 40 mA from 3° to 40° 2θ, at a scanning speed of $0.05°s^{-1}$ and a step size of 0.010°. The crystallinity of the samples was determined as ratio between areas beneath characteristic and separate peaks of physical mixtures and samples and was expressed as percentage (%). These peaks are specific for each material; none of them is a double peak, or covered by the peak of the semi crystalline PEG. All manipulations of diffractograms and the calculation of area under curves were performed with DIFFRACTplus EVA software.

Differential scanning calorimetry (DSC)

DSC data were recorded with a Netzsch STA-409 (Selb, Germany) instrument with an intercooler. 4.5–5.5 mg samples were crimped in aluminium pans with two holes and were examined in the temperature interval 298.15–473.15 K under an argon gas flow at 100–150 mL min^{-1}, heating rate was 10 K min^{-1}.

Results and discussion

Determination of crystallinity of mannitol

The DSC measurements indicated that the ratio T_g/T_m *(K/K)* for pure β-D-mannitol (T_g 285.75 K T_m 440.05 K) is lower than 0.7, suggesting that this compound has only a low tendency to exist in amorphous form. β-D-mannitol has linear molecules and an orthorhombic crystal structure, which is preferable for the development of strong long-range order among the molecules.

Thermoanalytical techniques such as DSC or DTA are suitable methods for investigation of the crystallinity of samples. From the areas under the peaks of melting of the

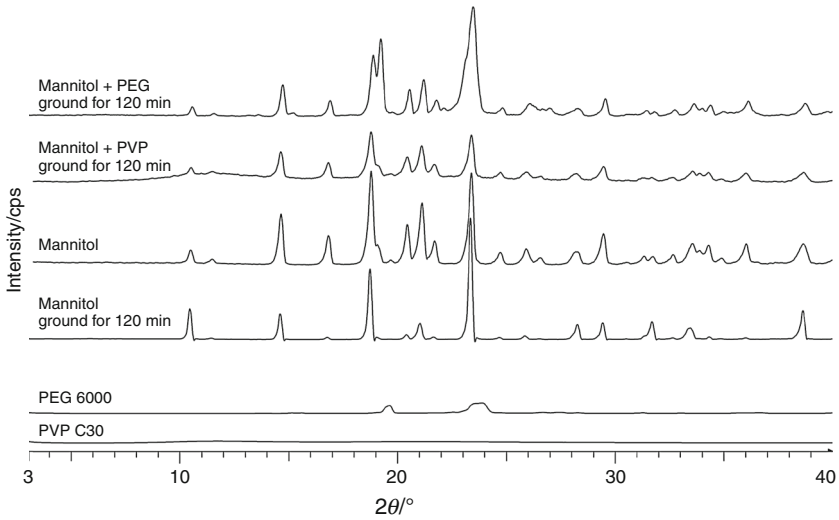

Fig. 1 X-ray diffractograms of pure PVP C30, PEG 6000, and mannitol; and mannitol samples ground for 120 min with PVP C30 and PEG 6000

samples can be concluded. DSC measurements demonstrated that the raw mannitol during the grinding process did not suffer any loss in crystallinity, and it exhibited a similar characteristic melting peak at the same temperature (440.05 ± 3.1 K), with identical enthalpy ($\Delta H = 41.02 \pm 1.13$ J g^{-1}) as for raw mannitol itself. The mannitol samples made with polymer additives behaved similarly to pure mannitol: the amorphous PVP has no peak in the DSC curve, while the semi crystalline PEG has a broad melting peak at around 338 K; the mannitol in the mixtures displayed identical melting action to that without polymers. Specific peaks relating to the melting point of mannitol appeared in the curves with slightly varying enthalpy ($\Delta H = 22.04 \pm 0.83$ J g^{-1}) indicating that the mannitol maintained it well-defined long-range order in the crystal structure.

XRPD measurements can also be used to investigate the crystal structure of ingredients. As it was shown before the limit of quantification (LOQ) of XRPD methods is low enough to use it for quantitative measurements. In case of clopidogrel bisulphate polymorphs and olanzapine polymorphs the LOQ were 1.0–1.5 % (w/w) and 1.22 % (w/w), respectively [33, 34]. The areas under diffraction peaks are related to the crystallinity from the changes of the independent characteristic peaks the decrease of crystallinity can be calculated.

XRPD measurements were performed on each of the raw materials and samples. Amorphous PVP exhibited a halo with no specific peaks in the diffractogram, PEG, as a semi crystalline polymer gave few broad peaks in the investigated range (Fig. 1). Pure mannitol displayed peak characteristics of the β-D form (sharp peaks at the following 2θ values: 10.441°, 14.572°, 18.722°, 21.019°, 23.374°, 28.282°, 29.444°, 31.728°, 38.645°, 44.052°). After 120 min of grinding, the same peaks were found in the curve. No shifts were observed, no peaks disappeared and no new peaks appeared. The areas under peaks at 9.5–11° 2θ; 13.7–15.5° 2θ and 17.7–19.9° 2θ were calculated for each sample that were withdrawn. This revealed that, although some peaks decreased to an insignificant extent, no fundamental change in crystallinity occurred during grinding (Fig. 2).

Same grinding and investigation method was applied in the presence of the polymer additives. The samples containing PEG gave the peaks characteristic of mannitol and the broad peak relating to PEG at around 22–24° 2θ. Crystallinity determination (based on the same peaks as utilised in the case of raw mannitol) proved that minor amorphization took place after 40 min of milling. No polymorph transition was observed: no peaks underwent a shift or disappeared and no new peaks were detected. Slightly different behaviour was observed for the samples containing PVP. The peaks were specific for mannitol, but the areas under the curves decreased with increasing grinding duration. The degree of this decrease exceeded the quantification limit and could not be interpreted in terms of a decrease in particle size. The change in crystallinity did not exceed 70 % during the milling. After 40 min of grinding an apparent equilibrium set between the crystalline and amorphous phases.

Crystallinity determination of sorbitol

The ratio T_g/T_m (T_g and T_m in K) measured for D-sorbitol was 0.75 (T_g 273.92 K T_m 364.55 K), which predicted this material is a good glass-former.

The DSC measurements showed that the sorbitol used was a mixture of the epsilon (T_m 364.55 K) and gamma (372.05 K) polymorphs. During the grinding process, the proportions of the polymorphs changed. The pure material

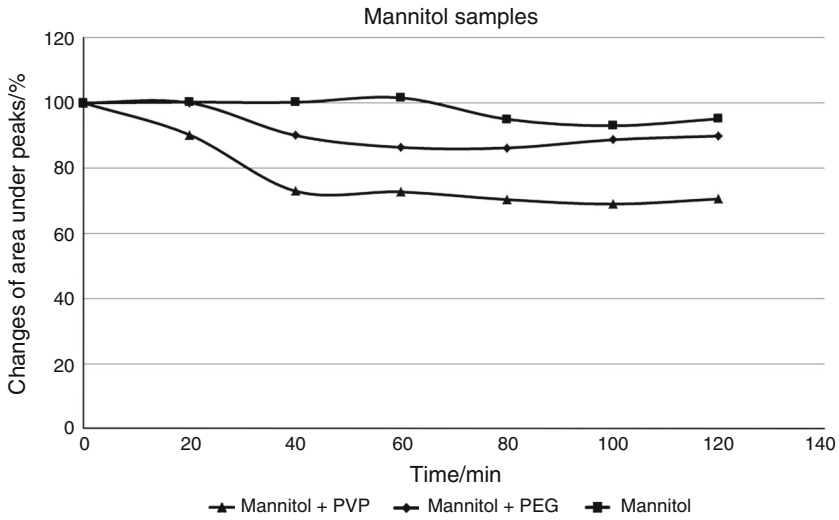

Fig. 2 Crystallinity change of mannitol and mannitol ground with polymer additives by milling time

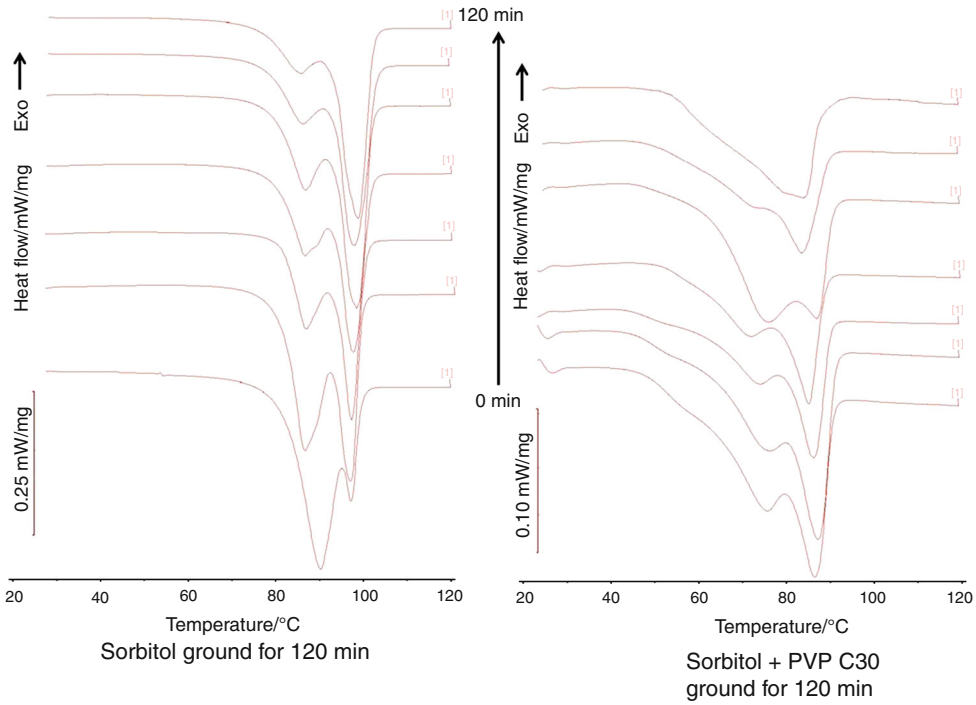

Fig. 3 DSC curves of pure sorbitol grinding, and sorbitol ground with PVP C30

contained a predominance of the epsilon form. The milling led to a decrease in the amount of the epsilon form, while the amount of the gamma polymorph slightly increased (Fig. 3). This means that the mechanical energy broke down the crystal structure of the crystalline epsilon sorbitol. Some of the amorphous material recrystallized due to the mechanical impact.

A similar phenomenon was observed in the DSC curves of sorbitol co-ground with PVP. The melting point of the sorbitol was lowered by the polymer excipient. Both polymorphs gave characteristic DSC curve. Similarly as when no additive was present, the epsilon polymorph amount decreased during the milling. In this case, the content of gamma polymorph also decreased, as demonstrated by the decrease of the area under the curve. The bulk part of the system lost its well-defined long-range order of the crystal structure.

The DSC investigation of sorbitol samples containing PEG did not show any significant change in crystallinity. The melting point of the semi crystalline polymer and the melting of sorbitol were to be seen in the curves. The areas under the melting peak of sorbitol varied only slightly during the milling ($\Delta H = 25.04 \pm 1.25$ J g^{-1}), within the error of the measurement. No amorphization or polymorphic alteration was noted during the milling of these two materials.

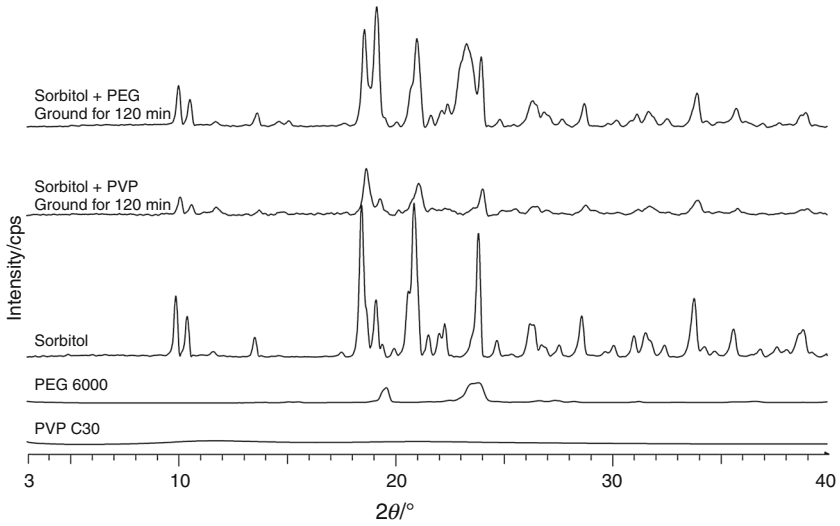

Fig. 4 X-ray diffractograms of pure PVP C30, PEG 6000, and sorbitol; and sorbitol samples ground for 120 min with PVP C30 and PEG 6000

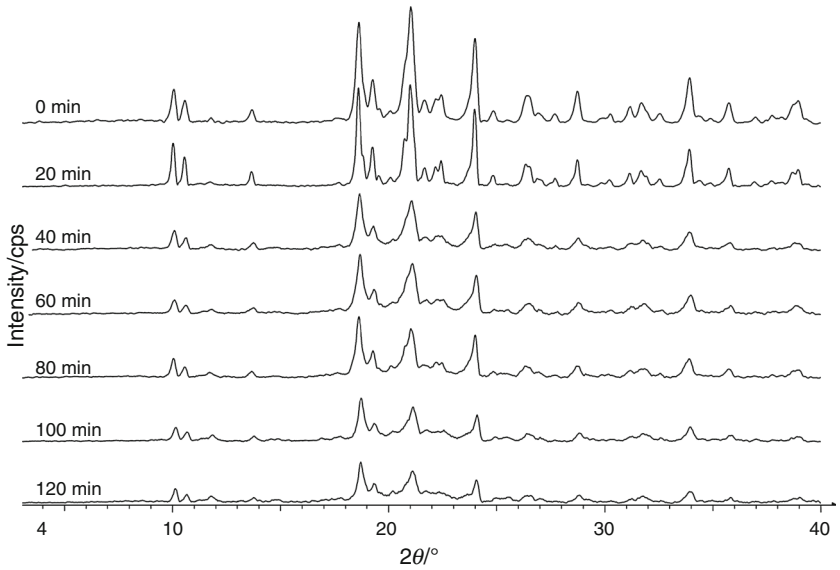

Fig. 5 X-ray diffractograms of sorbitol samples ground with PVP and withdrawn in every 20 min

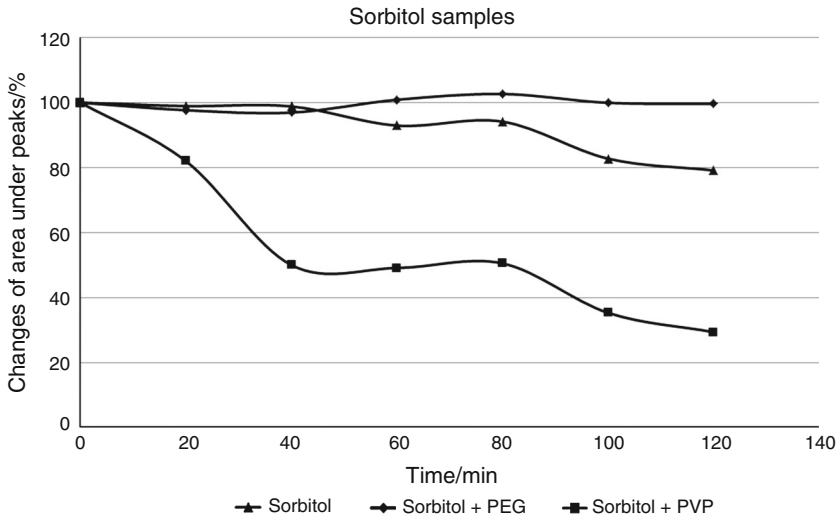

Fig. 6 Crystallinity change of sorbitol and sorbitol ground with polymer additives by milling time

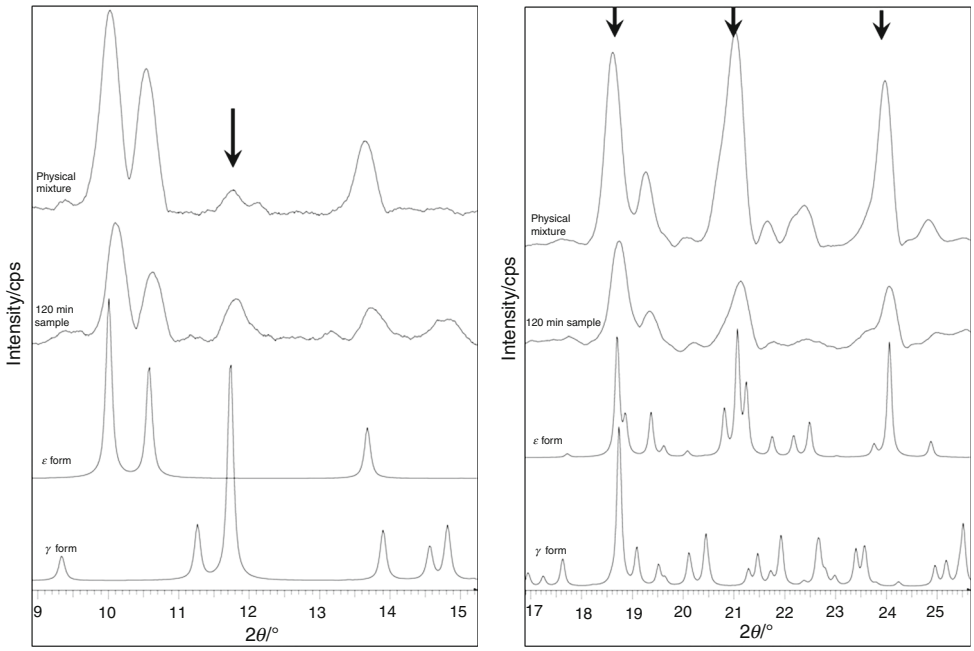

Fig. 7 Polymorphic transition of sorbitol during milling with PVP excipient. While the amount of epsilon form decreases by the milling time, the amount of gamma form increases. Diffractograms of epsilon and gamma forms are acquired from Cambridge Crystallographic Data Centre (CCDC)

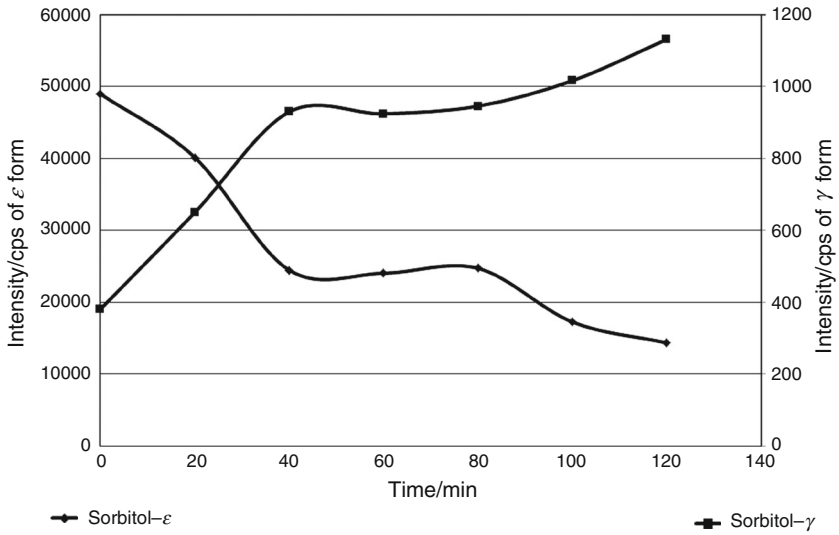

Fig. 8 Crystallinity change of different sorbitol polymorphs. The left "*y*" axis is for the epsilon form, the right one is for the gamma form. It shows the similar course of the decrease of the epsilon and the increase of the gamma form

To investigate the change in crystallinity of the co-ground sorbitol and to calculate the extent of amorphization, XRPD method was also carried out on the samples (Fig. 4).

The peaks of X-ray diffractograms of pure sorbitol were mostly characteristic of the epsilon form, though the peaks of the gamma form were also present. The determination of the polymorphs was based on the calculated X-ray powder diffractograms to be found in Cambridge Crystallographic Data Centre (CCDC). During the milling process the areas under the peaks relating to the epsilon form noticeably decreased with milling time. In parallel the peaks of the gamma polymorph became slightly larger at a similar rate. This phenomenon which affected slightly more than 20 % of the ground sorbitol could occur in two ways: mechanical energy converted some of the material into the amorphous phase and the gamma form recrystallized from this; or the epsilon form was transformed directly to the gamma form.

A similar polymorph transition took place during the grinding of sorbitol with PVP: peaks relating to both polymorph forms were found in the diffractogram of the physical mixture. During the milling process the areas under the peak characteristics of the epsilon form decreased markedly (Fig. 5). From the areas under the peaks of the epsilon form at 9.5–11° 2θ, 23.15–24.53° 2θ and 28.2–29.6° 2θ, the degree of reduction in crystallinity was measured (Fig. 6). During the first 40 min the system lost about 50 % of its well-defined crystal structure. After 40 min there was an apparent lag phase. At the end of the

milling, slightly more than 30 % of the sorbitol remained in the epsilon polymorph form. Most of the remaining 70 % had lost its well-defined order of molecular packing and a minor part had been transformed into the gamma polymorph (Fig. 7). Only the peak at 11.5–12.1° 2θ is related clearly to the gamma form. All the other peaks were characteristic either of epsilon form or of both polymorphs. This gamma sorbitol peak was used to evaluate the polymorphic transition. Figure 8 illustrates the decrease in the epsilon form and the increase in the gamma form with the milling time. The figure has two "*y*" axes scaled differently to demonstrate the similar courses of the changes in proportions of the two polymorphs. There was a strong decrease in epsilon form initially, which was accompanied by a comparable rapid increase in the gamma form. After apparent lags, phase between 40 and 80 min both changes (increasing of gamma and decreasing of epsilon from) continued similarly. This polymorph alteration was confirmed by the changes in the other peaks. Whereas the peaks clearly relating to the epsilon form (for example those at 23.15–24.53° 2θ and 28.2–29.6° 2θ) decreased continuously with the grinding time, the common peaks (at 18.1–19.1° 2θ) diminished only slightly. All the changes observed are indicative of a constant crystallinity decrease as the milling time becomes longer, some of the sorbitol recrystallizing and changing into the gamma polymorphic form during the process.

The samples containing PEG displayed different behaviour during mechanical activation. The degree of crystallinity changed by around 100 % during the overall procedure. The sorbitol did not suffer any loss in crystal structure. As the sorbitol itself, in the absence of excipient did lose its crystallinity noticeably, it can be concluded, that PEG stabilized the crystal structure of this sugar alcohol and helped it maintain its crystallinity. No polymorphic transformation was detected in the X-ray pattern.

Discussion

Our study highlighted the problem that analogous materials can react differently to a high energy impact and therefore it can alter their physical and physical–chemical properties so critically, that can exclude their use as a pharmaceutical additive. Two chemically equivalent sugar alcohols (mannitol and sorbitol), as model materials, were subjected to milling both alone and in presence of polymer excipients (PVP C30 and PEG 6000) to accentuate the different behaviour of analogous materials. As a poor glass-former mannitol did not show any decrease in crystallinity when it was milled alone or together with PEG. In presence of PVP the crystal structure of mannitol was slightly lost. When ground alone or together with PVP, sorbitol suffered amorphization and underwent polymorph transformation when co-ground together: the initial mostly epsilon form continuously transited into gamma form, while parallel lost more than 70 % of its crystallinity. PEG preserved the well-ordered molecular packing of sorbitol and stabilized the crystal structure therefore the sorbitol could not amorphize. It can be concluded that these sugar alcohols which have the same chemical structure, went through different rate of crystallinity loss.

Acknowledgements The work was supported by the European Union and cofunded by the European Social Fund (TÁMOP-4.2.2.A-11/1/KONV-2012-0035). The authors wish to acknowledge the cooperation supported by MÖB/DAAD. The help of Kati Bergt, Lydia Helmdach and Kristin Wendt with the XRPD and DSC measurements is gratefully acknowledged.

References

1. Chen H, Khemtong C, Yang X, Chang X, Gao J. Nanoization strategies for poorly-water soluble drugs. Drug Discov Today. 2011;16:354–60.
2. De Jong WH, Borm PJA. Drug delivery and nanoparticles: applications and hazards. Int J Nanomed. 2008;3(2):133–49.
3. Kurti L, Kukovecz A, Kozma G, Ambrus R, Deli MA, Szabo-Revesz P. Study of the parameters influencing the co-grinding process for the production of meloxicam nanoparticles. Powder Technol. 2011;212(1):210–7.
4. Mallick S, Pattnaik S, Swain K, De PK, Saha A, Ghoshal G, Mondal A. Formation of physically stable amorphous phase of ibuprofen by solid state milling with kaolin. Eur J Pharm Biopharm. 2008;68:346–51.
5. Sharma P, Denny WA, Garg S. Effect of wet milling process on the solid state of indomethacin and simvastatin. Int J Pharm. 2009;380:40–8.
6. Brodka-Pfeiffer K, Langguth P, Grafi P, Hausler H. Influence of mechanical activation on the physical stability of salbutamol sulphate. Eur J Pharm Biopharm. 2003;56:393–400.
7. Yonemochi E, Kitahara S, Maeda S, Yamamura S, Oguchi T, Yamamoto K. Physicochemical properties of amorphous clarithromycin obtained by grinding and spray drying. Eur J Pharm Sci. 1999;7:331–8.
8. Mártha C, Kürti L, Farkas G, Jójárt-Laczkovich O, Szalontai B, Glässer E, Deli MA, Szabó-Révész P. Effects of polymers on the crystallinity of nanonized meloxicam during a co-grinding process. Eur Polym J. 2013;49:2426–32.
9. Lin SY, Hsu CH, Ke W. Solid-state transformation of different gabapentin polymorphs upon milling and co-milling. Int J Pharm. 2010;396:83–90.
10. Chieng N, Rades T, Saville D. Formation and physical stability of the amorphous phase of ranitidine hydrochloride polymorphs prepared by cryo-milling. Eur J Pharm Biopharm. 2008;68:771–80.
11. Yu S, Adams MJ, Gururajan G, Reynolds G, Roberts R, Wu CY. The effects of lubrication on roll compaction, ribbon milling and tableting. Chem Eng Sci. 2013;86:9–18.
12. Arias MJ, Moyano JR, Gines JM. Investigation of the triamterene-β-cyclodextrin system prepared by co-grinding. Int J Pharm. 1997;153:181–9.
13. Bettinetti G, Mura P, Faucci MT, Sorrenti M, Setti M. Interaction of naproxen with noncrystalline acetyl β- and acetyl γ-cyclodextrins in the solid and liquid state. Eur J Pharm Sci. 2002;15:21–9.

14. Izutsu K, Yoshioka S, Terao T. Effect of mannitol crystallinity on the stabilization of enzymes during freeze-drying. Chem Pharm Bull. 1994;42:5–8.
15. Kim AI, Akers MJ, Nail SL. The physical state of mannitol after freeze-drying: effects of mannitol concentration, freezing rate, and a noncrystallizing cosolute. J Pharm Sci. 1998;87:931–5.
16. Maury M, Murphy K, Kumar S, Mauerer A, Lee G. Spray-drying of proteins: effects of sorbitol and trehalose on aggregation and FT-IR amide I spectrum of an immunoglobulin G. Eur J Pharm Biopharm. 2005;59:251–61.
17. Tee SK, Marriot C, Zeng XM, Martin GP. The use of different sugars as fine and coarse carriers for aerosolised salbutamol sulphate. Int J Pharm. 2000;208:111–23.
18. Reitz E, Vervaet C, Neubert RHH, Thommes M. Solid crystal suspensions containing griseofulvin—preparation and bioavailability testing. Eur J Pharm Biopharm. 2013;83:193–202.
19. Gombás Á, Szabó-Révész P, Regdon G Jr, Erős I. Study of thermal behaviour of sugar alcohols. J Therm Anal Calorim. 2003;73:615–21.
20. Pomázi A, Ambrus R, Sipos P, Szabó-Révész P. Analysis of co-spray-dried meloxicam–mannitol systems containing crystalline microcomposites. J Pharm Biomed Anal. 2011;10/56(2):183–90.
21. Hamishehkar H, Emami J, Najafabadi AR, Gilani K, Minaiyan M, Mahdavi H, Nokhodchi A. Effect of carrier morphology and surface characteristics on the development of respirable PLGA microcapsules for sustained-release pulmonary delivery of insulin. Int J Pharm. 2010;15/389(1–2):74–85.
22. Cavatur RK, Vemuri NM, Pyne A, Chrzan Z, Toledo-Velasquez D, Suryanarayanan R. Crystallization behavior of mannitol in frozen aqueous solutions. Pharm Res. 2002;19:6.
23. Nezzal A, Aerts L, Verspaille M, Henderickx G, Redl A. Polymorphism of sorbitol. J Cryst Growth. 2009;311:3863–70.
24. Martini A, Torricelli C, De Ponti R. Physico-pharmaceutical characteristics of steroid-crosslinked polyvinylpyrrolidone co-ground systems. Int J Pharm. 1991;75(2-3):141–6.
25. Wu JZ, Ho PC. Evaluation of the in vitro activity and in vivo bioavailability of realgar nanoparticles prepared by cryo-grinding. Eur J Pharm Sci. 2006;29(1):35–44.
26. Mura P, Cirri M, Faucci MT, Ginès-Dorado JM, Bettinetti GP. Investigation of the effects of grinding and co-grinding on physicochemical properties of glisentide. J Pharm Biomed Anal. 2002;30(2):227–37.
27. Ambrus R, Aigner Z, Catenacci L, Bettinetti G, Szabó-Révész P, Sorrenti M. Physico-chemical characterization and dissolution properties of nifluminic acid-cyclodextrin-PVP ternary systems. J Therm Anal Calorim. 2011;104:291–7.
28. Yam N, Li X, Jasti BR. Interactions of topiramate with polyethylene glycol 8000 in solid state with formation of new polymorph. Int J Pharm. 2011;411(1-2):86–91.
29. Bailey FE, Koleske JV. Poly(ethylene oxide). New York: Academic; 1976.
30. Craig DQM, Royall PG, Kett VL, Hopton ML. The relevance of the amorphous state to pharmaceutical dosage forms: glassy drugs and freeze dried systems. Int J Pharm. 1999;179:179–207.
31. Yu L. Amorphous pharmaceutical solids: preparation, characterization and stabilization. Adv Drug Deliv Rev. 2001;48:27–42.
32. Jójárt-Laczkovich O, Szabó-Révész P. Formulation of tablets containing an 'in-process' amorphized active pharmaceutical ingredient. Drug Dev Ind Pharm. 2011;37:1272–81.
33. Uvarov V, Popov I. Development and metrological characterization of quantitative X-ray diffraction phase analysis for the mixtures of clopidogrel bisulphate polymorphs. J Pharm Biomed Anal. 2008;46:676–82.
34. Tiwari M, Chawla G, Bansal AK. Quantification of olanzapine polymorphs using powder X-ray diffraction technique. J Pharm Biomed Anal. 2007;43:865–72.

IV

Csaba Mártha
Orsolya Jójárt-Laczkovich
Piroska Szabó-Révész

University of Szeged, Department of Pharmaceutical Technology, Szeged, Hungary.

Effect of Co-Grinding on Crystallinity of Clopidogrel Bisulfate

A high energy input during pharmaceutical formulation is capable of decreasing the crystallinity of compounds in the product. The presence of the amorphous form can cause serious problems at any stage of the formulation. Crystallinity changes of a model powder mixture containing clopidogrel bisulfate (CLP) and a colloidal silicon dioxide as additive were investigated during a long-time co-grinding process. The crystallinity of CLP was reduced sigmoidally by co-grinding with longer co-grinding time. X-ray powder diffraction and differential scanning calorimetry examinations confirmed that the product had become totally amorphous after four hours of grinding. Thermogravimetric results proved that no major mass reduction happened and FT-IR changes referred to formulation of a secondary bond between the components.

Keywords: Clopidogrel bisulfate, Co-grinding, Crystallinity, FT-IR

Received: February 24, 2014; *revised:* April 25, 2014; *accepted:* May 06, 2014

DOI: 10.1002/ceat.201400120

1 Introduction

In pharmaceutical processing, the amorphous form of compounds frequently appears. It can be prepared deliberately when the properties of a poorly water-soluble active pharmaceutical ingredient (API) need to be changed, or accidentally when any of the ingredients convert into their amorphous form during the formulation process [1]. In the deliberate case, the amorphous form can be prepared in three ways: quench-cooling of melts [2, 3], rapid solvent evaporation [4, 5], and grinding [6–8]. Accidentally, the crystallinity of materials can decrease during many formulation processes, e.g., lyophilization [9], spray-drying [10], tableting [11], nano-crystallization, grinding etc. [12]. Generally, amorphous materials exhibit a faster dissolution rate, but sometimes the other properties can cause major problems in formulation: above the glass transition temperature they become sticky, gummy, and viscous, thereby making the formulation impossible. Mostly, the amorphous form of the material is physically and chemically less stable than the crystalline form [13, 14].

Grinding is a widely used process in pharmaceutical formulation for particle size decreasing, micronization, and nanonization [15–19]. By increasing the specific area and making spherical shapes, grinding can improve the dissolution rate of poorly water-soluble drugs. Processes like grinding are often accompanied by changes in the crystallinity of the material because of high energy input. It can cause polymorphic transformations, e.g., the amorphous form of a crystalline API may appear [20, 21]. This is especially true for co-grinding [22, 23], when an appropriate excipient is used which is able to reduce the free energy of the system and the energy demand of the amorphization process. This can lead to a major decrease in crystallinity [24].

Some materials show a higher tendency to exist in amorphous form. One of these materials which are named in literature as good glass formers, is CLP (methyl(+)-(*S*)-*α*-(2-chlorophenyl)-6,7-dihydrothieno[3,2-c]pyridine-5(4*H*)-acetate sulfate). Several researchers prepared and analyzed the amorphous and polymorphic forms of CLP [25–28]. The most popular and easy way to turn CLP into its amorphous phase is solvent evaporation. For this method, any of its good organic solvents are suitable, as demonstrated in a work formerly published by our team. In that article, a physically stable amorphous form of CLP was prepared and stabilized by Aerosil 200. The optimized mass ratio of the components was 7:3 of CLP:Aerosil 200. In this process, a generated hydrogen bond was also discovered between silanol groups of Aerosil 200 and CLP molecules [29].

CLP is also appropriate for co-grinding because of its high melting point (181.2 °C) since it does not melt during milling. Through the grinding process, the temperature of the system had to be below the glass transition temperature $(T)_g$[1)] of the CLP, which is 83 °C [28], because below the T_g the free energy and enthalpy of the system is much lower. Aerosil 200 was used because of its amorphous properties, so it has neither any thermal sign nor any peak on X-ray powder diffraction (XRPD) diffractograms [30].

Correspondence: Prof. Piroska Szabó-Révész (revesz@pharm.u-szeged.hu), University of Szeged, Department of Pharmaceutical Technology, Eötvös u. 6, 6720 Szeged, Hungary.

1) List of symbols at the end of the paper.

The changes of crystallinity of a model powder mixture containing CLP and Aerosil 200 during a long time co-grinding process were determined. The interaction between CLP and Aerosil 200 was studied to detect whether a H-bond forms also by grinding. Finally, the changes of the crystallinity of the system were quantified.

2 Materials and Methods

2.1 Materials

Pure polymorphic form II clopidogrel bisulfate (methyl(+)-(*S*)-α-(2-chlorophenyl)-6,7-dihydrothieno[3,2-c]pyridine-5(4*H*)-acetate sulfate) was obtained from EGIS Nyrt., Budapest. Aerosil 200, a colloidal SiO_2 with hydrophilic properties, was purchased from Nippon Aerosil Co., Japan.

2.2 Co-Grinding

Co-grinding of the mixture of the two components was performed in a planetary ball mill (Retsch PM 100, Retsch GmbH & Co., Germany). The mass ratio of CLP and Aerosil 200 was 7:3, based on a previous work of our team. The maximum grinding time was 240 min. Samples were withdrawn for investigation after 15, 30, 45, 60, 90, 120, 150, 180, and 240 min. During the grinding procedure, the temperature was controlled by an infrared thermometer. The temperature was not higher than 60 °C through milling.

2.3 Differential Scanning Calorimetry (DSC) and Thermogravimetry (TG)

The DSC investigation was recorded with a Mettler-Toledo DSC 821e instrument with an intercooler and the TG curve was obtained by a TGA/DSC (Mettler-Toledo, Switzerland). Sample portions of 4.5–5.5 mg were crimped in aluminum pans with two holes and examined in the temperature interval 25–200 °C under an argon gas flow at 100–150 mL min^{-1}. The heating rate was 20 °C min^{-1}.

2.4 X-Ray Powder Diffraction (XRPD)

XRPD analysis was performed on a Bruker D8 Advance diffractometer (Bruker AXS GmbH, Karlsruhe, Germany) system with hot-humidity stage, with Cu K λI radiation (λ = 1.5406 Å). The samples were scanned at 40 kV and 30 mA from 3° to 50° 2θ using a scanning speed of 0.1° s^{-1} and a step size of 0.010°. The relative humidity was 60 %, the temperature range was 25, 80, and 95 °C, and the heating rate was 20 °C min^{-1}. Crystallinity determination was based on the total area below the curve between 8° and 36° 2θ.

The quantification was based on the result of the XRPD measurement. The crystallinity of the investigated material is proportional to the area below the peak of the diffractogram. Using this correlation, the crystallinity of each sample can be quantified. The quantification is based on the total area below the diffractograms between 8° and 36° 2θ after smoothing and background removal.

For linearization of this function Avrami's equation was applied:

$$X(t) = \ln[-\ln(1-\Delta A_f/\Delta A_0)] \quad (1)$$

where A_f is the netto area below the peaks and A_0 is the netto area below the peaks at 0 min.

2.5 FT-IR Spectroscopy

FT-IR spectra were obtained with a Bio-Rad Digilab Division FTS- 65A/896 FTIR spectrometer between 4000 and 400 cm^{-1}, at an optical resolution of 4 cm^{-1}, operating Harrick's Meridian SplitPea single reflection, diamond, ATR accessory. Thermo Scientific GRAMS/AI Suite software was used for spectral analysis.

3 Results and Discussion

3.1 DSC Determination

As thermal analysis techniques are widely used for characterization of amorphous forms [30, 31], the raw CLP, the Aerosil 200, and the prepared samples were investigated by DSC. The curve of the raw CLP gave a characteristic sharp peak at 181.2 °C, corresponding to the melting point of the material. Any other changes were not observed on the curve, which means that the CLP contained no moisture or any rest solvent. The amorphous additive Aerosil 200 did not exhibit any thermal signal, so it is practically amorphous and had no moisture or any rest solvent either.

The curves of samples display that an endothermic peak of the CLP's melting point appears on each curve of the samples, except for the last one at 240 min (Fig. 1). The heights of the peaks belonging to the melting point decreased with increasing grinding time until they practically disappeared after 240 min of grinding. The peak of the physical mixture was similar to the peak of the raw CLP, with a smaller area according to the mass ratio. It indicates the decreasing crystallinity of the CLP which was finally converted into the amorphous phase. The peaks during grinding are slightly shifted to lower temperatures. It was impossible to determine the exact peak areas because of the imprecise pre- and post-baseline fittings of the melting peaks. The DSC method was not applicable for further semi-quantitative determination.

3.2 X-Ray Diffraction

The XRPD process is an appropriate method to determine the crystallinity of materials. The X-ray pattern of the raw CLP exhibits characteristic high-intensity diffraction peaks, which proves the crystalline nature of the unprocessed API. A comparison of the CLP determination with data from the Cam-

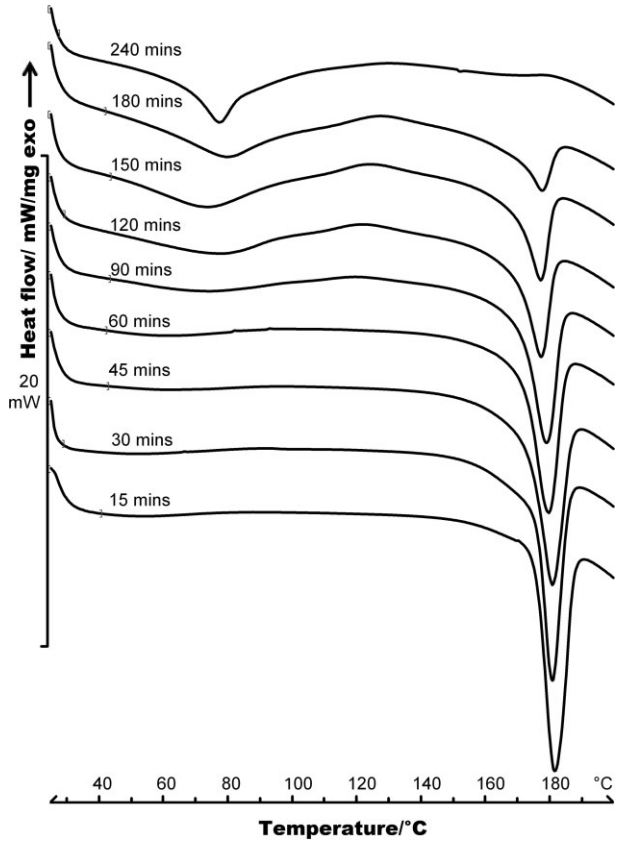

Figure 1. DSC curves of the samples were ground for 15, 30, 45, 60, 90, 120, 150, 180, and 240 min. The endothermic peak of CLP appears on each curve, and the areas below the peaks are decreasing with the grinding time. After 120 min of grinding an emerging peak can be observed at 80 °C.

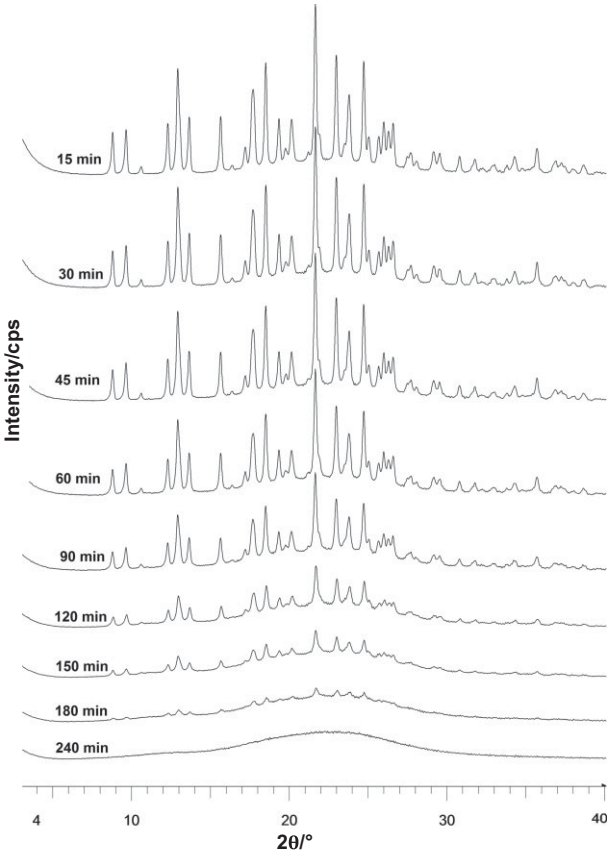

Figure 2. XRPD diffractograms of samples. The characteristic peaks of CLP are decreasing with longer grinding time. The last sample at 240 min shows no peaks, so it is practically amorphous.

bridge Crystallographic Data Centre (CCDC ID: AI631510) proved that this API is of the polymorphic form II. The pattern of Aerosil 200 does not show any peaks in the measured interval, which means that the excipient is practically amorphous.

The typical peaks of the CLP emerge clearly on the diffractograms of the ground products (Fig. 2). The intensities of these peaks were lower than those of the peaks for the raw API corresponding to the concentration of the materials in the samples. The amorphous Aerosil 200 does not show any further reflection. The intensities of these peaks are decreasing with longer grinding time and practically disappear after co-grinding for 240 min. The diffractogram of the last sample displays the amorphous halo. During the co-grinding process no other polymorphic form of the CLP appeared because no shifting of the peaks or appearance any new peak can be observed on the pattern.

Quantification of the crystallinity decrease was performed according to Avrami's equation and is displayed in Fig. 3. Obviously, the decrease of the crystallinity changes sigmoidally upon longer grinding time. The rise of the fitted trend line refers to the speed coefficient of the formation of the amorphous product. The regression line equation is:

$y = -0.0233x + 1.619$; $R^2 = 0.9935$.

According to this phenomenon, the crystallinity of the products starts to decrease slowly. After a certain time is elapsed, the decrease is getting faster, and at the end of the procedure the curve of amorphization is flattening. This procedure can be caused by an in-process formed secondary bond between the API and the excipient because the formation of the bond is an energy-intensive process.

3.3 TG and Hot-Humidity Stage XRPD

In the curves of the samples ground more than 120 min an endothermic peak can be observed at 80 °C (Fig. 1). The area below this peak is increasing and sharpening with longer grinding time. To find the source of the peaks, the last sample, i.e., ground for 240 min, was investigated by TG and hot-humidity stage XRPD.The TG curve revealed that the product is thermodynamically stable. Only 3.33 % of mass decrease was detected until the melting point of the CLP (Fig. 4). At 80 °C, the determination did not show salient mass decrease which means that the peak observed on the DSC pattern could not be ascribed to dissolution or solvent evaporation. No major decrease was

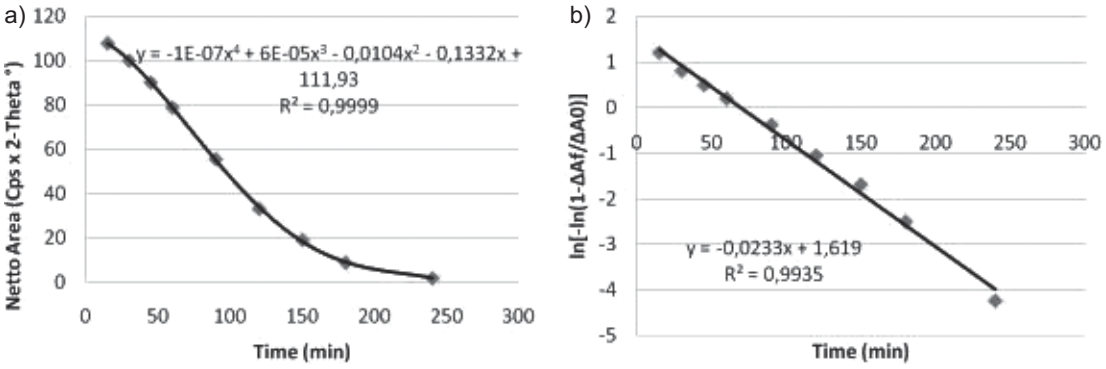

Figure 3. Crystallinity changes during grinding time. Function A shows the area below the curves decreasing with longer grinding time; function B is the linearization of the first one.

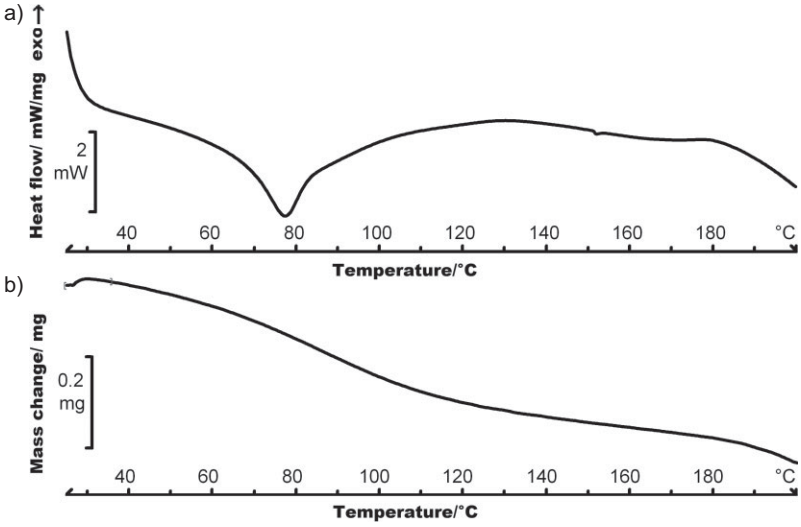

Figure 4. DSC (A) and TG (B) analysis of sample ground for 240 min. No major mass decrease was detected at 80 or 100 °C.

found at 100 °C which means that the sample was sufficiently dry.

The last sample, ground for 240 min, was determined by XRPD using the hot-humidity chamber at room temperature of 25 °C, at the temperature of the peak at 80 °C, and at a hotter temperature than the peak at 95 °C. The diffractograms showed an amorphous halo at all three times, so this peak does not refer to any change of crystallinity (Fig. 5).

The outlined phenomenon could be the glass transition of the amorphous complex since the T_g of the amorphous CLP is around 83 °C [28], although this signal change is more similar to an endothermic peak and has not the shape of T_g, which is just a baseline shift. This phenomenon is probably an emerging secondary bond between the API and the additive. The detected endothermic peak at 80 °C displays the split of the bond. At higher temperatures, the CLP-Aerosil 200 complex separates and a solid dispersion of the two independent materials arises.

3.4 FT-IR Spectroscopy

FT-IR spectroscopy is a suitable method for investigating interactions between pharmaceutical materials and polymers [33]. For FT-IR determination, the attenuated total reflection (ATR) method was chosen because sample preparation such as particle size reduction or KBr tableting is not required, which would expose the samples to further physical stress.

FT-IR results demonstrated that the grinding process caused several small changes in the spectra of the samples. One of the most spectacular alterations was observed at 1752 cm^{-1}, which displays the $\nu_{C=O}$ valence vibration of the CLP. These peaks of the samples ground more than 120 min expanded, shifted to lower wavenumbers, and slightly increased in intensity with longer grinding time (Fig. 6).

Another change was observed at 865 cm^{-1} where a band with high intensity starts to decrease after 120 min of grinding, while a double peak at 858 and 838 cm^{-1} fuses into one peak

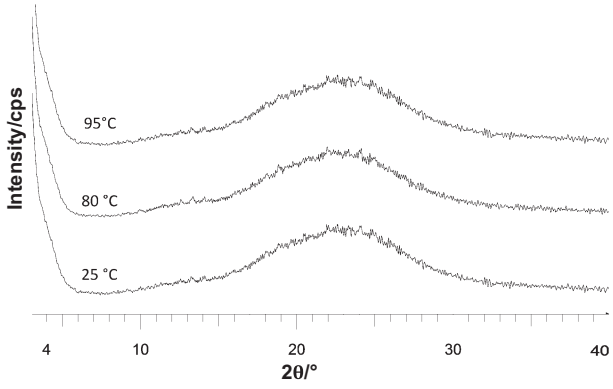

Figure 5. Hot-XRPD diffractograms of sample ground for 240 min at 25, 80, and 95 °C. Each diffractogram shows the amorphous halo. No changes happened in the crystallinity at these temperatures.

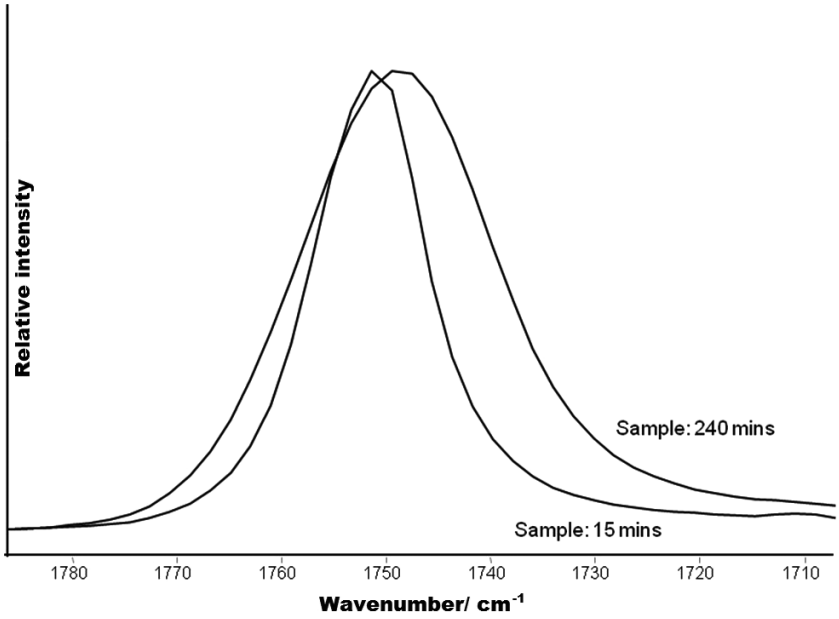

Figure 6. FT-IR investigation of samples ground for 15 and 240 min. The area below the peak at 1750 cm^{-1} increased, and the peak shifted to lower wavenumbers.

with a higher intensity (Fig. 7). These changes proportionally follow the change at 1752 cm^{-1} which is also remarkable after 120 min of grinding. The same phenomenon can be found between 1200 and 1135 cm^{-1}: the peak at 1188 cm^{-1} decreases, while the peak at 1150 cm^{-1} slightly increase parallel after 120 min of co-grinding.

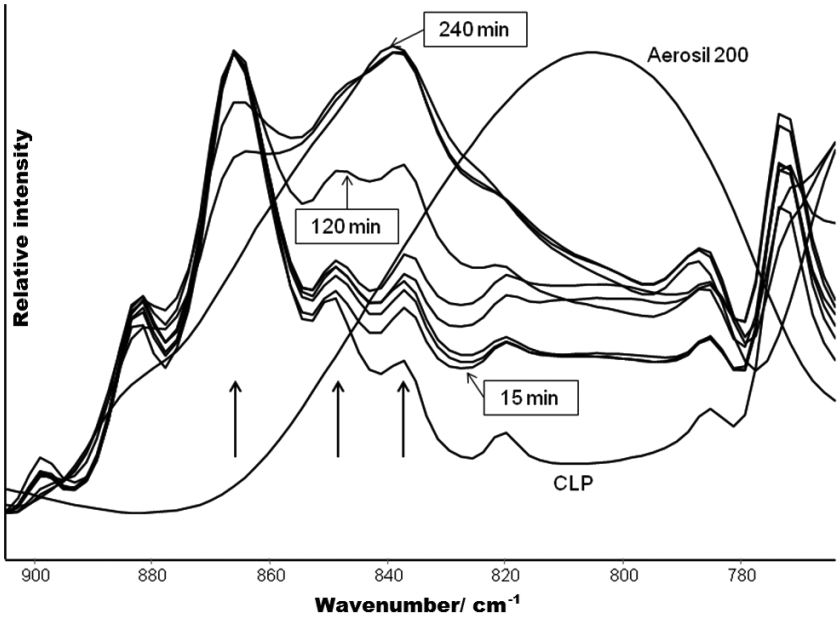

Figure 7. Bands of Aerosil 200, CLP, and nine samples ground from 15 to 240 min. The area under peak at 865 cm^{-1} is decreasing after 120 min of grinding, while the double peak at 858 and 838 cm^{-1} fuses into one peak with a higher intensity.

After 120 min of grinding a weak secondary bond appears between the CLP and the silanol groups of the CLP. This bond is strong enough to keep the CLP in amorphous phase. Based on previous work [29], this secondary bond can be considered as a hydrogen-bond.

4 Conclusions

Results proved that major alterations can be caused in the crystal structure of materials during co-grinding. Already a few minutes of grinding can be enough to break the long range order of the crystal, while grinding for sufficiently long time can convert the whole amount of the sample into the amorphous phase. In this case, the system containing CLP and the colloidal silicon dioxide Aerosil 200 started to lose its crystallinity from the beginning of grinding and needed 240 min to become fully amorphous. DSC and XRPD measurements demonstrated the course of decrease of crystallinity. TG and FT-IR determinations confirmed that no dissolution or solvent evaporation happened during grinding. TG and hot-humidity stage XRPD proved that the discovered peak at 80 °C was neither moisture or rest solvent nor change in crystallinity. FT-IR also determined a formatting secondary H-bond between CLP and Aerosil 200 molecules after 120 min of grinding. The previous peak on the DSC curve is a common signal of the split of this hydrogen bond. This bond can stabilize the molecularly disperse system in the amorphous phase. Finally, quantification of the phenomenon was performed by XRPD diffractograms, and the speed coefficient was calculated using Avrami's equation.

Acknowledgment

This work was supported by the European Union and co-funded by the European Social Fund. Project number: TÁMOP-4.2.2.A-11/1/KONV-2012-0035.

The authors have declared no conflict of interest.

References

[1] L. Yu, *Adv. Drug Delivery Rev.* **2001**, *48 (1)*, 27–42.
[2] L. Carpentier, S. Desprez, M. Descamps, *J. Therm. Anal. Calorim.* **2003**, *73 (2)*, 577–586.
[3] S. Qi, F. Avalle, R. Saklatvala, D. Q. Craig, *Eur. J. Pharm. Biopharm.* **2008**, *69 (1)*, 364–371.
[4] F. Taneri, T. Güneri, Z. Aigner, O. Berkesi, M. Kata, *J. Therm. Anal. Calorim.* **2004**, *76 (2)*, 471–479.
[5] S. Sethia, E. Squillante, *Int. J. Pharm.* **2004**, *272 (1–2)*, 1–10.
[6] K. Brodka-Pfeiffer, P. Langguth, P. Grab, H. Häusler, *Eur. J. Pharm. Biopharm.* **2003**, *56 (3)*, 393–400.
[7] T. Watanabe, I. Ohno, N. Wakiyama, A. Kusai, M. Senna, *Int. J. Pharm.* **2002**, *241 (1)*, 103–111.
[8] E. Yonemochi, S. Kitahara, S. Maeda, S. Yamamura, T. Oguchi, K. Yamamoto, *Eur. J. Pharm. Biopharm.* **1999**, *7 (4)*, 331–338.
[9] L. Kumar, A. Baheti, A. Mokashi, A. K. Bansal, *Eur. J. Pharm. Sci.* **2011**, *44 (1–2)*, 136–141.
[10] A. Pomázi, R. Ambrus, P. Sipos, P. Szabó-Révész, *J. Pharm. Biomed. Anal.* **2011**, *56 (2)*, 183–90.
[11] B. C. Hancock, G. J. Zografi, *Pharm. Sci.* **1997**, *86 (1)*, 1–12.
[12] M. Meier, E. John, D. Wieckhusen, W. Wirth, W. Peukert, *Eur. J. Pharm. Sci.* **2008**, *34 (1)*, 45–55.
[13] V. B. Pokharkar, L. P. Mandpe, M. N. Padamwar, A. A. Ambike, K. R. Mahadik, *Powder Technol.* **2006**, *167 (1)*, 20–25.
[14] D. Q. M. Craig, P. G. Royall, V. L. Kett, M. L. Hopton, *Int. J. Pharm.* **1999**, *179 (2)*, 179–207.
[15] J. T. Fuchs, C. Mattern, *Chem. Eng. Technol.* **2010**, *33 (9)*, 1464–1470.
[16] E. Merisko-Liversidge, G. G. Liversidge, *Adv. Drug Delivery Rev.* **2011**, *63 (6)*, 427–440.
[17] M. Juhnke, J. Berghausen, C. Timpe, *Chem. Eng. Technol.* **2010**, *33 (9)*, 1412–1418.
[18] R. Ambrus, N. N. Amirzadi, P. Sipos, P. Szabó-Révész, *Chem. Eng. Technol.* **2010**, *33 (5)*, 827–832.
[19] L. Kürti, A. Kukovecz, G. Kozma, R. Ambrus, M. A. Deli, P. Szabó-Révész, *Powder Technol.* **2011**, *212 (1)*, 210–217.
[20] M. J. Arias, J. M. Gines, J. R. Moyano, *Int. J. Pharm.* **1997**, *153 (2)*, 181–189.
[21] S. Y. Lin, W. T. Cheng, S. L. Wang, *Int. J. Pharm.* **2006**, *318 (1–2)*, 86–91.
[22] P. Mura, M. Cirri, M. Faucci, J. Ginas-Dorado, G. Bettinetti, *Pharm. Biomed. Anal.* **2002**, *30 (2)*, 227–237.
[23] C. Mártha, L. Kürti, G. Farkas, O. Jójárt-Laczkovich, B. Szalontai, E. Glässer, M. A. Deli, P. Szabó-Révész, *Eur. Polym. J.* **2013**, *49 (9)*, 2426–2432.
[24] Z. Aigner, O. Berkesi, G. Farkas, P. Szabó-Révész, *J. Pharm. Biomed. Anal.* **2012**, *57 (1)*, 62–67.
[25] D. K. Raijada, B. Prasad, A. Paudel, R. P. Shah, S. Singh, *J. Pharm. Biomed. Anal.* **2010**, *52 (3)*, 332–344.
[26] V. Uvarov, I. Popov, *J. Pharm. Biomed. Anal.* **2008**, *46 (4)*, 676–682.
[27] Z. Német, A. Demeter, G. Pokol, *J. Pharm. Biomed. Anal.* **2009**, *49 (1)*, 32–41.
[28] O. Jójárt-Laczkovich, P. Szabó-Révész, *J. Therm. Anal. Calorim.* **2010**, *102 (1)*, 243–247.
[29] O. Jójárt-Laczkovich, P. Szabó-Révész, *Drug. Dev. Ind. Pharm.* **2011**, *37 (11)*, 1272–1281.
[30] H. Takeuchi, S. Nagira, H. Yamamoto, Y. Kawashima, *Int. J. Pharm.* **2005**, *293 (1–2)*, 155–164.
[31] J. A. Baird, L. S. Taylor, *Adv. Drug Delivery Rev.* **2012**, *64 (5)*, 396–421.
[32] A. Sharples, *Introduction to Polymer Crystallization*, Edward Arnold Ltd., London **1966**.
[33] D. Hegyesi, T. Sovány, O. Berkesi, K. Pintye-Hódi, G. Regdon Jr., *Microchem. J.* **2013**, *110*, 36–39.

